

ผลของเกลือโคโตซานต่อประสิทธิภาพในการถ่ายโอนยีนเข้าสู่เซลล์เพาะเลี้ยงในหลอด  
ทดลองสำหรับการนำส่งยีน

โดย

นายวัลลภ วีชะรังสรรค์

วิทยานิพนธ์นี้เป็นส่วนหนึ่งของการศึกษาตามหลักสูตรปริญญาวิทยาศาสตรดุษฎีบัณฑิต

สาขาวิชาเทคโนโลยีเภสัชกรรม

บัณฑิตวิทยาลัย มหาวิทยาลัยศิลปากร

ปีการศึกษา 2550

ลิขสิทธิ์ของบัณฑิตวิทยาลัย มหาวิทยาลัยศิลปากร

**EFFECT OF CHITOSAN SALTS ON IN VITRO TRANSFECTION  
EFFICIENCY FOR GENE DELIVERY**

**By**

**Wanlop Weecharangsan**

**A Thesis Submitted in Partial Fulfillment of the Requirements for the  
Degree of Doctor of Philosophy  
Program of Pharmaceutical Technology  
Graduate School  
SILPAKORN UNIVERSITY  
2007**

The Graduate School, Silpakorn University accepted thesis entitled “EFFECT OF CHITOSAN SALTS ON *IN VITRO* TRANSFECTION EFFICIENCY FOR GENE DELIVERY” by Wanlop Weecharangsan in partial fulfillment of the requirements for the degree of Doctor of Philosophy, program of Pharmaceutical Technology.

.....  
(Assoc. Prof. Sirichai Chinatungkul, Ph.D.)  
Dean of Graduate School  
...../...../.....

Thesis advisors

1. Assoc. Prof. Praneet Opanasopit, Ph.D.
2. Assoc. Prof. Tanasait Ngawhirunpat, Ph.D.
3. Asst. Prof. Auayporn Apirakaramwong, Ph.D.

Thesis committee

.....Chairman  
(Parichat Chomto, Ph.D.)  
...../...../.....

..... Member ..... Memeber  
(Assoc. Prof. Praneet Opanasopit, Ph.D.) (Assoc. Prof. Tanasait Ngawhirunpat, Ph.D.)  
...../...../.....

..... Member .....Memeber  
(Asst. Prof. Auayporn Apirakaramwong, Ph.D.) (Uracha Ruktanonchai, Ph.D.)  
...../...../.....

46353902: สาขาวิชาเทคโนโลยีเภสัชกรรม

คำสำคัญ: กลีโกลิโคซาน/ การนำส่งยีน/ ประสิทธิภาพในการนำส่งยีน

วัลลภ วีระรังสรรค์: ผลของกลีโกลิโคซานต่อประสิทธิภาพในการถ่ายโอนยีนเข้าสู่เซลล์เพาะเลี้ยงในหลอดทดลองสำหรับการนำส่งยีน (EFFECT OF CHITOSAN SALTS ON *IN VITRO* TRANSFECTION EFFICIENCY FOR GENE DELIVERY) อาจารย์ผู้ควบคุมวิทยานิพนธ์: รศ.ดร.ปราณีต โอปณะโสภิต, รศ.ดร.ชนะเศรษฐ์ งามหิรัญพัฒน์ และ ผศ.ดร.อวยพร อภิรักษ์อร่ามวง. 148 หน้า.

การวิจัยนี้มีวัตถุประสงค์เพื่อศึกษาผลของกลีโกลิโคซานต่อประสิทธิภาพในการถ่ายโอนยีนเข้าสู่เซลล์เพาะเลี้ยงในหลอดทดลอง โดยศึกษาความสามารถในการเกิดสารประกอบเชิงซ้อนกับพลาสมิดดีเอ็นเอ ประสิทธิภาพในการถ่ายโอนยีนเข้าสู่เซลล์ และความเป็นพิษในเซลล์ COS-1 (Green monkey fibroblast) และ CHO-K1 (Chinese hamster ovary) กลีโกลิโคซานที่ใช้ในการศึกษาได้แก่ โกลิโคซานอะซีเตต โกลิโคซานแอสพาเตต โกลิโคซานกลูตามาต โกลิโคซานไฮโดรคลอไรด์ และโกลิโคซานแลคเตต ที่เตรียมจากการพ่นแห้งและจากการละลายโกลิโคซานในสารละลายกรด โดยใช้โกลิโคซานน้ำหนักโมเลกุล 20, 45, 200 และ 460 kDa นำกลีโกลิโคซานมาเตรียมสารประกอบเชิงซ้อนกับพลาสมิดดีเอ็นเอ pSVβ-gal และ pcDNA3-CMV-Luc ในอัตราส่วนระหว่างโกลิโคซานกับพลาสมิดดีเอ็นเอ (N/P) ต่างๆ กัน ผลการศึกษาพบว่าสารประกอบเชิงซ้อนระหว่างโกลิโคซานกับพลาสมิดดีเอ็นเอที่เตรียมจากโกลิโคซานจากการพ่นแห้งและจากการละลายโกลิโคซานในสารละลายกรด เกิดสารประกอบเชิงซ้อนสมบูรณ์ที่อัตราส่วน N/P มากกว่า 4 และ 2 ตามลำดับ จากการศึกษาประสิทธิภาพในการถ่ายโอนยีนเข้าสู่เซลล์ พบว่ากลีโกลิโคซานที่เตรียมจากการพ่นแห้งมีประสิทธิภาพในการถ่ายโอนยีนเข้าสู่เซลล์ไม่แตกต่างจากกลุ่มควบคุมทั้งในเซลล์ COS-1 และ CHO-K1 จากการศึกษาผลของสภาวะต่างๆ ต่อประสิทธิภาพในการถ่ายโอนยีนเข้าสู่เซลล์พบว่า pH ของตัวกลางในการนำส่งยีนมีผลต่อประสิทธิภาพในการถ่ายโอนยีนเข้าสู่เซลล์อย่างมีนัยสำคัญ จึงได้ควบคุมสภาวะการศึกษาที่ pH เท่ากันคือ 6.5 โดยใช้โกลิโคซานที่เตรียมจากการละลายโกลิโคซานในสารละลายกรดศึกษาผลของกลีโกลิโคซานต่อประสิทธิภาพในการถ่ายโอนยีนเข้าสู่เซลล์ CHO-K1 ผลการศึกษาพบว่ากลีโกลิโคซานชนิดต่างๆ มีประสิทธิภาพในการถ่ายโอนยีนเข้าสู่เซลล์ขึ้นกับชนิดของกลีโกลิโคซาน น้ำหนักโมเลกุลของโกลิโคซาน และอัตราส่วน N/P โดยกลีโกลิโคซานต่างกันให้ประสิทธิภาพในการถ่ายโอนยีนเข้าสู่เซลล์สูงสุดที่อัตราส่วน N/P ต่างกัน โกลิโคซานไฮโดรคลอไรด์ โกลิโคซานแลคเตต โกลิโคซานอะซีเตต โกลิโคซานแอสพาเตต และโกลิโคซานกลูตามาตมีประสิทธิภาพในการถ่ายโอนยีนเข้าสู่เซลล์สูงสุดที่อัตราส่วน N/P เท่ากับ 12, 12, 8, 6 และ 6 ตามลำดับ ประสิทธิภาพในการถ่ายโอนยีนเข้าสู่เซลล์มีแนวโน้มเพิ่มขึ้นเมื่ออัตราส่วน N/P เพิ่มขึ้น โกลิโคซานน้ำหนักโมเลกุลต่ำ (20 และ 45 kDa) มีประสิทธิภาพในการถ่ายโอนยีนเข้าสู่เซลล์สูงกว่าโกลิโคซานน้ำหนักโมเลกุลสูง (200 และ 460 kDa) จากการศึกษาความเป็นพิษต่อเซลล์ COS-1 และ CHO-K1 พบว่าสารประกอบเชิงซ้อนระหว่างกลีโกลิโคซานกับพลาสมิดดีเอ็นเอมีความเป็นพิษต่อเซลล์ต่ำ จากการวิจัยนี้แสดงให้เห็นว่ากลีโกลิโคซานมีความสามารถในการนำส่งยีนเข้าสู่เซลล์ และมีศักยภาพในการเป็นตัวพาที่ยีนที่ปลอดภัย

---

สาขาวิชาเทคโนโลยีเภสัชกรรม บัณฑิตวิทยาลัย มหาวิทยาลัยศิลปากร ปีการศึกษา 2550

ลายมือชื่อนักศึกษา.....

ลายมือชื่ออาจารย์ผู้ควบคุมวิทยานิพนธ์

1).....2).....3).....

46353902: MAJOR: PHARMACEUTICAL TECHNOLOGY

KEY WORDS: CHITOSAN SALT/ GENE DELIVERY/ TRANSFECTION EFFICIENCY

WANLOP WEECHARANGSAN: EFFECT OF CHITOSAN SALTS ON *IN VITRO* TRANSFECTION EFFICIENCY FOR GENE DELIVERY. THESIS ADVISORS: ASSOC. PROF. PRANEET OPANASOPIT, Ph.D., ASSOC. PROF. TANASAIT NGAWHIRUNPAT, Ph.D., ASST. PROF. AUAYPORN APIRAKARAMWONG, Ph.D. 148 pp.

The aim of this research was to investigate the effect of chitosan salts (CS) on *in vitro* transfection efficiency for gene delivery. CS was investigated for their DNA complexing ability with plasmid DNA, their transfection efficiency, and cytotoxicity in COS-1 (Green monkey fibroblast) and CHO-K1 (Chinese hamster ovary) cells. CS with various chitosan molecular weights (MW 20, 45, 200 and 460 kDa) including chitosan acetate (CAc), chitosan aspartate (CAs), chitosan glutamate (CGI), chitosan hydrochloride (CHy) and chitosan lactate (CLa) were prepared by spray drying and by dissolving chitosan base with acidic solutions. CS were formed a complex with pSV $\beta$ -gal or pcDNA3-CMV-Luc at various N/P ratios. Chitosan/DNA complexes prepared from spray dried chitosan salts and CS solution were completely formed at N/P ratios above 4 and 2, respectively. Spray dried chitosan salts yielded transfection efficiency not significantly different from naked DNA in both COS-1 and CHO-K1 cells. Optimization of transfection condition showed that pH of transfection medium significantly affected the transfection efficiency. Therefore, transfection condition was controlled at the same pH (6.5). CS solution was used to investigate the effect of the salt form of chitosan on the transfection efficiency in CHO-K1 cells. The results showed that the transfection efficiency of CS/DNA complexes depended on the salt form and MW of chitosan, and the N/P ratio of CS/DNA complexes. Of different CS, maximum transfection efficiencies were found in different N/P ratios. CHy/DNA, CLa/DNA, CAc/DNA, CAs/DNA and CGI/DNA complexes showed maximum transfection efficiencies at N/P ratios of 12, 12, 8, 6, and 6, respectively. The transfection efficiency had a tendency to increase as the N/P ratio increased. Low chitosan MW (20 and 45 kDa) had higher transfection efficiency than high chitosan MW (200 and 460 kDa). Cytotoxicity results showed that all CS/DNA complexes had low cytotoxicity. In conclusion, all CS had effective transfection efficiencies. This study suggests that CS have the potential to be used as safe gene delivery vectors.

---

Program of Pharmaceutical Technology, Graduate School, Silpakorn University

Student's signature.....

Thesis Advisor's signature 1) .....2).....3).....

## ACKNOWLEDGEMENTS

I would like to express my sincere gratitude and appreciation to my thesis advisor, Associate Professor Dr. Praneet Opanasopit, for her invaluable advices, guidance, attention and encouragement throughout my study.

I wish to express appreciation to my thesis co-advisors, Associate Professor Dr. Tanasait Ngawhirunpat and Assistant Professor Dr. Auayporn Apirakaramwong for their invaluable advices, suggestions and comments.

I also like to thank to my collaborate advisor, Associate Professor Dr. Robert J. Lee, College of Pharmacy, The Ohio State University for his invaluable guidance and comments.

I would like to appreciate for my thesis committee for their worthwhile suggestion and comment.

I am indebted to the Silpakorn University Research and Development Institute, the Nanotechnology for drug/gene delivery systems group, Faculty of Pharmacy, Silpakorn University, and the Office of the Commission for Higher Education, Ministry of Education, for granting financial support to fulfill this study.

I would like to express my thank to the National Nanotechnology Center (Nanotec) for the use of zetasizer and atomic force microscopy.

The acknowledgement is given to the staff of the Department of Pharmaceutical Technology and the Department of Biopharmacy, Faculty of Pharmacy, Silpakorn University, and the Division of Pharmaceutics, College of Pharmacy, The Ohio State University for their assistance and support.

Finally, I would like to express my love to my parents, brothers and sisters for their love, understanding, support, care and encouragement throughout my study.

# CONTENTS

	<b>Page</b>
THAI ABSTRACT.....	iv
ENGLISH ABSTRACT.....	v
ACKNOWLEDGEMENTS.....	vi
LIST OF TABLES.....	viii
LIST OF FIGURES.....	ix
ABBREVIATIONS.....	xii
CHAPTER	
I INTRODUCTION.....	1
II LITERATURE REVIEWS.....	3
III MATERIALS AND METHODS.....	40
IV RESULTS AND DISCUSSION.....	54
V CONCLUSION.....	107
BIBLIOGRAPHY.....	110
APPENDIX.....	127
BIOGRAPHY.....	148

## LIST OF TABLES

Table	Page
1 Chitosan in gene therapy.....	22
2 Example used cell lines for gene delivery.....	33
3 Physicochemical properties of the acids used to prepare the CS solutions.....	43
4 Calculation of N/P ratio for chitosan/DNA complex.....	47
5 Calculation of N/P ratio for PEI/DNA complex.....	48
6 Molar ratio of D-glucosamine unit and acids.....	55
7 pH of SD-CS in various solutions.....	73
8 Protonated amine and unprotonated amine of chitosan in the complex solution at various pH of complex solution.....	80

## LIST OF FIGURES

Figure	Page
1	Structure of chitosan.....1
2	Structure of cationic lipids.....14
3	Structure of cationic polymers.....21
4	Structure of plamid DNA.....29
5	Numbering of a DNA sequence.....30
6	Consensus sequences in the promoter regions of prokaryotic and eukaryotic DNA.....31
7	Transmission infrared spectrum of chitosan base, SD-CAs, SD-CGI and SD-CLa.....57
8	Solid-state <sup>13</sup> C-NMR spectrum of chitosan base, SD-CAs, SD-CGI and SD-CLa.....58
9	DSC thermogram of chitosan base, SD-CAs, SD-CGI and SD-CLa.....59
10	TGA thermogram of chitosan base, SD-CAs, SD-CGI and SD-CLa.....60
11	Powder X-ray diffraction pattern of chitosan base, SD-CAs, SD-CGI and SD-CLa.....61
12	Gel electrophoresis of SD-CS/DNA complexes with different chitosan salts and MW.....63
13	Relative fluorescent intensity of DNA/EtBr complex at varying N/P ratios of SD-CS.....64
14	Zeta potential and particle size at varying N/P ratios of SD-CS-20kDa/DNA complexes.....66
15	Zeta potential and particle size at varying N/P ratios of SD-CS-45kDa/DNA complexes.....67
16	Zeta potential and particle size at varying N/P ratios of SD-CS-200kDa/DNA complexes.....68
17	Zeta potential and particle size at varying N/P ratios of SD-CS-460kDa/DNA complexes.....69

## LIST OF FIGURES (Continued)

Figure	Page
18	Transmission electron microscope images of SD-CLa-20kDa/DNA complexes.....70
19	Relative fluorescent intensity of DNA/EtBr complex at varying N/P ratios of SD-CGI.....72
20	Transfection efficiency of SD-CS/DNA complexes in COS-1 cells .....75
21	Transfection efficiency of SD-CS/DNA complexes in CHO-K1 cells.....76
22	Effect of SD-CS/DNA complexes on COS-1 cell viability.....77
23	Gel electrophoresis of CAc-45kDa/DNA complexes at pH 3.0, 5.0 and 6.5.....79
24	Particle size at varying N/P ratios of CS-45kDa/DNA complexes with different chitosan salts at pH 3.0 and 6.5.....82
25	Particle size at varying N/P ratios of CGI/DNA complexes with different chitosan MW at pH 3.0 and 6.5.....83
26	Zeta potential at varying N/P ratios of CS-45kDa/DNA complexes with different chitosan salts at pH 3.0 and 6.5.....85
27	Zeta potential at varying N/P ratios of CGI/DNA complexes with different chitosan MW at pH 3.0 and 6.5.....86
28	Gel electrophoresis of CS-45kDa/DNA complexes with different chitosan salts.....88
29	Zeta potential and particle size at varying N/P ratios of CS-45kDa/ DNA complexes with different chitosan salts.....89
30	Gel electrophoresis of CGI/DNA complexes with different chitosan MW.....91
31	Zeta potential and particle size at varying N/P ratios of CGI/DNA complexes with different chitosan MW.....92

## LIST OF FIGURES (Continued)

Figure	Page
32 Topological image of atomic force microscopy image of CS-45kDa/DNA complexes at an N/P of 2.....	95
33 Phase contrast image of atomic force microscopy of CLa-20/DNA complexes at an N/P of 12.....	96
34 Transfection efficiency of CAc-45kDa/DNA complexes at 0.1%, 0.2% and 0.6% acetic acid solution in CHO-K1 cells.....	97
35 Transfection efficiency of CAc-45kDa/DNA complexes at pH of transfection medium 6.0 and 7.4 in CHO-K1 cells.....	99
36 Transfection efficiency of CAc-45kDa/DNA complexes at incubation time 1, 2, 4, 6 and 24 hours in CHO-K1 cells.....	100
37 Transfection efficiency of CS-45kDa/DNA complexes with different chitosan salts in CHO-K1 cells.....	101
38 Transfection efficiency of CGI/DNA complexes with different chitosan MW in CHO-K1 cells.....	103
39 Effect of CS-45kDa/DNA complexes with different chitosan salts on CHO-K1 cell viability.....	105
40 Effect of CGI-45kDa/pcDNA3-CMV-Luc complexes with different chitosan MW on CHO-K1 cell viability.....	105

## ABBREVIATIONS

AFM	atomic force microscopy
BCA	bicinchoninic acid
bp	basepair
BSA	bovine serum albumin
CAC	chitosan acetate
CAs	chitosan aspartate
CGI	chitosan glutamate
CHy	chitosan hydrochloride
CLa	chitosan lactate
CS	chitosan salt
CHO-K1	Chinese hamster ovary
CO <sub>2</sub>	carbon dioxide
COS-1	green kidney fibroblast
<sup>13</sup> C-NMR	carbon13-Nuclear magnetic resonance
°C	degree celcius
DMEM	dulbecco's modified eagle's medium
DMSO	dimethylsulfoxide
DNA	deoxyribonucleic acid
DSC	differential scanning calorimetry
e.g.	exempli gratia, 'for example'
et al.	et alii, 'and others'
EtBr	ethidium bromide
FTIR	fourier transformed infrared
FBS	fetal bovine serum
h	hour
i.e.	id est, 'that is'
kDa	kilodalton
min	minute
ml	milliliter
MTT	3-(4,5-dimethylthiazol-2-yl)-2,5-diphenyltetrazoliumbromide

## ABBREVIATIONS (Continued)

mV	milivolt
MW	molecular weight
N	normal (concentration)
NaOH	sodium hydroxide
nm	nanometer
N/P ratio	ratio of positively charged chitosan to negatively charged DNA
pK <sub>a</sub>	minus logarithm base 10 of K <sub>a</sub> , -log K <sub>a</sub>
RLU	relative light unit
RNA	ribonucleic acid
rpm	revolution per minute
RPMI-1640	roswell park memorial institute (medium)
SD	standard deviation
SD-CAs	spray dried chitosan aspartate
SD-CG1	spray dried chitosan glutamate
SD-CLa	spray dried chitosan lactate
SD-CS	spray dried chitosan salt
sec	second
TEM	transmission electron microscopy
TGA	thermogravimetric analysis
μl	microliter
%w/v	% weight by volume
XRPD	X-ray powder diffraction

## CHAPTER I INTRODUCTION

Chitosan [a (1→4) 2-amino-2-deoxy-β-D-glucan] is a copolymer of *N*-acetyl-D-glucosamine and D-glucosamine produced by alkaline deacetylation of chitin (Figure 1). Chitosan is a weak base with a pK<sub>a</sub> value of the D-glucosamine residue of about 6.2-7.0 (Hejazi and Amiji 2003: 151-165); therefore, it is insoluble at neutral and alkaline pH values. It makes salts with inorganic and organic acids such as hydrochloric acid and acetic acid which allows it to be soluble in water. Chitosan has been used in drug delivery as an absorption enhancer (Tengamnuay et al. 2000: 53-67; Maestrelli et al. 2004: 257-267; Florea et al. 2006: 353-361) and as a vector for gene delivery (Kumar et al. 2003: 3; Zhao et al. 2006: 223-228).

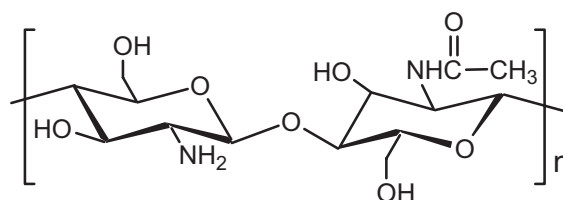


Figure 1 Structure of chitosan.

As a non viral vector for gene delivery, chitosan has several advantages over viral vectors that they have major drawbacks such as virally-induced inflammatory responses, immunological reactions and oncogenic effects (Simon et al. 1993: 771-780; Ferber 2001: 1638-1642; Somia and Verma 2000: 91-99). Chitosan can be used for the efficient transfection of cells with DNA. In addition, chitosan is biocompatible, biodegradable and non-toxic; therefore, it has been proposed as a safer alternative to other non viral vectors such as cationic lipids and cationic polymers (Lee et al. 2001: 427-431; Thanou et al. 2002: 153-159; Corsi et al. 2003: 1255-1264).

At acidic pH, below  $pK_a$ , the primary amines in the chitosan backbone become positively charged. These protonated amines enable chitosan to bind to negatively charged DNA and condense it into particles. Chitosan has shown promise to protect DNA from DNase I and II degradation (Richardson, Kolbe and Duncan 1999: 231-243; Köping-Höggård et al. 2004: 1441-1452; Haung et al. 2005: 391-406) and transfect into different cell types such as African green monkey (COS-1) (Maclaughlin et al. 1998: 259–272; human osteosarcoma (MG63) and human embryonic kidney (HEK293) cells (Corsi et al. 2003: 1255-1264). Formulation variables such as MW, degree of deacetylation, N/P ratio (ratio of positively charged chitosan to negatively charged DNA), and pH of transfection medium were found to affect the transfection efficiency of chitosan/DNA complexes (Sato, Ishii and Okahata 2001: 2075-2080; Rómóren et al. 2003: 115-127; Kiang et al. 2004: 5293-5301; Lavertu et al. 2006: 4815-4824).

Although chitosan salts (CS) were reported to be used for drug delivery, protein delivery and transfection of DNA, these methods employed the dissolution of the chitosan base with the acidic solutions (Tengamnuay et al. 2000: 53-67; Hino et al. 2000: 413-419; Lavertu et al., 2006: 4815-4824; Zhao, Yu, et al., 2006: 223-228) or spray-dried chitosan salts (hydrochloride, glutamate, aspartate, lactate, etc) (Luangtananan et al., 2005: 189-196; Weecharangsan et al., 2006: E1-E6). Because different acids possess their different physicochemical properties such as  $pK_a$ , solubility, charge, and size. These properties might affect the physicochemical properties of respective chitosan, resulting in different transfection efficiencies. Although chitosan and chitosan derivatives have been extensively reported to effective methods for transfection, each experiment was separately performed by different investigators. No previous study compared the effect of different salt forms on the chitosan/DNA complexes and transfection efficiency in the same experiment.

Therefore, the objective of this study was to investigate different CS including chitosan acetate (CAc), chitosan aspartate (CAs), chitosan glutamate (CGI), chitosan hydrochloride (CHy) and chitosan lactate (CLa) for their ability to form complexes with plasmid DNA and their transfection efficiencies in COS-1 and CHO-K1 cells. In addition, the cytotoxicity of chitosan/DNA complexes formulated with various CS was investigated.

## CHAPTER II

### LITERATURE REVIEWS

#### 1. Gene therapy

Gene therapy is one of the new therapeutic approaches emerging from molecular biology and biotechnology revolution. Gene therapy involves the modification of cells of patient in order to achieve a therapeutic goal. There are basic distinctions in the types of cells modified, and the type of modification effected. The types of cells modified can be divided in germ-line and somatic cell gene therapy. Germ-line gene therapy produces a permanent transmissible modification. This might be achieved by modification of a gamete, a zygote or an early embryo. Germ-line therapy is banned in many countries for the types of modification effected. Somatic cell gene therapy aims to modify specific cells or tissues of the patient in a way that is confined to that patient. All current gene therapy trials and protocols are for somatic cell therapy. Somatic cell gene therapy might be modified in a number of different ways such as gene supplementation, gene replacement, targeted inhibition of gene expression, and targeted killing of specific cells. Gene supplementation, also called gene augmentation, aims to supply a functioning copy of defective gene. This would be used to treat loss of function conditions where the disease process is the result of a gene not functioning. Gene replacement aims to replace a mutant gene by a correctly functioning copy. Targeted inhibition of gene expression where essential functions of the pathogen are targeted. It is relevant in infectious diseases. It could also be used to silence activated oncogenes in cancer, unwanted responses in autoimmune disease and mutant allele in inherited disease. Targeted killing of specific cells aims to kill unwanted cells. This application is capable for cancer treatment (Stracham and Read 2004: 616).

A gene can be transferred to the cells in the body by two general strategies, *ex vivo* and *in vivo*. In *ex vivo* gene transfer, the cells are removed from the patient. These cells are cultured in the laboratory and then used as the recipient for a desired gene. The cells that have the desired gene are then cultured and returned to the patient and continue to divide and develop into a number of different cells in the body (Bouragaize, Jewell, and

Buiser 2000: 224-230; Evans et al. 2006: 243-258). For *in vivo* gene delivery, genes are administered directly to the body. By this way, genes can be encountered with biological barriers from the point of injection to the surface of the cellular target such as degradation in the blood circulation, scavenging by circulating or resident macrophage, extravasation from vascular layer, permeation across endothelial barrier, and distribution within tissue (Pouton and Seymour 2001: 187-203). For each strategy of gene transfer, efficient delivery of gene to the cells can be aided by the application of vectors.

A variety of genetic diseases have been characterized. Many of these diseases are caused by lack of production of a single gene product or are due to the production of a mutated gene product incapable of carrying out its natural function. Gene therapy represents a seemingly straightforward therapeutic option which could correct such genetic-based diseases. This would be achieved by facilitating insertion of a healthy copy of the gene into appropriate cells of the sufferer. In theory, it is possible to transform either somatic cells or cells of the germline such as sperm cells, ova, and their stem cell precursors. All gene therapy to date on humans has been directed at somatic cells, whereas germline engineering in humans remains controversial. For the introduced gene to be transmitted normally to offspring, it needs not only to be inserted into the cell, but also to be incorporated into the chromosomes by genetic recombination (Walsh 1998: 396-402; Wikipedia, FL, USA 2007c).

The importance of gene therapy to the future practice of medicine is no longer being seriously questioned. However, in addition to technical difficulties, a number of non-technical issues must be satisfactorily addressed before its practice becomes widespread. Chief among these issues are the questions of public perception, ethics and costs. The strict regulations overseeing the use of this technology are required. Without proper controls, the danger exists that gene therapy could eventually be used to improve human characteristics. The technical know-how to underpin a new era of eugenics is now almost a reality. The most important safeguard aimed at preventing eugenic-type developments is already in place. Currently, gene therapy is restricted to somatic cells. The genetic manipulation of human germ cells is banned. Any genetic alterations achieved will thus not be transmitted to future generations (Walsh 1998: 396-402).

In most gene therapy studies, a carrier molecule called a vector must be used to deliver the therapeutic gene to the target cells. The desired gene must usually be packaged into a vector system capable of delivering it safely inside the intended

recipient cells. A variety of vectors can be used to affect gene transfer. The vectors for gene delivery can be divided into two major groups, viral and non viral vectors. Viruses such as adenovirus and retrovirus are the most common vectors that have been genetically altered to carry normal human DNA (Schiedner et al. 1998: 180-183; Blaese et al. 1995: 475-480). Viral vectors have very high level of gene expression, while also significant limitations such as virally-induced inflammatory responses, immunological reactions and oncogenic effects. For this reason, considerable effort has been put into the development of nonbiological delivery systems in gene therapy. Of these, the most promising system appears to be based on cationic vectors such as cationic polymers and cationic lipids which can be used to carry DNA and transfect the cells (Felgner et al. 1987: 7413-7427; Wu and Wu 1987: 4429-4432). The advantage in using nonbiological delivery systems in gene therapy includes the lack of immunological reactions, the ability to perform repeated administration *in vivo* without adverse consequence, the ease in creating targeted complexes for delivery and expression in specific cell types, and the safety for patient due to few or no viral sequences used for delivery (Zhang et al. 2004: 165-180; Templeton 2002: 283-295).

## **2. DNA vaccines**

DNA vaccines are the vaccines based on the induction of an immune response to a protein expressed *in vivo* from a gene the introduction of its encoding DNA. (Tang, DeVit and Johnston 1992: 152-154) demonstrated the elicitation of an immune response against a foreign protein by introducing a plasmid encoding an antigen protein directly to mouse skin with a gene gun. Ulmer et al. (1993) and Fynan et al. (1993) showed that immunization with plasmid DNA could protect mice against a lethal influenza challenge. Subsequently, several studies have been published demonstrating that the DNA vaccine is potentially effective for a wide variety of diseases including infectious diseases (Kang et al. 2003: 270-276), cancers (Todorova et al. 2005: 4727-4732), and allergic disease (Hartl et al. 2004: 65-73).

A DNA vaccine can be generated by inserting an interesting antigen-encoding gene into a bacterial plasmid under the control of an appropriate eukaryotic promoter e.g., the CMV promoter from cytomegalovirus in most cases. Due to the difference in codon usage preference between bacteria and eukaryotic cells, the antigen gene is often modified by point mutation to improve the efficiency of gene expression. The plasmid

that has been purified and detoxified is then administered into the host animal. The plasmids that are uptaken by appropriate cells and processed their way into nucleus, the host cell will use its own gene transcription and protein expression to produce corresponded antigen (Cui 2005: 258-289).

The ideal vaccine would have the following properties: safe for all individuals; easily administered, preferably by oral means; induction of the full range of immune responses; long-lasting effect from a single dose; easy and inexpensive to manufacture; simplified with rigorous quality assessment and control; and heat-stability. Classical vaccination involves administration of an immunogen, which could be subdivided into three general types: subunit, live attenuated and killed vaccines. Subunit vaccines involve administration of selected components of the pathogen (virus or bacteria). The disadvantage of these vaccines is that the induction of immunity is effective for certain pathogens. Another drawback is that they induce only short-term immunity. Live vaccines consist of viruses or bacteria grown for prolonged periods under abnormal conditions so that they become attenuated i.e. non-pathogenic. They usually provide excellent immunity due to prolonged exposure to immunogen and synthesis in self-cells. The most important drawback for live attenuated vaccines is the possibility of reversion to a virulent form. Killed vaccines are produced from viruses or bacteria killed by treatment with heat or chemicals. The disadvantage of these vaccines may include infection due to incomplete inactivation, loss of immunogenicity owing to denaturation (Dickson 1995: 368-372).

The potential advantages of DNA vaccination, in contrast to classical vaccination where antigens are administered, the genetic material encoding the antigen is synthesized *in vivo*. The immunological responses are similar to subunit vaccines except that the antigen is produced within the cells of individual to be immunized. There are two unique features of DNA-based vaccines that make them particularly interesting. The first is the possibility of long-live gene expression resulting in sustained presentation of antigen at low levels to the immune system. The second unique feature of DNA-based vaccines is due to the synthesis of antigen *in vivo* and presentation by major histocompatibility complex (MHC) surface glycoproteins. As such, DNA vaccines should induce cell mediated immunization (CMI) by activation of cytotoxic T lymphocytes (CTL), as do the live viral or bacterial vaccines, but without the risk of inadvertent infection, an important consideration for use in immunosuppressed

individuals. Furthermore, multiple component DNA vaccines can be engineered to include specific immunogens, which could optimize and amplify desirable immunological responses (Dickson 1995: 368-372; Kim and Weiner 2000: 551-559).

The mechanism for DNA immunization is likely to be similar to traditional antigen presentation. In general, immune responses include the induction of humoral and cell-mediated immunity. Humoral immunity is the production of neutralizing antibodies by B lymphocytes. When B cells are activated by binding with circulating soluble antigen, most B cells differentiate into plasma cells that produce and secrete neutralizing antibodies. Some activated B cells become memory cells which react quickly to a secondary challenge of antigen with higher and more sustained level of antibody. In cell-mediated immunity, the infected cells are destructed by CTL (Dickson 1995: 368-372). T lymphocytes do not recognize circulating antigen, but recognize antigen presented on the surface of antigen-presenting cells (APCs) by MHC glycoprotein surface molecules. Four primary components are critical in the professional APCs ability to present the antigen to T cells and activate them for appropriate immune responses. These components are MHC-antigen complexes, costimulatory molecules primarily CD80 and CD86, intracellular adhesion molecules, and soluble cytokines. Naïve T cells circulate through the body across lymph nodes and secondary lymphoid organs such as spleen. Their migration is mediated by intracellular adhesion molecules and cytokines. As the T cells travel, they bind to and dissociate from various APCs. This action is mediated through adhesion molecules. When a naïve T cell binds to an APC expressing a relevant MHC-peptide complex, the T cell expresses high levels of high affinity interleukin-2 receptor. When this T cell receives a costimulatory signal through CD80/CD86-CD-28 interaction does the T cell make soluble interleukin-2, which then binds to the receptors and drives the effector T cell to activate and proliferate (Kim and Weiner 2000: 551-559).

DNA vaccine in variety of animal models propelled it into a number of human clinical trials for diseases or pathogens including acquired immunodeficiency syndrome (AIDS) (Tavel et al. 2007:601-605), malaria (Dunachis et al. 2006: 5933-5942), hepatitis B (Rebedea et al. 2006: 5320-5326), and cancers (Cassaday 2007: 540-549).

### 3. Vectors for gene delivery

#### 3.1 Viral vectors

Viral vectors are genetically modified viruses, which are able to transfer their genetic material to a host cells. Viral vectors used in gene therapy include integrating vectors based on retrovirus and adeno-associated virus, as well as non-integrating vectors based on adenovirus and herpes simplex virus.

##### 3.1.1 Retroviral vectors

The pioneer work on gene delivery *in vivo* was performed with retroviral vectors, typically using murine leukemia virus (MLV). Advantageous features of retroviruses are their ability to integrate into the host genome and therefore sustain heterologous gene expression for extended time periods. Retroviruses are small RNA viruses that replicate through a DNA intermediate. The retrovirus infects target cells through a specific interaction between the viral envelope protein and a cell surface receptor on the target cell. The virus is then internalized, where it is uncoated the RNA reverse-transcribed into proviral double-stranded DNA (dsDNA) by means of the virally encoded polymerase gene. The dsDNA is then transported to the nucleus, where it is stably integrated into the host genome. The ability of retroviruses to insert their genome into the host DNA allows stable genetic modification for the life of the host cell (Robbins and Ghivizzani 1998: 35-47). Retroviral vector was subjected to the first clinical trial on human gene therapy to correct adenosine deaminase (ADA) deficiency (Blaese et al. 1995: 475-480). White blood cells isolated from patients were *ex vivo* with MLV-based vector expressing ADA and a neomycin marker gene. After selection with G418, neomycin-resistant, the transduced cells were isolated and reintroduced into patients. The treatment improved the physical condition of the patients and the ADA-containing provirus was stable in the blood for several years. Retroviral vector also demonstrated some promising results in cancer therapy by the introduction of retrovirus particles expressing herpes simplex virus-thymidine kinase (HSV-TK) and administration of the prodrug ganciclovir (GCV). HSV-TK converts the GCV to its active form and kills the cancer cells (Bonini et al. 1997: 1719-1724). The disadvantage of retroviral vectors is that they require cell division. Thus, the current retroviral vectors are better suited for *ex vivo* gene therapy.

### 3.1.2 Adenoviral vectors

Adenovirus is a non-enveloped virus with a dsDNA genome of 26-45 kb, which replicates in the nucleus after infection of either quiescent or dividing cells. The features that have made adenovirus a popular gene therapy vector are the ability to generate high titer virus stocks and high level heterologous gene expression (Shenk 2001: 2265-2300). Adenovirus can infect a wide variety of cells through a specific interaction between the viral fiber protein and cell surface receptor. Entry of the virus into the cell is further enhanced through a specific interaction of the fiber with an integrin co-receptor. The host range can be altered by modifying the fiber protein so that it can bind more efficiently to other components of the cell surface (Wickham, Carrion and Kovesdi. 1995: 750-756; Wickham et al, 1996: 6831-6838). Antibodies against tissue-specific cell surface can also be coupled to the fiber protein to facilitate partial targeting of the virus (Kranykh et al. 1996: 6839-6846). Adenoviral vector has been predominantly for treatment of cystic fibrosis because the natural site for adenoviral infection is the airway. Cystic fibrosis is the result of recessive mutation of cystic fibrosis transmembrane conductance regulator (CFTR) gene. CFTR gene is responsible for the transport chloride ions across the cell membrane. Lack of this function has major effects on the cells that line the lungs and gut. The engineered virus containing the functional gene can be delivered to patients as an aerosol (Perricone et al. 2001:1383-1394).

### 3.1.3 Adeno-associated viral vectors

Adeno-associated virus (AAV) is a single stranded DNA virus that requires helper virus such as adenovirus or herpes simplex virus for replication. AAV is a non pathogenic virus. Its genome contains two open reading frames flanked by inverted terminal repeats (ITRs). AAV vectors have most of the viral DNA deleted, leaving only the ITRs, giving a transgene capacity. The most widely used AAV vectors use heparin sulfate proteoglycans as the primary receptor and co-receptors fibroblast growth factor 1 receptor and  $\alpha_v\beta_5$  integrin, giving access to a wild range of tissue types. (Summerford and Samulski 1998: 1438-1445; Summerford, Bartlett and Samulski 1999: 78-82). Different AAV serotypes have shown remarkably different expression patterns because of differences in cell entry and intracellular activities. AAV-1 is suitable for expression in skeletal muscle and retina. AAV-5 packaged vectors have tropism for airway epithelial cells in murine and human models (Rabinowitz et al. 2002: 791-801).

AAV-6 shows very efficient uptake into skeletal muscle (Blankinship et al. 2004: 671-678). AAV-8 shows liver tropism and has been developed for hepatic delivery of Factor IX for haemophilia (Davidoff et al. 2005: 875-888; Nathwani, McIntosh and Davidoff 2005: 287-293). The major hurdles remain for the use of AAV vectors: the small transgene capacity and the effect of neutralizing antibodies. AAV can package 4.9 kb, which is too small for many applications. Many people have neutralizing antibodies to AAV due to prior infection. The administration of AAV also elicits a strong humoral response which can interfere with subsequent doses (Chirmule et al. 1999: 1574-1583; Kok et al. 2005: 432-441).

### **3.1.4 Herpes Simplex viral vectors**

Herpes Simplex virus (HSV) is a linear dsDNA virus of approximately 150 kb, encoding over 70 viral proteins. Using two viral glycoproteins B and D, the virus binds to the cells through an interaction with heparin sulfate moieties on the cell surface, and then enters the cells by fusion. HSV is a natural human pathogen, replicating in epithelial cells but able to stay in a latent state in nondividing cells (neurons). Although full genome HSV is cytotoxic to neurons, multiple gene deletions can be made to generate viable HSV vectors. The deletion of four immediate early genes ICP0, ICP4, ICP22 and ICP47 resulted in an entirely nontoxic vector, which persists for extended time in host cells. HSV vectors have advantages of being able to infect nondividing cells, establishing latency in some cell types, and having the capacity to carry large regions of exogenous DNA. The ability to establish latency in neuronal cells make HSV an attractive vector for treating neurological disorders such as Parkinson's and Alzheimer's (Sun et al. 2005: 119-129; Hong et al. 2006: 1068-1079).

### **3.2 Non viral vectors**

Non viral gene delivery methods are the techniques employing either chemical or physical approaches. The first is mainly based on lipids or polymers which on interaction with DNA form lipid/DNA complexes called lipoplexes and polymer/DNA complexes called polyplexes (Felgner et al. 1997: 511-512). Cationic vectors interact with negatively charged DNA through electrostatic interaction. The total charge maintains a positive net value. This will enable the carrier of efficiently interacting with

the negatively charged cell membranes and internalizes into the cell, which occurs mainly through endocytosis pathway (Colin et al. 2000: 139-152).

### 3.2.1 Lipoplexes

Cationic lipids used for DNA delivery are composed of three basic domains: a positively charged headgroup, a hydrophobic chain, and a linker such as amide or carbamate which joins these molecules together covalently (Gao and Hui 2001: 855-863). Lipids with monovalent cationic headgroups e.g., N-[1-(2,3-dioleoyloxy)propyl]-N,N,N-trimethylammonium chloride (DOTMA), N-[1-(2,3-dioleoyloxy)propyl]-N,N,N-trimethylammonium methylsulfate (DOTAP), N-[1,2-dimyristyloxypropyl]-N,N-dimethyl hydroxyethyl (DMRIE), 3- $\beta$  [N-(N',N'-dimethylaminoethane)-carbamoyl] cholesterol (DC-Chol) and those with multivalent cationic headgroups e.g., 2,3-dioleoyloxy-N-[2(sperminecarboxamido)ethyl]-N,N-dimethyl-1-propane ammonium trifluoroacetate (DOSPA) and dioctadecylamidoglycyl spermine (DOGS) have been utilized as DNA delivery agents (Felgner et al. 1987: 7413–7417; Ewert et al. 2002: 5023-5029). Neutral lipids, such as dioleoyl phosphatidylethanolamine (DOPE), cholesterol and dioleoyl phosphatidyl choline (DOPC) are utilized in many formulations for improving transfection efficiency (Farhood, Serbini and Huang 1995: 289-295). The structure of cationic lipids is shown in Figure 2.

Cationic lipids are amphiphilic molecules, consisting of a hydrophilic and a hydrophobic region. An important property of the amphiphile with regard to its application as a vector, is its geometry. Like any amphiphile, when suspended in an aqueous environment, cationic lipids adopt various structural phases, including the micellar, lamellar, cubic and inverted hexagonal phases.

Cationic lipids were first introduced by Felgner et al., following early attempts to transfer DNA via encapsulation in liposomes (Nicolau and Sene 1982: 185-190; Nicolau et al. 1983: 1068-1072). Thus the first reported lipid was DOTMA, which consists of a quarternary amine connected to two unsaturated aliphatic hydrocarbon chains via ether groups (Felgner et al. 1987: 7413–7417). Synthesis of the multivalent lipopolyamine e.g., DOSPA and DOGS was subsequently reported (Gao and Huang 1991: 280-285). For transfection application, cationic lipids are often mixed with so-called helper lipids, such as DOPE and cholesterol. These lipids potentially promote

conversion of the lamellar lipoplex phase into a non-lamellar, which presumably enhance endosomal escape of the lipoplexes into the cytoplasm as they are thought to have fusogenic properties important for endosomal membrane disruption (Farhood, Serbini and Huang 1995: 289-295; Vidal and Hoekstra 1995: 17823-17829; Ellen, Bentz and Szoka 1986: 4141-4147).

Cationic lipid/DNA complexes are formed by an electrostatic interaction between the cationic lipid and the DNA. Spontaneous self-assembly into nanometric particles results, leading to shielding of the DNA from the nucleases of the extracellular medium. Use of an excess of lipid equips the lipoplex surface with a positive charge, which is presumed to mediate subsequent cellular uptake via interaction with negative cell surface structures (Labat-Moleur et al 1996: 1010-1017; Friend, Papahadjopoulos and Debs 1996: 41-50; Mislick and Baldeschwieler 1996: 12349-12354). Cationic lipids in liposomal formulation serve the same function as cationic polymers to form a complex with anionic DNA. There are several ready-to-use cationic liposomes in the market with different lipid compositions e.g., Lipofectamine and Lipofectin (Invitrogen, Carlsbad, CA, USA).

It is generally agreed that the length and type of the aliphatic chains incorporated into cationic lipids significantly affect their transfection efficiency. A set of results in terms of transgene expression obtained with DMRIE (Felgner et al. 1994: 2550-2561), glycine betaine derivatives (Floch et al. 1998: 360-365), alkyl acyl carnitine esters (Wang et al. 1998: 2207-2215), lactic derivatives (Laxmi et al. 2001: 1057-1062) and bis-ether lipids related to DOTAP (Heyes et al. 2002: 99-114), have shown that a comparison of vectors based solely on the lengths of the two saturated aliphatic chains led to identify the order C14 > C16 > C18. It was therefore proposed that a shorter chain length may facilitate intermediate mixing, an important in endosomal escape (Felgner et al. 1994: 2550-2561).

The structure of cationic lipids is readily amenable to chemical modification, allowing attachment of other functional groups like PEG (Maruyama et al. 1997: 177-180; Song et al. 2002: 1-13; Rejimen et al. 2004: 41-52), thus conveying so-called stealth properties to cationic vectors, which precludes their rapid elimination from the blood circulation by macrophages, upon injection *in vivo* (Woodle 1998: 139-152). By attachment of sugar residues, sugar-linked biosurfactants have been prepared, thereby providing targeting properties to particular cellular receptors, thus promoting

cell type-dependent vector specificity and a potential enhancement of its cellular internalization. Thus inclusion of a sugar-linked biosurfactant into dimethylaminoethane carbamoyl cholesterol (DC-Chol)/DOPE based lipoplexes improved the transfection efficiency of the lipoplex due to an enhancement of cell attachment and subsequent internalization (Igarashi, Hattori and Maitani 2006: 362-368).

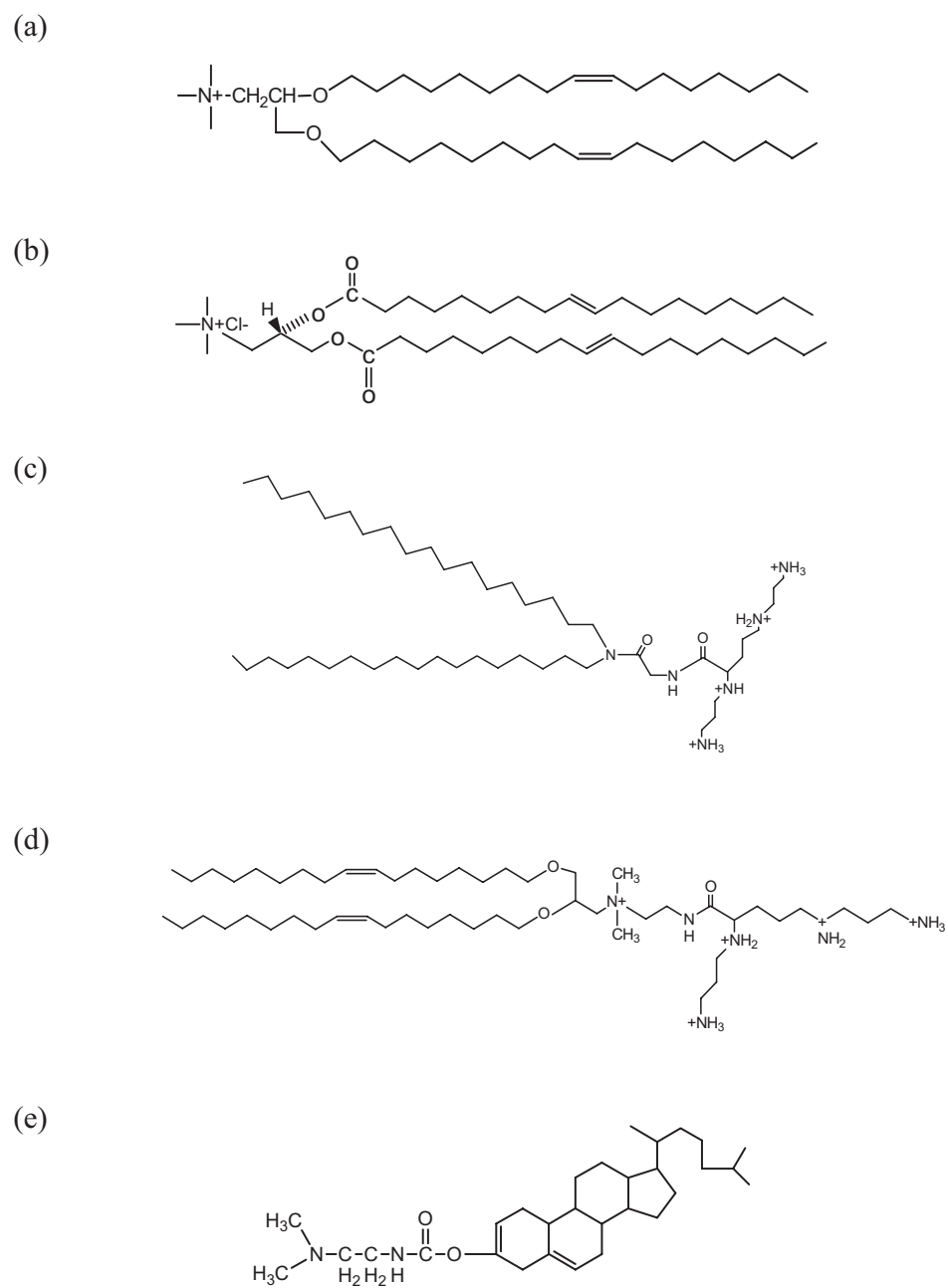


Figure 2 Structure of cationic lipids (a) DOTMA, (b) DOTAP, (c) DOGS (d) DOSPA and (e) DC-Chol.

### 3.2.2 Polyplexes

Cationic polymers form complexes with DNA by electrostatic interaction between positively charged amine groups of polycations and negatively charged phosphate groups of the DNA. Cationic polymer/DNA complexes with positive charge can interact with negative cell surface molecules such as glycoproteins and glycolipids, and enter the cell by endocytosis. Cationic polymers including poly(L-lysine) (PLL) (Toncheva et al. 1998: 354-368), protamine (Maruyama et al. 2004: 3267-3273), polyamidoamine (PAMAM) (Toth et al. 1999: 93-99), polyethylenimine (PEI) (Kichler et al. 2001: 135-144) and chitosan (Li et al. 2003: 7-18) have been investigated for gene delivery. The structure of cationic polymers is shown in Figure 3.

#### 3.2.2.1 Poly(L-lysine) (PLL)

PLL is a biodegradable polymer of lysine amino acid. PLL is synthesized by polymerization of the N-carboxy-anhydride of lysine. PLL is a linear polypeptide with amino acid lysine as the repeat unit; thus, it possesses a biodegradable nature (Zhang et al. 2004: 165-180). PLL has a sufficient number of primary amines with positive charges to interact with negatively charged DNA. PLL/DNA complexes are prone to aggregation under physiological conditions. This drawback was improved by coupling PLL with hydrophilic dextran to increase its solubility. The dextran chains of PLL-graft-dextran do not considerably hinder the electrostatic interaction between PLL and DNA but increase the solubility of the complexes (Maruyama et al. 1998: 292-299; Ferdous et al. 1998: 1400-1405).

In addition to the undesirable effect of aggregation of PLL/DNA complexes, PLL is toxic to the cells. To decrease the cytotoxicity, PLL has been covalently linked to polyethylene glycol (PEG). PLL-graft-polyethylene glycol (PLL-g-PEG) was found to be relatively low toxic to the cells when compared to PLL. In addition, the transfection efficiency of PLL-g-PEG/DNA complexes was higher than that of PLL/DNA complexes (Choi et al. 1998: 39-48). Conjugation of PEG to PLL could stabilize PLL/DNA complexes at neutral charge ratios by shielding their surfaces to prevent aggregation and interaction with serum components. PLL-g-PEG/DNA complexes also had effective gene delivery *in vivo* (Kwoh et al. 1999: 171-190). Coating PLL-g-PEG/DNA complexes with a fusogenic peptide, KALA, could improve the transfection efficiency of PLL/DNA complexes with minimal cellular toxicity (Lee,

Jeong and Park 2002: 283-291). Modification of PLL as dendritic PLL could improve their transfection efficiency by proton sponge effect from highly branch unit of dendritic PLL (Yamagata et al. 2007: 526-532).

### **3.2.2.2 Protamine**

Protamine is a biodegradable protein. It was introduced for gene delivery because the positively charged amino groups of protamine facilitate charge interaction with negatively charged phosphate of DNA. Protamine has low transfection efficiency due to its low density of amine groups. Maruyama et al. (2004: 3267-3273) improved the transfection efficiency of protamine/DNA complexes on HepG2 cells by coating the protamine/DNA complexes with polyethylene glycol having lactose pendant (Lac-PEG-COOH). Lac-PEG-COOH coating reduced surface electrical potential of protamine/DNA complexes and avoided the albumin-induced aggregation. Protamine/DNA/Lac-PEG-COOH complexes had high gene expression on the HepG2 cells and their cytotoxicity was low. Enzymatic digestion of protamine to low molecular weight protamine showed significantly enhanced gene transfer of protamine/DNA complexes, and exhibited a markedly reduced cytotoxicity compared to PEI/DNA complexes (Park et al. 2003: 700-711.). Protamine has been used co-associated with liposome to generate liposome/DNA complexes, and exhibited high levels of transfection activity and resistance to serum protein (Sun and Zhang 2004: 797-805; Faneca, Simoes and Pedroso de Lima 2004: 681-692).

### **3.2.2.3 Polyamidoamine (PAMAM)**

PAMAM dendrimer is a cationic polymer containing amine and amido groups. PAMAM is synthesized by reiterative reaction sequences with methacrylate and ethylenediamine. PAMAM is a class of highly branched spherical polymers. It is also referred as starburst dendrimer. The branched shape is presumed to enhance gene delivery. Terminal amino groups of PAMAM bind DNA by electrostatic interactions. An increase in the level of terminal amino groups has been shown to enhance gene delivery (Toth et al. 1999: 93-99). The advantage of highly branched spherical shape is that the DNA be able to interact with the surface primary amines, leaving the internal tertiary amines available for neutralization of the acid pH within the endosomal compartment. The release of PAMAM/DNA complexes by endosome has

been attributed to the protonation of the internal tertiary nitrogens by endosomal protons which results in a swelling of the endosome and release the DNA to the cytoplasm (Tang, Redemann and Szoka 1996: 703-714).

PAMAM produces high transfection efficiency; however, its toxicity is also significant (Hill et al. 1999: 161-174). Conjugation of PAMAM with L-arginine (Arg) could enhance the transfection efficiency of plasmid DNA compared to native PAMAM, PEI and Lipofectamine. It is presumed that the increased gene expression might be due to the cell penetrating activity during uptake or nuclear localizing efficiency after entry into the cytosol of the affluent arginine residues oriented on the surface of PAMAM-Arg/DNA complexes (Choi et al. 2004: 445-456; Kim et al. 2006: 110-117).

#### **3.2.2.4 Polyethylenimine (PEI)**

PEI is a cationic polymer available in branched and linear forms. PEI is synthesized by polymerization of aziridine. PEI is composed of about 25% primary amines, 50% secondary amines and 25% tertiary amines. PEI has high charge density due to every third atom on the PEI backbone which is amino nitrogen capable of being protonated. In linear PEI, all of these nitrogen atoms are protonable, whereas in branched PEI, only two-thirds of them can be charged (Garnett et al. 1999: 147-207). At the pH 7, about 17% of amines in PEI will be protonated, whereas at pH 5, about 45% of the nitrogens are protonated (Suh et al. 1994: 318-327). This knowledge led to the hypothesis that molecules with unprotonated functional groups may inherently buffer endosomes. PEI is considered to be one of the most effective cationic polymers for gene delivery. In the presence of PEI in endosome, the accumulation of protons brought in by the endosomal ATPase coupled to an influx of chloride anion. This results in a large increase in the proton concentration within the endosome, resulting in osmotic swelling of endosome. Therefore, PEI enhances intracellular trafficking by buffering the endosomal compartments, thus protect the DNA from lysosomal degradation by endosomal DNA release via lysosomal disruption, leading to high transfection efficiency (Kichler et al. 2001: 135-144).

PEI has been shown to effectively condense plasmid DNA into colloidal particles that effectively transfect plasmid DNA into a variety of cells both *in vitro*. PEI/DNA complexes are prone to aggregation and are toxic to the cells.

PEGylation of PEI/DNA complexes have been found to enhance the water solubility and reduce the toxicity of PEI/DNA complexes (Ogris et al. 1999: 595-605). Inclusion of cyclodextrins to PEI could enhance the cellular uptake of plasmid DNA in PEI-cyclodextrin/DNA complexes and decrease the cytotoxicity of PEI (Forrest, Gabrielson and Pack 2005: 416-423; Yamashita et al. 2006: 297-302). Acetylation of PEI with acetic anhydride could enhance the gene transfection of acetylated PEI/DNA complexes due to acetylated PEI are more easily dissociated into free polymer and DNA. The toxicity of acetylated PEI was also lower than unmodified PEI (Gabrielson and Pack 2006: 2427-2435).

PEI has been shown to be effective in various *in vivo* transfection studies. PEI/nerve growth factor cDNA complexes have been transferred to rat dorsal root ganglion through lumbar intrathecal injection and improved regeneration of transected rat sciatic nerves (Wang et al. 2005: 314-320). Biodistribution and tissue expression of PEI/DNA complexes have been found to be dependant on the structure and the molecular weight of PEI and the N/P ratio of PEI/DNA complexes. Linear PEI had high level of plasmid expression efficiency in lung, whereas branched PEI was beneficial in kidney and spleen (Jeong et al. 2007: 118-125).

### 3.2.2.5 Chitosan

Chitosan is a non toxic biodegradable polysaccharide derived by deacetylation of natural polymer chitin. Chitosan is composed of D-glucosamine and *N*-acetyl-D-glucosamine glucosamine units, linked by  $\beta$  (1,4) glycosidic bond. Chitosan comprises a series of polymers varying in their degree of deacetylation, molecular weight and viscosity. The presence of a number of amino groups permits chitosan to chemically react with anionic systems, thereby resulting in alteration of physicochemical characteristics of such combinations.

Chitosan was first introduced as a delivery system for DNA by Mumper et al. (1995). Chitosan/DNA complexes can be formed by electrostatic interaction between positively charged amine of chitosan and negatively charged phosphate of DNA. The amine groups of chitosan are predominantly in primary amine form which is able to neutralize the proton within the endosome, resulting in enhancing the transfection efficiency. Formulation variables such as MW and degree of deacetylation of chitosan, the N/P ratio of chitosan/DNA complexes, and pH of

transfection medium were found to affect the physicochemical properties and transfection efficiency of chitosan/DNA complexes (Sato, Ishii, and Okahata 2001: 2075-2080; Rómoren et al. 2003: 115-127; Kiang et al. 2004: 5293-5301; Lavertu et al. 2006: 4815-4824).

The physicochemical properties of chitosan/DNA complexes have been investigated by several techniques including ethidium bromide fluorescence assay, gel retardation, atomic force microscopy, and dynamic and electrophoretic light scattering. Liu et al. (2005: 2705-2711) reported that the binding affinity of chitosan to DNA depended on the pH of medium. The morphology of chitosan/DNA complexes depended on the charge ratios. The strong interaction between chitosan and DNA might stem from the strong compact of DNA caused by highly charged chitosan. By using ethidium bromide fluorescence assay and gel retardation, Strand et al. (2005: 3357-3366) found that the charge density of chitosan and the number of charges per chain is the dominating factors for the structure and stability of chitosan/DNA complexes.

Several cell lines such as African green monkey (COS-1), human osteosarcoma (MG63) and human embryonic kidney (HEK293) cells (Maclaughlin et al. 1998: 259-272; Corsi et al. 2003: 1255-1264) have been transfected with chitosan/DNA complexes. The transfection efficiency of chitosan/DNA complexes is cell type-dependent. To obtain high level of transfection, a fine balance needs to be achieved between extracellular DNA protection which is better with high MW chitosan, and efficient intracellular dissociation which is better with low MW chitosan (Köping-Höggård et al. 2004: 1441-1452). Chitosan has shown the promise in delivery of plasmid DNA encoding reporter genes such as pSV $\beta$ -gal (Gao et al. 2005: 327-334) and pRSV- $\alpha$ 3 Luc (Thanou et al. 2002: 153-159), and therapeutic genes such as IFN- $\gamma$  cDNA (Kumar et al. 2003: 3) and pCXWN-hIL-2 (Özgel and Akbuğa 2006: 44-51).

Chitosan has been investigated for *in vivo* studies. Chitosan nanoparticles formulated with high MW chitosan and pCMVArah2 plasmid DNA encoding for a major peanut allergen elicited secretory IgA and serum IgG2a production in mice after oral administration. Challenge tests showed less severe and delayed anaphylactic responses in sensitized mice immunized with chitosan/ pCMVArah2 than non-treated mice (Roy et al. 1999: 387-391). Chitosan-graft-PEG/DNA complexes have been delivered to rat liver through bile duct and portal vein infusions. The transfection efficiency of chitosan-graft-PEG/DNA complexes in the liver was three times higher

than that of chitosan/DNA complexes. Grafting of PEG to chitosan could prevent the DNA from the degradation in serum and bile, and reduce acute liver toxicity toward chitosan/DNA complexes (Jiang et al. 2006: 477-487). Chitosan/DNA complexes have been delivered to mouse lung by intratracheal administration. Chitosan/DNA complexes were less efficient gene expression than PEI/DNA complexes, but comparable to DOTMA/DNA complexes (Köping-Höggård et al. 2001: 1108-1121). The cytotoxicity of chitosan/DNA complexes was low compared to other cationic complexes (Lee et al. 2001: 427-431; Thanou et al. 2002: 153-159; Corsi et al. 2003: 1255-1264; Özgel and Akbuğa 2006: 44-51). Chitosan in gene therapy are summarized in Table 1.

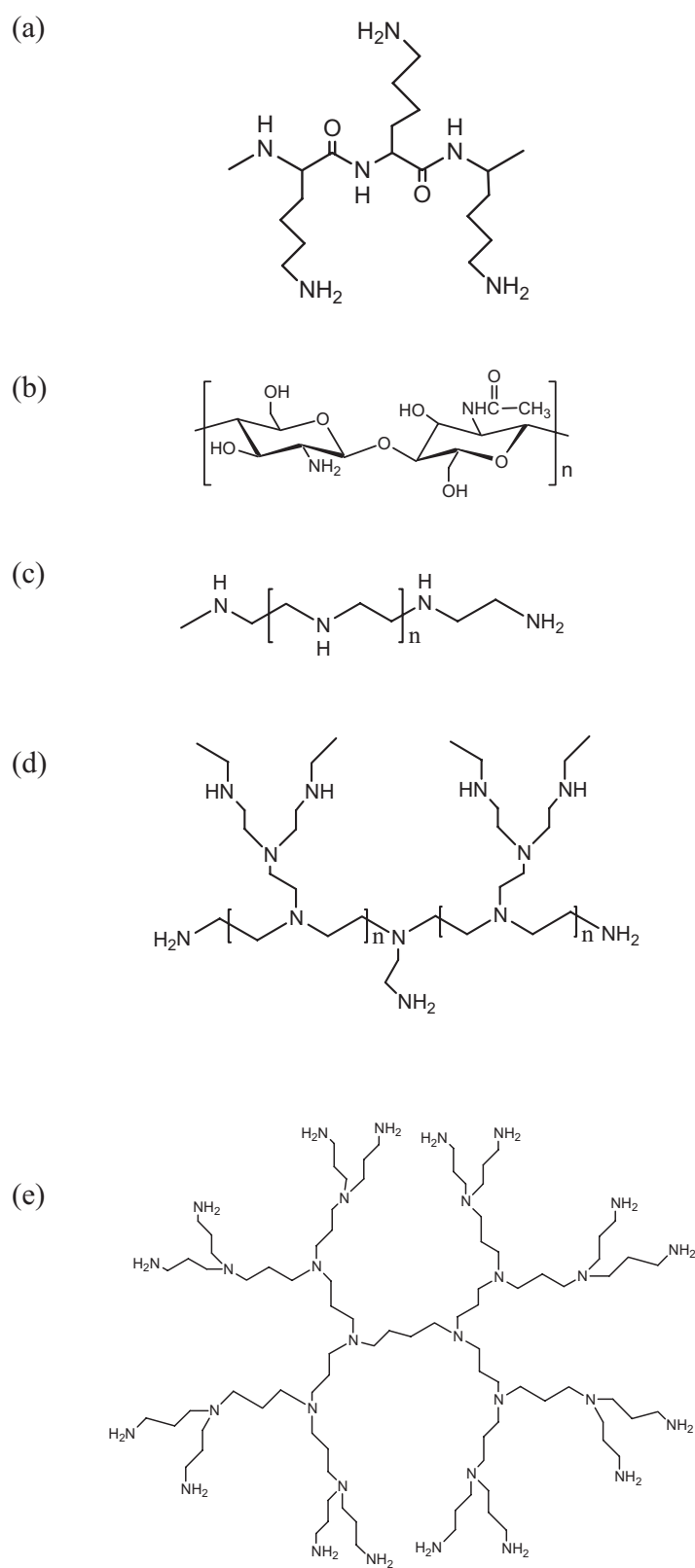


Figure 3 Structure of cationic polymers (a) PLL, (b) chitosan (c) linear PEI (d) branched PEI and (e) PAMAM.

Table 1 Chitosan in gene therapy.

Vector	Plasmid DNA	Protein expressed	<i>In vitro/ in vivo</i>	Result/effect	Reference
<b>Formulation variable study</b>					
Chitosan/ depolymerized chitosan	pCMV-Luc	Luciferase	COS-1	Chitosan MW and particle size of chitosan/DNA complex affected transfection efficiency.	MacLaughlin et al. (1998)
Chitosan hydrochloride (MW 15, 52, 100 kDa)	pGL3	Luciferase	A549 B16 HeLa	pH of medium, N/P ratio, amount of DNA, chitosan MW and cell type affected transfection efficiency.	Sato, Ishii and Okahata (2001)
Chitosan (MW 6.6, 90, 160 kDa; DDA 85, 68, 75%)	pcDNA3-Luc	Luciferase	EPC	N/P ratio, amount of DNA, chitosan MW and DDA affected transfection efficiency.	Romóren et al. (2003)
Chitosan glutamate (MW 150 kDa; DDA 75%)	pGL3	Luciferase	CHO-K1 293	Chitosan/DNA nanoparticle had a sustained expression.	Li et al. (2003)
Chitosan (MW 15, 52, 100 kDa)	pVR1412	$\beta$ -galactosidase	MG63 MSCs HEK293	Cell type affected transfection efficiency.	Corsi et al. (2003)
Chitosan oligomer (DP10-14, 18, 15-21, 22-35, 36-50)	pCMV-Luc	Luciferase	BALB/c mice	Low MW chitosan dissociated more easily than those of high MW chitosan.	Köping-Höggård et al. (2004)
Chitosan (MW 390 kDa; DDA 90, 61, 70%)	pcDNA-CMV-Luc	Luciferase	HEK293 HeLa SW756 BALB/c mice	Decrease in chitosan DDA decreased in transfection efficiency <i>in vitro</i> . Decrease in DDA increased in transfection efficiency <i>in vivo</i> .	Kiang et al. (2004)
Chitosan (MW 213, 98, 48, 17, 10 kDa; DDA 46, 61, 88%)	pEGFP-C2	Green fluorescent protein	A549	Cellular uptake reduced by decreasing of chitosan MW and DDA. Transfection efficiency was correlated with cellular uptake and zeta potential of chitosan/DNA nanoparticle.	Huang et al. (2005)
Chitosan (MW 150, 80, 40, 10 kDa; DDA 72, 80, 92, 98%)	pEGFPLuc	Green fluorescent protein; luciferase	HEK293	Maximum expression was obtained a certain combination with DDA and MW that depended on N/P ratio and pH.	Lavertu et al. (2006)
Chitosan (MW 6, 46, 85, 200, 300, 899 kDa; DDA 80, 85, 88%)	pEGFP	Green fluorescent protein	Primary chondrocyte	Transfection efficiency depended on pH, chitosan MW and amount of DNA.	Zhao et al. (2006)
Chitosan (spraydried chitosan post-mixed with lactose-lipid-polycation)	pEGFP-N1	Green fluorescent protein	A549	Chitosan mediated lactose-lipid-polycation-pDNA (LPD) enhanced level of gene expression.	Li and Birchall (2006)

MW = molecular weight  
DDA = degree of deacetylation

Table 1 Chitosan in gene therapy (continued).

Vector	Plasmid DNA	Protein expressed	<i>In vitro/ in vivo</i>	Result/effect	Reference
<b>Modification of chitosan chemistry</b>					
Deoxycholic acid-chitosan	pCMV-CAT	Chloramphenicol acetyl transferase	COS-1	Hydrophobically modified chitosan with deoxycholic acid had efficient transfection efficiency.	Lee et al. (1998)
Trimethylated chitosan oligomer	pRsv- $\alpha$ -Luc	Luciferase	COS-1 CaCo2	Trimethylated had higher transfection efficiency than chitosan oligomer. Transfection efficiency depended on the cell type.	Thanou et al. (2002)
Urocanic acid-chitosan	pGL3	Luciferase	293T	Transfection efficiency could be enhanced by urocanic acid- chitosan. Transfection efficiency increased with an increase of urocanic acid content.	Kim et al. (2003)
5 $\beta$ -cholanic acid-glycol chitosan	pCMV-Luc	Luciferase	COS-1	Hydrophobically modified glycol chitosan enhanced transfection efficiency <i>in vitro</i> and <i>in vivo</i> .	Yoo et al. (2005)
Deoxycholic acid-chitosan	pEGFP-N1	Green fluorescent protein	HEK293	Hydrophobically modified chitosan with deoxycholic acid affected Transfection efficiency. At MW 1-3 kDa, deoxycholic acid-chitosan had higher transfection efficiency than chitosan. At MW 3-10 kDa, deoxycholic acid-chitosan had lower transfection efficiency than chitosan.	Chae et al. (2005)
6-amino-6-deoxy-chitosan	pGL3	Luciferase	COS-1	6-amino-6-deoxy-chitosan had superior transfection efficiency to chitosan.	Satoh et al. (2006)
Stearic acid grafted chitosan oligosaccharide	pEGFP-C1	Green fluorescent protein	A549	Stearic acid grafted chitosan oligosaccharide form micelle like structure by self aggregation in aqueous solution. Optimal transfection efficiency of stearic acid grafted chitosan oligosaccharide micelle was higher than that of chitosan oligosaccharide.	Hu et al. (2006)
<b>Combination with other vectors</b>					
Galactosylated chitosan + PEI	pEGFP-N1	Green fluorescent protein	HepG2	PEI increased transfection efficiency of galactosylated chitosan targeted to HepG2.	Kim et al. (2005)
<b>Delivery of therapeutic DNA</b>					
Chitosan (MW 200, 400 kDa; DDA 87%)	pCXWN-hIL-2	Interleukin-2	MAT-LyLu	High level of interleukin-2 expression obtained with plasmid-loaded chitosan microspheres. Chitosan 200 kDa had higher interleukin-2 expression than chitosan 400 kDa.	Akbuğa et al. (2004)
Chitosan (MW 150 kDa; DDA 75-85%)	pCXWN-hIL-2	Interleukin-2	3T3 HeLa	Transfection efficiency of chitisan/ DNA complex was lower than that of PEI/DNA and DOTAP/DNA complexes.	Özgel and Akbuğa et al. (2006)

MW = molecular weight  
DDA = degree of deacetylation

Table 1 Chitosan in gene therapy (continued).

Vector	Plasmid DNA	Protein expressed	<i>In vitro/ in vivo</i>	Result/effect	Reference
<b>Delivery of therapeutic DNA (continued)</b>					
Chitosan (MW 390 kDa)	pcDNA3-VP1	Major structural protein of Coxsackievirus B3	BALB/c mice	Chitosan/pcDNA3-VP1 intranasal immunization had 42.9% protection of against lethal Coxsackievirus B3 infection.	Xu et al. (2004)
Chitosan (DDA 85%)	pcDNA3.1-IL-1Ra	Human IL-1Ra	Osteoarthritis rabbit	Expression of IL-1Ra was detected in knee joint synovial fluid of chitosan IL-1Ra-injected group. Severity of cartilage lesions in rabbit treated with chitosan IL-1Ra was significantly reduced.	Zhang et al. (2006)
Chitosan-gelatin scaffold	pCMV-TGF- $\beta$ 1	Transforming growth factor	Primary chondrocytes	Gene transfected into chondrocytes expressed TGF- $\beta$ 1 protein stably in 3 weeks. Primary chondrocytes cultured in chitosan gelatin scaffold had high secretion of extracellular matrix.	Guo et al. (2006)
Chitosan (low viscosity)	PEDF	PEDF (antiangiogenic factor)	BALB/c mice	Chitosan/PEDF resulted in a decrease in primary tumor growth, reduced bone lysis and reduced lung metastases in mice.	Dass et al. (2007)
<b>Cell specific targeting</b>					
Galactose-conjugated trimethylated chitosan	pSV- $\beta$ -gal	$\beta$ -galactosidase	HepG2	Galactose-trimethylated chitosan had efficient cell selective to HepG2 cells. The transfection efficiency of galactose-trimethylated chitosan was higher than that of trimethylated chitosan.	Murata, Ohya and Ouchi (1997)
Galactosylated chitosan (low, high MW)	pSV- $\beta$ -gal	$\beta$ -galactosidase	HepG2	Galactosylated low MW chitosan/DNA complex had lower cytotoxicity than galactosylated high MW chitosan/DNA complex and had efficient cell selective to hepatocyte.	Gao et al. (2003)
Lactosylated chitosan	pGL3-Luc	Luciferase	HepG2	Lactosylated chitosan/DNA complex had efficient cell selective to HepG2 cells. The transfection efficiency of lactosylated chitosan/DNA complex was greater than that of chitosan/DNA complex.	Hasimoto et al. (2006)
<b>Tissue and organ delivery</b>					
Trisaccharide-substituted chitosan oligomer	pCMV-Luc	Luciferase	BALB/c mice	24 h after lung administration (intra-tracheal injection) to mice, luciferase gene expression was 4-fold higher with trisaccharide-substituted chitosan than chitosan oligomer.	Mohamed et al. (2006)
PEG-graft-chitosan	pCMV-Luc	Luciferase	Wistar rats	PEG-graft-chitosan/DNA complex had significantly higher gene expression in liver than chitosan/DNA complex.	Jiang et al. (2006)
Chitosan (MW 1400 kDa; DDA 80%)	pnlacF	$\beta$ -galactosidase	Swiss albino mice	Gene expression was observed in histological stomach and small intestine after oral administration of chitosan/DNA microparticle.	Guliyeva et al. (2006)

MW = molecular weight  
DDA = degree of deacetylation

In addition to chemical and viral gene transfer techniques, several methodologies utilizing physical or mechanical means for translocating genes into cells have been developed. Such techniques have the advantage of avoiding the introduction of foreign substances, i.e., chemicals or viruses, into the target cells or tissues and therefore offer a safe alternative approach to gene delivery.

#### **4. Physical gene delivery methods**

The methods include microinjection, particle bombardment, and electroporation.

##### **4.1. Microinjection**

The most direct method to introduce DNA into cells is microinjection. It entails the direct injection of DNA into the cytoplasm or nucleus of target cells. The procedure is conducted on a single cell, using a fine glass needle (microcapillary pipette), a precision positioning device, and a microinjector. Extrusion of fluid containing the genetic material through micropipette uses hydrostatic pressure. Injections are typically carried out under direct vision control, using a microscope. The small tip diameters of these micropipettes, combined with the high precision of the micromanipulator, allow for accurate and precise DNA delivery (Mehier-Humbert and Guy 2005: 733-753). Conceptually, this technique is the simplest gene delivery method, but it one of the most difficult to apply. While pronuclear injection of DNA is very efficient, it is a laborious procedure; only one cell at a time can be injected, typically allowing for only a few hundred cells to be transfected per experiment. Some recent advances in this technology utilizing automated systems have promised to increase the speed and decrease the labor required (Genlantis, CA, USA 2006).

##### **4.2 Particle bombardment**

One method for the direct introduction of DNA into various tissues is gene mediated particle bombardment or so called “gene gun”. The technique was first used in 1987 to overcome the inherent difficulty of transgene expression in plant cells. This approach was then extended to mammalian cells and living tissues in the early 1990s (Yang et al. 1990: 9568–9572). To date, however, few clinical trials using the gene gun have been reported. DNA delivery utilizes heavy metal particles propelled at a sufficient velocity into the target cell. Acceleration is achieved by a high-voltage electric spark, or

a helium discharge. The particles must be non-toxic, non-reactive and smaller than the diameter of target cell. Naked DNA can be precipitated onto these microparticles, and gradually released within the cell post-bombardment. The major application of this technology is genetic immunization (Mehier-Humbert and Guy 2005: 733-753).

### 4.3 Electroporation

A common physical tool to introduce DNA into cells is an electric field. This technique exposes the cell membrane to high-intensity electrical pulses that can cause transient and localized destabilization of the barrier. During this perturbation, the pores in the cell membrane are temporarily opened. This allows exogenous DNA to pass through the pores and into the cytoplasm of the cells. The transient increase in permeability is believed to result from the creation of electric field-induced pores. Using freeze-fracture electron microscope, the size of these membrane openings was shown to be between 20 and 120 nm in red blood cells (Chang 1992: 9-27). Electroporation has been extensively used for the transfection *in vitro* and *in vivo*. This technology has now been applied to a variety of tissues including muscles, skin, liver, lung, artery, kidney, retina, cornea, spinal cord, brain, and tumors. The efficiency of gene transfer by electroporation is influenced by several factors. The morphology of cells can affect the applied voltage required to porate the membrane. The smaller cells are less likely to be porated and the large size of cells, the lower the field strength is required for poration to occur (Neuman et al. 1996: 868-877). It has also been suggested that in asymmetric cells (e.g., muscle cells and dendritic cells), the acute membrane curvature associated with processes or the ends of muscle fibers can also influence the required field strength for poration (Somari et al. 2000: 178-187). Viscosity of extracellular fluid also influences electroporation. The increase in viscosity of the media in which cells are grown results in decreased electroporation efficiencies (Klenchin et al. 1991: 804-811). Another factor thought to affect electroporation efficiency is the presence of divalent cations. When  $\text{Ca}^{2+}$  ions are delivered by electroporation before or after DNA administration, the transgene expression is reduced, probably because they abolish the electrostatic interactions between electrical field and DNA molecules (Zhao et al. 2006: 307-310).

## 5. Plasmid DNA

It is virtually impossible to take small pieces of DNA and insert them into normal cells so that they will direct the production of protein products. DNA does not enter a cell easily. Linear pieces of DNA are rapidly destroyed in the cells. Even the DNA could get into the cells intact, it will not necessarily contain the proper signals for transcription, translation and replication. The DNA might not be used by the cell transcription, translation and replication systems. However, if the genes are incorporated within other DNA molecules that can exist within the cells, they could then be safely introduced into the cells. Such a carrier DNA is called a vector. DNA vectors are used to carry genes of interest. There are many types of vectors such as plasmid, cosmid and bacteriophage, but most common type is a plasmid (Bourgaize, Jewell and Buiser 2000: 138-169).

Plasmids are circular pieces of DNA, found in many different kinds of microorganisms that are replicated by the cells but exist separate from the chromosomes of the organism. Most commonly vector used to carry DNA is from *Escherichia coli*. Plasmid contains a DNA sequence that serves as an origin of replication (*ori*), which enables the plasmid to be duplicated independently from the chromosomal DNA. Thus, any DNA inserted into a plasmid will be replicated along with the plasmid DNA. Plasmid can be digested with a restriction enzyme that can cut it at a single site converting it from a circular molecule into a linear molecule with sticky ends. The foreign DNA can also be digested with the restriction enzyme to produce the same sticky ends. When the plasmid and the foreign DNA are mixed, molecules of plasmid become joined to molecules of foreign DNA via their common sticky ends and circular recombinant plasmids are obtained. DNA ligase is then used to covalently join the two. By using a plasmid vector to carry gene of interest, the difficulties of replication and degradation of linear DNA molecules can be overcome. The technology is called recombinant DNA technology (Bourgaize, Jewell and Buiser 2000: 138-169; Winter, Hickey and Fletcher 2002: 255-294).

A plasmid DNA containing a reporter gene can be introduced into cultured animal cells. This process is called transfection. The cultured animal cells must be treated to facilitate their uptake of the plasmid DNA. This can be done by exposing cells to viral or non viral gene delivery vectors, or physical gene delivery methods. Usually, the plasmid DNA is added in sufficient concentration to ensure that a large proportion of the

cultured cells will receive the plasmid DNA. The plasmid DNA also carries an origin of replication derived from a virus that infects mammalian cells. Once such a plasmid DNA enters a mammalian cell, the viral origin of replication allows it to replicate efficiently, generating numerous plasmids from which the protein is expressed (Lodish et al 2004: 378-380). After the plasmid DNA with a reporter gene is delivered to cultured animal cells, the gene expression can be obtained by measuring the product of the reporter gene after gene transcription and translation. The reporter genes that have been used in gene delivery are the genes encoding  $\beta$ -galactosidase (Buttgereit et al. 2000: 1145-1155; Corsi et al. 2003: 1255-1264), chloramphenicol acetyltransferase (CAT) (Lee, K.Y. et al. 1998: 213-220), luciferase (Girão da Cruz, Simões and Pedroso de Lima 2004: 65-75; Gabrielson and Pack 2006: 2427-2435), and green fluorescent protein (GFP) (Zhang, Yadava and J. Hughes 2004: 144-150; Salvati et al. 2005: 21-29). The  $\beta$ -galactosidase activity can be measured using either the substrate X-gal, which turns blue upon cleavage or o-nitrophenyl- $\beta$ -D-galactopyranoside (ONPG), which turns yellow upon reaction. The CAT activity in transfected cells can be measured by mixing the cell extract with radioactive chloramphenicol and an acetyl donor (acetylCoA). Thin layer chromatography is used to separate chloramphenicol from its acetylated products. The concentration of these products is proportional to their CAT activity. The luciferase activity can be determined by mixing the luciferase with luciferase substrate, luciferin. The luciferase converts the luciferin to a chemoluminescent compound that emits light. The light can be detected with a scintillation counter (Weaver 1999: 95-134). The GFP is a protein from the jelly fish *Aequorea victoria* that fluoresces green when exposed to blue light. Upon transfection, the transfected cells can be detected by a fluorescence microscope (Salvati et al. 2005: 21-29). Figure 4 shows the structure of plasmid DNA pSV- $\beta$ -Galactosidase (Promega, Madison, IL, USA 2007) and gWiz<sup>TM</sup> Luc (Aldevron, Fargo, ND, USA 2007).

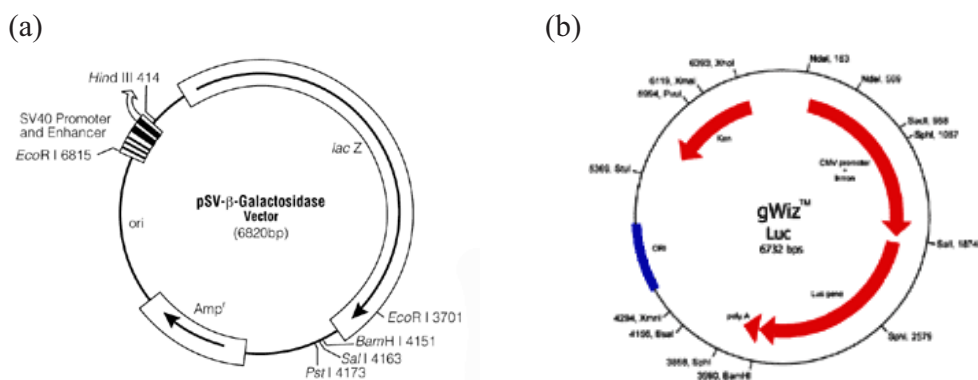


Figure 4 Structure of plasmid DNA (a) pSV-β-Galactosidase (Promega, Madison, IL, USA 2007) and (b) gWiz<sup>TM</sup> Luc (Aldevron, Fargo, ND, USA 2007).

## 6. Promoters

Promoter is the sequence of DNA to which RNA polymerase binds to initiate RNA synthesis. As the RNA strand being synthesized, the RNA strand grows in the 5' to 3' direction, and the template strand is read in the 3' to 5' direction. The numbers to the base pairs in the promoter region are assigned to indicate their positions relative to the site of transcription initiation (Figure 5). The transcription initiation site is assigned to the number +1. Base pairs preceding this site are given negative numbers and are not transcribed. Base pairs following the initiation site are given positive numbers. Proceeding toward the 5'-end of the coding strand is termed moving upstream; the opposite direction is downstream (Bolsover et al. 1997 148-151; Stenesh 1998: 454-455).

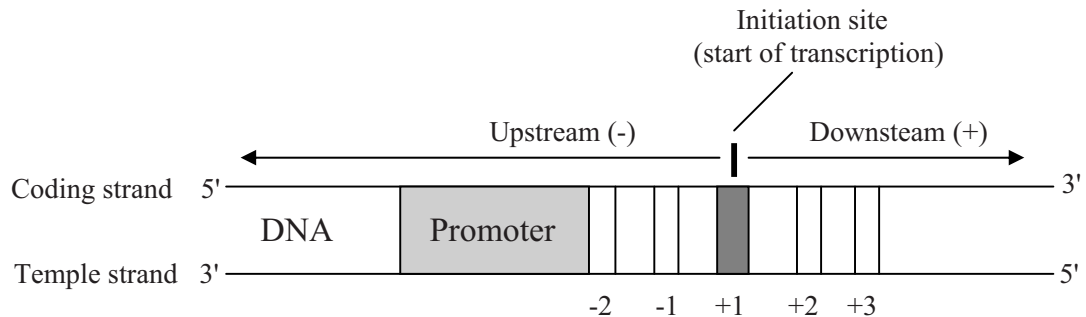


Figure 5 Numbering of a DNA sequence (Stenesch 1998: 454).

The transcription involves four discrete stages: promoter recognition, chain initiation, chain elongation, and chain termination. To start transcription, RNA polymerase binds to the promoter sequence to form the closed promoter complex. After the initial binding step, the RNA polymerase melts the DNA double helix, causing the strand that is to be transcribed to separate strand and become accessible to the polymerase. An open promoter complex develops when the two strands of DNA unwind enabling one strand to act as the template for the synthesis of an RNA molecule. The RNA polymerase then initiates RNA synthesis at a nearby transcription start site (number +1, Figure). The first nucleoside triphosphate is placed at this site, and synthesis proceeds in the 5' to 3' direction. RNA polymerase moves progressively along the transcribed DNA strand, adding nucleotides to the growing RNA chain. When RNA polymerase reaches a chain-termination sequence, both the newly synthesized RNA molecule and polymerase are released. Initiation of a second round of transcription need not await completion of the first round, because the promoter becomes available once RNA polymerase has polymerized from 50 to 60 nucleotides (Bolsover et al 1997: 148; Hartl and Jones 2000:452-455).

A promoter consists of consensus sequences in its sequence. Each nucleotide in the consensus sequence is the nucleotide most often observed at that position in actual sequence. Most promoters differ from a consensus sequence by at most one or two nucleotides. Both prokaryotic and eukaryotic promoters usually contain two consensus sequences (Figure 6). In prokaryotes, these sequences occur at about -10 and -35 and are named the -10 region (Pribnow box) and the -35 region, respectively. In eukaryotes,

consensus sequences occur at about -25 and -75 and are named the -25 region (TATA box or Hogness box) and the -75 region (CAAT box), respectively (Stenesh 1998: 454-455).

The strength of the binding of RNA polymerase of different promoters varies greatly, which causes differences in the extent of expression from one gene to another. Most of the differences in promoter strength result from variations in the consensus sequence and the space between them. In general the more closely the promoter elements resemble the consensus sequence, the stronger the promoter. Mutations that change the nucleotide sequence in a promoter can alter the strength of the promoter. Mutations that destroy matches with the consensus sequences tend to be down mutations. That is, they make the promoter weaker, resulting in less transcription. Mutations that make the promoter sequences more like the consensus sequences are called up mutations. That usually makes the promoters stronger (Weaver 1999: 141-145; Hartl and Jones 2000:452-455; Jewis 2003: 193-194).

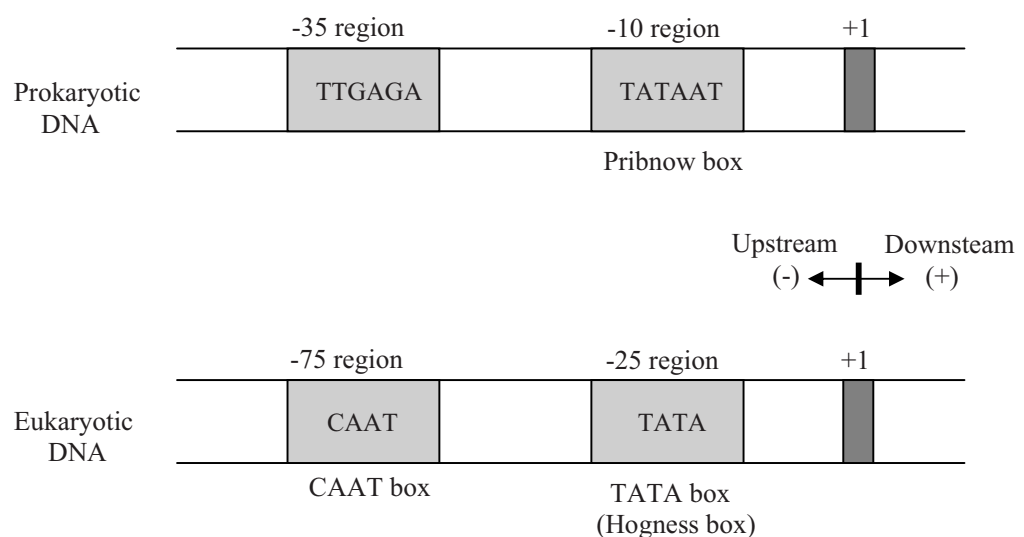


Figure 6 Consensus sequences in the promoter regions of prokaryotic and eukaryotic DNA (Stenesh 1998: 455).

## 7. Cell culture

There are two types of gene therapy: somatic cell or nonheritable gene therapy, germ line or heritable gene therapy. In higher animals such as humans, the reproductive or germ line cells are produced by a cell lineage separate from all somatic cell lineages. Thus, somatic cell gene therapy will treat the disease symptoms of the individual but not cure the disease. That is, the defective genes will still be present in the germ line cells of the patient after somatic cell gene therapy and may be transmitted to the next generation. All of the gene therapy treatments of human diseases are currently somatic cell gene therapy. Germ line gene therapy is being performed on mice and other animals, but not on humans (Snustud and Simmons 2006: 492-523).

Cell cultures used in the development of gene delivery are achieved from various mammalian cells such as ovary, fibroblast, lymphoma and epitheloid cells. Table 2 shows the examples of cell lines used for gene delivery. The type of cells or tissue to which genes will be transferred is a parameter considered when selecting a gene delivery vector. For a number of different reasons, the difficulty of cellular gene delivery varies from cell type to cell type. Because of this, it is important to review the literature to determine if cell type of interest has previously been utilized for gene transfer experiments, which exact methods have been used, and what delivery efficiencies were achieved, i.e., what percentage of cells actually transfected or transduced, with each method. Certain cell types often described as difficult to transfect include various kinds of lymphoma cells and primary cell cultures of many varieties. Successful gene transfer to certain cells usually requires an optimization of transfection condition (Genlantis, CA, USA 2006; Buttgereit et al. 2000: 1145-1155).

Table 2 Examples of cell lines used for gene delivery study.

Cell line	Source	Reference
A549	human lung carcinoma	Seville, Kellaway and Birchall (2002) Smrekar, B. et al. (2003)
B	human lymphoma	Buttgereit et al. (2000)
C6	rat glioma	Congiu et al. (2004) da Cruz, Simões and de Lima (2004)
CaCo2	human colon carcinoma epithelial	Thanou et al. (2002) Schmitz et al. (2007)
CHO	Chinese hamster ovary	Vanderbyl, Macdonald and de Jong (2001) Salvati et al. (2005)
COS-1	monkey kidney fibroblast	Fominaya, Uherek and Wels (1998) Matsuura et al. (2003)
HEK293	human embryonic kidney	Corsi et al. (2003) Forrest, Gabrielson and Pack (2005)
HeLa	human cervix epitheloid carcinoma	Song et al. (2002) Kilk et al. (2005)
HepG2	human hepatocarcinoma	Song et al. (2002) Lee et al. (2003)
HuH-7	human hepatoma	Bandyopadhyay et al. (1998) Mady et al. (2004)
KB	human oral epidermoid carcinoma	Mislick et al. (1995) Smrekar et al. (2003)
K562	human chronic myelogenous leukemia	Li et al. (2003) Schakowski et al. (2004)
MG63	human osteosarcoma	Corsi et al. (2003) Liang et al. (2006)
Neuro2A	mouse neuroblastoma	Kircheis et al. (2002) Walker et al. (2005)
SMC	rabbit smooth muscle	Lampela et al. (2002) Appleby et al. (2003)

## 8. Measurement of intracellular protein

Protein is a major content of cellular macromolecules. The amount of protein in the cell culture can be determined by the measurement of protein concentration in solutions. Following is the assays that can be used to determine the protein concentration.

### 8.1 Biuret protein assay

The Biuret reaction involves a reagent containing copper (cupric ions) in alkaline solution. When substances containing two or more peptide bonds react with the Biuret reagent, alkaline copper sulfate, a purple complex is formed with maximum absorbance of 540 nm. The colored product is the result of coordination of peptide nitrogen atoms with cupric ions ( $\text{Cu}^{2+}$ ). The purple color of the complex can be measured independently of the blue color of the Biuret reagent itself with a spectrophotometer or colorimeter. Using the Biuret assay to determine protein concentration in an unknown sample requires construction of a standard curve made by assaying a series of a standard protein solution with known concentrations. The best protein to use as a standard is a purified preparation of the protein to be assayed. Since this is rarely available, another protein, bovine serum albumin (BSA), is used as a relative standard. BSA provides a similar color yield. BSA is also widely available and low price. The protein concentration is determined from the standard curve. Few substances interfere with the Biuret assay. There is abnormal color development with amino acid buffers and Tris buffer. The Biuret assay has several advantages including speed, similar color development with different proteins, and few interfering substances. The disadvantage of this assay is the lack of sensitivity (Peterson 1983: 95; Boyer 1993: 51-58).

### 8.2 Lowry protein assay

The Lowry protein assay is one of the most sensitive and, hence, widely used. The Lowry procedure can detect protein levels as low as 5  $\mu\text{g}$ . The principle of this assay is identical to that of the Biuret assay except that a second reagent (Folin-Ciocalteu) is added to increase the amount of color development. The principle of the Lowry method lies in the reactivity of the peptide nitrogen with the cupric ions ( $\text{Cu}^{2+}$ ) under alkaline conditions (Biuret reaction) and the subsequent reduction of the Folin-Ciocalteu reagent (phosphomolybdate-phosphotungstate) to heteropolymolybdenum blue by the copper-catalyzed oxidation of tyrosine and tryptophan in the protein. The

heteropolymolybdenum blue is detectable at 750 nm. A standard curve is prepared with BSA or other pure protein, and the concentration of unknown protein solutions is determined from the graph. The Lowry assay is sensitive to pH changes and therefore the pH of assay solution should be maintained at 10.0-10.5. The advantage of Lowry assay is its sensitivity, which is up to 100 times greater than that of the Biuret assay; however, more time is required for the Lowry assay. The disadvantage of the Lowry assay is their accuracy within narrow pH range. However, very small volumes of sample will have little or no effect on pH of the reaction mixture. A variety of compounds interfere with the Lowry procedure. These include some amino acid derivatives, certain buffers, drugs, lipids, sugars, salts, nucleic acids and sulphhydryl reagents. Ammonium ions, zwitterionic buffers, nonionic buffers, and thiol compounds can also interfere with the Lowry reaction. These substances should be removed or diluted before running Lowry assays (Dunn 1992; Boyer 1993: 51-58; Ausubel 2002: 277-284).

### **8.3 Bradford protein assay**

The Bradford assay is a method to determine the protein concentration based on protein binding of a dye. This assay provides numerous advantages over other methods. The binding of Coomassie Brilliant Blue dye to the positively charged residues of protein in acidic solution causes a shift in wavelength of maximum absorption of the dye from 465 nm to 595 nm. The absorption at 595 nm is directly related to the concentration of protein. A calibration curve is prepared using BSA or bovine plasma gamma globulin as a standard. The assay requires only a single reagent, an acidic solution of Coomassie Brilliant Blue G-250. The reaction is complete in two minutes and the color remains stable up to 1 hours. The sensitivity of the Bradford assay rivals and may surpass that of the Lowry assay. The assay can be used to determine proteins in the range of 1 to 20  $\mu$ g. The interfering substances in the Bradford assay are detergents, Triton X-100 and sodium dodecyl sulfate (SDS). The Bradford assay is recommended for general use, especially for determining protein content of cell fractions and assessing protein concentrations for gel electrophoresis (Bradford 1976: 248-254; Boyer 1993: 51-58; Ausubel 2002: 277-284).

#### 8.4 Bicinchoninic acid (BCA) protein assay

The BCA protein assay is detergent-compatible formulation based on bicinchoninic acid (BCA) for the colorimetric detection and quantitation of total protein. It is a two-step assay, in which cupric ion ( $\text{Cu}^{2+}$ ) is first oxidized to cuprous ion ( $\text{Cu}^+$ ) forming a complex with protein amide bond in an alkaline medium (Biuret reaction). Secondly, bicinchoninic acid forms a purple complex with cuprous ion which is detectable at 562 nm. Samples of unknown proteins and relative standard are treated with the reagent, and the concentrations of protein are determined from a standard curve. This assay has the same sensitivity level as the Lowry and Bradford assays, and is relatively fast with incubating at 37 °C. The advantage of BCA protein assay is that the BCA reagent is fairly stable under alkaline conditions and is usefulness in the presence of 1% detergent such as Triton or sodium dodecyl sulfate (SDS), and the BCA reagent can be included in the copper solution to allow a one step procedure (Stoscheck 1990: 50-69; Boyer 1993: 51-58).

#### 8.5 Spectrophotometric assay

Spectrophotometric assay is the direct measurement of protein concentration. This assay is simple and rapid, since no additional reagents or incubations are required. Most proteins have intense ultraviolet light absorption at 280 nm due to the presence of tyrosine and tryptophan residues in the protein. The relationship of absorbance to protein concentration is linear. Because different proteins have widely varying absorption characteristics, there may be considerable error, especially for unknowns or protein mixtures. Cellular extracts containing many other compounds that absorb in the vicinity of 280 nm will interfere with the assay. Nucleic acids, which would be common contaminants in a protein extract, absorb strongly at 280 nm ( $\lambda_{\text{max}} = 260 \text{ nm}$ ). Although the spectrophotometric assay of proteins is fast, relatively sensitive, and requires only a small sample size, it is used for estimating of protein concentration. The advantage of this assay is that most buffers do not interfere with the assay. The spectrophotometric assay is commonly suited to monitor protein fractions from chromatography columns (Boyer 1993: 51-58; Caprette 2006).

## **9. Morphological examination of cationic vector/DNA complexes**

Cationic vector/DNA complexes can be examined by using transmission electron microscopy (TEM) and atomic force microscopy (AFM).

### **9.1 Transmission electron microscopy (TEM)**

Transmission electron microscopy (TEM) is an image technique whereby a beam of electrons is transmitted through a specimen, then an image is formed, magnified and directed to appear either on a fluorescent screen or layer of photographic film (Wikipedia, FL, USA 2007b). The electron signal is detected after it has passed through the specimen. The TEM consists of four systems: the illuminating system, the image system, the image recording system, and the high vacuum system.

The illuminating system serves to produce the required radiation and direct it onto the specimen. It consists of the electron gun which generates electron and the condenser lens assembly which directs the electron beam onto the sample. The major prerequisite for the filament is that it be composed of a material capable of generating an intense beam of electrons. Most microscopes meet these requirements by using a V-shaped tungsten wire, which can be electrically heated to incandescence. Another component of illuminating system is the condenser lens assembly. It serves the dual function of demagnifying the electron beam and focusing it onto the sample (Gabriel 1982: 1-12).

The second system of TEM is the image system. It composed of a series of electromagnetic lenses that produce the final magnified image of the specimen. These are the objective, intermediate, and projector lenses. The objective lens forms the initial enlarged image of illuminated portion of the specimen in a plane that is suitable for further magnification by intermediate lens. The intermediate lens magnifies a portion of the image emerging from the objective lens and directs it toward the projector lens. The projector lens enlarges a portion of the intermediate image and projects it onto the observation screen (Gabriel 1982: 1-12).

The image recording system converts the electron image observed on a fluorescent screen into a permanent record or electron micrograph. The observation screen and photographic film comprise the image record system. Because electrons are invisible to human eye, the screen and film essentially translate that signal into light. Fluorescent screens coated with a layer of zinc and cadmium sulfides are used for localization, focusing, and observation of the image (Gabriel 1982: 1-12).

The final system of the TEM is the high vacuum system. It is used to reduce the amount of gases within the microscope which would otherwise degrade resolution by interacting with the electron beam. Gas can interact with the electrons and scatter them randomly, giving rise to reduced contrast and noise. The ionization of gas molecules can cause random electrical discharges and fluctuations in the beam. Residual gases can react with the heated filament, eroding it, and gases also can contaminate the sample (Gabriel 1982: 1-12).

## **9.2 Atomic force microscope (AFM)**

Atomic force microscope (AFM) is a very high resolution type of scanning probe microscope with resolution of fractions of a nanometer. AFM utilizes a sharp probe moving over the surface of a sample in a raster scan. The probe of AFM is a tip on the end of a cantilever which bends in response to the force between the tip and the sample. The cantilever is moved by a mechanical scanner over the surface to be observed. Every variation of the surface height varies the force acting on the tip and therefore varies the bending of the cantilever. This bending is measured by an integrated stress sensor at the base of the cantilever spring and recorded line by line in the electronic memory. As the cantilever flexes, the light from the laser is reflected onto the split photo-diode. By measuring the different signals, changes in the bending of the cantilever can be measured (Hidber and Tonin 2007, Wikipedia, FL, USA 2007a; Carberry 2007).

The constant height of a scanned tip may have a risk that the tip would collide with the sample surface, causing damage. Therefore, in most cases a feedback mechanism is employed to adjust the tip-to-sample distance to maintain a constant force between the tip and sample. Traditionally, the sample is mounted on a piezoelectric tube that can move the sample in the z direction for maintaining a constant force, and the x and y directions for scanning the sample. Alternatively, a tripod configuration of three piezo crystals may be employed with each responsible for scanning in the x, y and z directions. This eliminates some of the distortion effects from a tube scanner (Wikipedia, FL, USA 2007a).

The way in which image is obtained can be achieved in many ways. The three main classes of interaction are contact mode, tapping mode and non-contact mode. Contact mode is the most common method of operation of the AFM. The tip and sample remain in close contact as the scanning proceeds. One of the drawbacks of remaining in

contact with the sample is that there exist large lateral forces on the sample as the drip is dragged over the specimen. Tapping mode is also the most common mode used in AFM. When the AFM is operated in air or other gases, the cantilever is oscillated at its resonant frequency and positioned above the surface so that it only taps the surface for a very small fraction of its oscillation period. Recently, there has been much interest in phase imaging by measuring the phase difference between the oscillations of the cantilever driving piezo and the detected oscillations. It is thought that image contrast is derived from image properties such as stiffness and viscoelasticity. Non-contact operation is another method which may be employed when imaging by AFM. The cantilever must be oscillated above the surface of the sample. This is a very difficult mode to operate in ambient conditions with the AFM. The thin layer of water contamination which exists on the surface of the sample will invariably form a small capillary bridge between the tip and the sample and cause the tip to jump-to-contact (Carberry 2007).

## CHAPTER III

### MATERIALS AND METHODS

Materials

Equipments

Methods

1. Preparation of CS
  - 1.1 Preparation of SD-CS
  - 1.2 Preparation of CS solution
2. Characterization of SD-CS
3. Plasmid preparation
4. Complex formation between CS and plasmid DNA
5. Characterization of CS/DNA complexes
  - 5.1 Agarose gel electrophoresis
  - 5.2 Binding affinity
  - 5.3 Size and zeta potential measurements
  - 5.4 Surface morphology
6. *In vitro* transfection study in COS-1 cells
  - 6.1 Transfection of SD-CS/DNA complexes
  - 6.2  $\beta$ -galactosidase activity assay
  - 6.3 Bradford protein assay
7. *In vitro* transfection study in CHO-K1 cells
  - 7.1 Transfection of CS/DNA complexes
  - 7.2 Luciferase activity assay
  - 7.3 Bicinchoninic acid (BCA) protein assay
8. Evaluation of cytotoxicity
9. Statistical analysis

## Materials

1. Chitosan, MW 20, 45, 200 and 460 kDa, 87% degree of deacetylation (Seafresh chitosan Lab, Bangkok, Thailand)
2. Acetic acid, glutamic, hydrochloric acid, sodium hydroxide, ethylene diamine tetraacetic acid (EDTA), Tris base, ethidium bromide (Merck, Darmstadt, Germany)
3. Aspartic acid (Acros Organics, Geel, Belgium)
4. Lactic acid and dimethyl sulfoxide (BDH Laboratories, Poole, England)
5. Endotoxin-free Plasmid Maxiprep Kit, Tris-EDTA buffer (Qiagen, Santa Clarita, CA, USA)
6. Agarose (ISC Bioexpress, Kaysville, UT, USA)
7. Dulbecco's modified Eagle's medium, Opti-MEM, fetal bovine serum, Trypsin-EDTA, penicillin-streptomycin (Gibco-Invitrogen, Carlsbad, CA, USA)
8. RPMI-1640 (Gibco BRL, Rockville, MD, USA)
9.  $\beta$ -galactosidase assay kit, pSV $\beta$ -gal containing bacterial  $\beta$ -galactosidase gene under the control of SV40 promoter with 6820 bp, Report Lysis Buffer (Promega, Madison, IL, USA)
10. Luciferase assay reagent,  $\lambda$ DNA/*Hind*III, Glo lysis buffer (Promega, Madison, IL, USA)
11. pcDNA3-CMV-Luc encoding luciferase under the control of CMV promoter with 7100 bp (Aldevron, Fargo, ND, USA)
12. Bicinchoninic acid protein assay reagent (Pierce, Rockford, IL, USA)
13. Polyethylenimine (PEI 25K) (Aldrich, Munich, Germany)
14. 3-(4,5-dimethylthiazol-2-yl)-2,5-diphenyl tetrazolium bromide (MTT), bovine serum albumin (Sigma Chemical, St Louis, MO, USA)
15. Bradford protein assay reagent (Bio-Rad Laboratories, Hercules, CA, USA)
16. COS-1, CHO-K1 cells (American Type Culture Collection, Rockville, MD, USA)

## Equipments

1. Spray dryer (Minispray Dryer, Büchi 190, Postfach, Switzerland)
2. Fourier transform infrared spectroscopy (1760X, Perkin-Elmer, CT, USA)
3. <sup>13</sup>C-NMR spectrometer (DPX-300, Faellenden Bruker, Switzerland)
4. Differential scanning calorimeter-thermogravimetric analyzer (SDT2960 DSC-TGA, TA Instruments, Inc, DE, USA)

5. X-ray diffractometer (JDX-8030 JEOL, Tokyo, Japan)
6. Transmission electron microscope (JEOL JEM-1230, Tokyo, Japan)
7. Atomic force microscopy (SPI4000-SPA400, Seiko Instruments, Chiba, Japan)
8. Spectrofluorometer (RF-1501, Shimadzu, Tokyo, Japan)
9. Spectrophotometer (Agilent Technologies, Waldbronn, Germany)
10. Zetasizer 3000 (Malvern Instruments, Southborough, MA, USA)
11. CO<sub>2</sub> Incubator (Contherm, Lower Hutt, New Zealand)
12. Laminar hood (Holten, Nino-lab, Sweden)
13. Optical microscope (Nikon, eclipse TE2000-S, Tokyo, Japan)
14. Incubator shaker (GFL, Burgwedel, Germany)
15. Microplate reader (Universal Microplate Analyzer, AOPUS01 and AI53601, Packard Biosciences, Meriden, CT, USA)
16. Gel electrophoresis (Alphaimager 2200, Alpha-Innotech, CA, USA)
17. Mini-Lum luminometer (Bioscan Inc., Washington DC, USA)
18. Cell culture plate (Corning, NY, USA)
19. pH meter (Horiba, Kyoto, Japan)

## **Methods**

### **1. Preparation of CS**

In this study, CS was prepared by two methods: (1) dissolving chitosan base in the acidic solutions and (2) dissolving chitosan base in the acidic solutions and then spray drying (SD). The protocol of each preparation was described as following:

#### **1.1 Preparation of CS solution**

CAC, CAs, CGI, CHy and CLa were prepared by dissolving chitosan base with different molecular weights in dilute acid solutions of acetic acid, aspartic acid, glutamic acid, hydrochloric acid and lactic acid, respectively, with a gentle stirring for at least 12 h. The final concentration of CS solution was adjusted to 1 mg/ml. CAC was prepared using 0.1%, 0.2 and 0.6% w/v acetic acid in order to achieve an optimal condition of transfection. The physicochemical properties of the acids used to prepare the CS solutions are shown in Table 3.

Table 3 Physicochemical properties of the acids used to prepare the CS solutions.

Acid	Structure	MW	pK <sub>a</sub> (25 °C)
Acetic	$\text{CH}_3-\overset{\text{O}}{\parallel}{\text{C}}-\text{OH}$	60.05	4.75
Aspartic	$\text{HO}-\overset{\text{O}}{\parallel}{\text{C}}-\underset{\text{H}_2}{\text{C}}-\underset{\text{NH}_2}{\overset{\text{H}}{\text{C}}}-\overset{\text{O}}{\parallel}{\text{C}}-\text{OH}$	133.10	pK <sub>a1</sub> = 1.88 pK <sub>a2</sub> = 3.65 pK <sub>a3</sub> = 9.6
Glutamic	$\text{HO}-\overset{\text{O}}{\parallel}{\text{C}}-\underset{\text{H}_2}{\text{C}}-\underset{\text{H}_2}{\text{C}}-\underset{\text{NH}_2}{\overset{\text{H}}{\text{C}}}-\overset{\text{O}}{\parallel}{\text{C}}-\text{OH}$	147.13	pK <sub>a1</sub> = 2.19 pK <sub>a2</sub> = 4.25 pK <sub>a3</sub> = 9.67
Hydrochloric	H—Cl	36.45	-
Lactic	$\begin{array}{c} \text{O} \\ \parallel \\ \text{C}-\text{OH} \\   \\ \text{HC}-\text{OH} \\   \\ \text{CH}_3 \end{array}$	90.08	3.86

## 1.2 Preparation of SD-CS

Chitosan base of different molecular weights was dissolved in dilute acid solutions of aspartic acid, glutamic acid and lactic acid in certain molar ratio. The amount of organic acids and chitosans (D-glucosamine unit) used was calculated based on the degree of deacetylation in order to form CS as shown in Equation 1. These solutions were adjusted with distilled water to make 1% w/v solutions and stirred for at least 12 h, filtered and then spray dried at a feed rate of 5 ml/min under the following conditions: inlet temperature of 125±2 °C and outlet temperature of 65±2 °C using a spray dryer (Minispray Dryer, Büchi 190, Switzerland). The obtained powder was stored in a dessicator containing dry silica gel prior to use in each experiment (Nunthanid et al. 2004: 15-26).

$$\text{Amount of chitosan for chitosan and acids ratio of 1:1} = \frac{\text{D-glucosamine unit}}{\text{D-glucosamine unit} + \text{N-acetyl-D-glucosamine unit}} \quad (1)$$

## 2. Characterization of SD-CS

The physicochemical characteristics of SD-CS were determined by Fourier transform infrared (FTIR) spectroscopy, <sup>13</sup>C Nuclear magnetic resonance (NMR) spectroscopy, Differential scanning calorimetry (DSC), Thermogravimetric analysis (TGA) and X-ray powder diffraction.

### 2.1 Fourier transformed infrared (FTIR) spectroscopy

FTIR spectra of SD-CS were obtained using a FTIR spectroscopy (1760X, Perkin-Elmer, CT, USA). The samples were previously ground and mixed thoroughly with potassium bromide (KBr), an infrared transparent matrix. The KBr disks were prepared by compressing the powder. The spectra were scanned over wave number range of 4000 to 400 cm<sup>-1</sup>.

### 2.2 <sup>13</sup>C Nuclear magnetic resonance (NMR) spectroscopy

The Carbon chemistry of SD-CS was assessed by solid-state <sup>13</sup>C-NMR spectroscopy using a DPX-300 (Faellenden Bruker, Switzerland) operating at a frequency of 400 MHz. Samples of 150-200 mg were packed in a silicon nitride rotor and spun at 5000±10 Hz.

### 2.3 Differential scanning calorimetry (DSC) and thermogravimetric analysis (TGA)

The thermal behavior of SD-CS was characterized by a Differential scanning calorimeter-thermogravimetric analyzer (SDT2960 DSC-TGA, TA Instruments, Inc, DE, USA). Samples of 2-4 mg were accurately weighed and sealed in an aluminum pan. The samples were heated at a constant rate of 5 °C/min over a temperature range of 25-300 °C. Inert atmosphere was maintained by purging nitrogen gas.

## 2.4 X-ray powder diffraction

X-ray powder diffraction was performed using an X-ray diffractometer (JDX-8030 JEOL, Tokyo, Japan) under the following conditions: target Cu; filter Ni; voltage 35 kV; current 20 mA; receiving slit 0.2 inches. The data were collected in the continuous mode using a step size of  $0.01^\circ$  at  $2\theta/\text{sec}$ . The scanned range was  $5-40^\circ$ .

## 3. Plasmid preparation

pSV $\beta$ -gal encoding the  $\beta$ -galactosidase reporter gene under the control of SV40 promoter and pcDNA3-CMV-Luc encoding the firefly luciferase reporter gene under control of the cytomegalovirus promoter were separately transformed to DH5- $\alpha$  *Escherichia coli*. DH5- $\alpha$  *E. coli* containing plasmid DNA was grown at  $37^\circ\text{C}$  in Luria Bertani (LB) broth containing solution of 100  $\mu\text{g}/\text{ml}$  ampicillin. Plasmid DNA was purified from the *E. coli* using the Qiagen endotoxin-free plasmid purification kit. The harvested bacterial cells was centrifuged at  $6000 \times g$  for 15 min at  $4^\circ\text{C}$ . The bacterial pellet was suspended in 10 ml of Buffer P1. 10 ml of Buffer P2 was added to the mixture of Buffer P1. The mixture of Buffer P2 was thoroughly mixed by vigorously inverting 4-6 times, and incubated at room temperature for 5 min. 10 ml of chilled Buffer P3 was added to the mixture of Buffer P2 and immediately mixed and thoroughly mixed by vigorously inverting 4-6 times, and incubated on ice for 5 min. The mixture of Buffer P3 was centrifuged at  $15,000 \times g$ . The supernatant containing plasmid DNA was applied to Qiagen-tip equilibrated with 10 ml of Buffer QBT. The Qiagen-tip was washed with ml of 2x30 Buffer QC. The plasmid DNA was eluted from the Qiagen-tip with 15 ml of Buffer QF. The plasmid DNA was precipitated in 10.5 ml of isopropanol. The plasmid pellet was collected and washed in 70% ethanol. The plasmid DNA was dried for 5-10 min, and redissolved in Tris-EDTA (TE) buffer, pH 8.0 (Qiagen, Santa Clarita, CA, USA 2005). DNA concentration were quantified by measurement of UV absorbance at 260 nm and 280 nm ( $\text{OD}_{260}/\text{OD}_{280}$  ratio  $\sim 1.9$ ) using a spectrophotometer (UV-160U; Shimadzu, Tokyo, Japan). The purity of plasmid was checked by gel electrophoresis (0.8% agarose gel) in Tris acetate-EDTA (TAE) buffer, pH 8.0.

## **4. Complex formation between cationic polymers and plasmid DNA**

### **4.1 Complex formation between SD-CS and plasmid DNA**

SD-CAs, SD-CGI and SD-CLa were dissolved in sterilized water. SD-CS/DNA complexes at N/P ratios of 2, 4, 12, 20 and 28 were prepared by adding plasmid DNA solution to SD-CS solution. The N/P ratio was calculated based on molar ratio of amine group in chitosan and phosphate group in DNA as shown in Table 4. The amount of CS at the N/P ratios of 2, 4, 12, 20 and 28 was 5, 10, 30, 50 and 70  $\mu\text{g}$ , respectively. The amount of plasmid DNA was 5  $\mu\text{g}$  for all N/P ratios. The mixture was gently pipetted and vortexed for 3-5 sec to initiate complex formation and left for 15 min at room temperature for the complexes to completely form. Complex formation was confirmed by agarose gel electrophoresis.

### **4.2 Complex formation between CS and plasmid DNA**

CAC, CAs, CGI, CHy and CLa were prepared by dissolving chitosan base in 0.1%, 0.2% or 0.6% w/v their respective acid solution. CS/DNA complexes at various N/P ratios were prepared by adding plasmid DNA solution to CS solution. The N/P ratio was calculated based on molar ratio of amine group in chitosan and phosphate group in DNA as shown in Table 4. The amount of CS at the N/P ratios of 0.5, 1, 2, 4, 6, 8, and 12 was 1.25, 2.5, 5, 10, 15, 20 and 30  $\mu\text{g}$ , respectively. The amount of plasmid DNA was 5  $\mu\text{g}$  for all N/P ratios. The mixture was gently pipetted and vortexed for 3-5 sec to initiate complex formation and left for 15 min at room temperature for the complexes to completely form. The pH of complex solutions was adjusted to pH 6.5 by adding 0.1 N NaOH. Complex formation was confirmed by agarose gel electrophoresis.

Table 4 Calculation of N/P ratio for chitosan/DNA complex.

N/P ratio	$\frac{\text{Amount of chitosan/MW of chitosan}}{\text{MW of chitosan/Nitrogen repeat unit of chitosan}} \times \frac{\text{Amount of DNA/Average MW of DNA}}{\text{MW of chitosan/Nitrogen repeat unit of chitosan}}$
0.5	$\frac{1.25 (\mu\text{g})/161 (\text{g/mol})}{5 (\mu\text{g})/330 (\text{g/mol})}$
1	$\frac{2.5 (\mu\text{g})/161 (\text{g/mol})}{5 (\mu\text{g})/330 (\text{g/mol})}$
2	$\frac{5 (\mu\text{g})/161 (\text{g/mol})}{5 (\mu\text{g})/330 (\text{g/mol})}$
4	$\frac{10 (\mu\text{g})/161 (\text{g/mol})}{5 (\mu\text{g})/330 (\text{g/mol})}$
6	$\frac{15 (\mu\text{g})/161 (\text{g/mol})}{5 (\mu\text{g})/330 (\text{g/mol})}$
8	$\frac{20 (\mu\text{g})/161 (\text{g/mol})}{5 (\mu\text{g})/330 (\text{g/mol})}$
12	$\frac{30 (\mu\text{g})/161 (\text{g/mol})}{5 (\mu\text{g})/330 (\text{g/mol})}$
20	$\frac{50 (\mu\text{g})/161 (\text{g/mol})}{5 (\mu\text{g})/330 (\text{g/mol})}$
28	$\frac{70 (\mu\text{g})/161 (\text{g/mol})}{5 (\mu\text{g})/330 (\text{g/mol})}$

### 4.3 Complex formation between PEI and plasmid DNA

PEI was dissolved in sterile water. PEI/DNA complexes at N/P ratios of 4 were prepared by adding plasmid DNA solution to PEI solution. The N/P ratio was calculated based on molar ratio of amine group in PEI and phosphate group in DNA as shown in Table 5. The amount of plasmid DNA was 1  $\mu\text{g}$ . The mixture was gently pipetted and vortexed for 3-5 sec to initiate complex formation and left for 15 min at room temperature for the complexes to completely form.

Table 5 Calculation of N/P ratio for PEI/DNA complex.

N/P ratio	Amount of PEI/MW of PEI
	MW of PEI/ Nitrogen repeat unit of PEI
	Amount of DNA/Average MW of DNA
4	$\frac{0.52 (\mu\text{g})/43 (\text{g/mol})}{1 (\mu\text{g})/330 (\text{g/mol})}$

## 5. Characterization of CS/DNA complexes

### 5.1 Agarose gel electrophoresis

Agarose gel was prepared by dissolving 0.3 g of agarose in 37.5 ml of Tris-acetate-EDTA (TAE) buffer, pH 8.0. The gel solution was warmed up in order to dissolve the agarose. 15  $\mu\text{l}$  of 1 mg/ml ethidium bromide was added into the gel solution before the gel was congealed. CS/DNA complexes and the plasmid DNA were loaded into the agarose gel in TAE buffer, pH 8.0. The volume of the sample loaded in the well was 15  $\mu\text{l}$  of CS/DNA complex solution containing 0.9  $\mu\text{g}$  of DNA. The electrophoresis was carried out at 100 V for 45 min. UV transillumination of the gel was employed to visualize DNA and the transilluminated gel was photographed using a gel documentation analyzer (AlphaImager 2200, Alpha-Innotech, CA, USA).

### 5.2 Binding affinity

Ethidium bromide (EtBr) displacement assay was performed in order to study the ability of CS to bind the DNA. EtBr (0.1 mg/ml) was dissolved in 0.01 M phosphate-buffered saline (PBS, pH 7.4). 20  $\mu\text{l}$  of EtBr solution was added to a 20  $\mu\text{l}$  of 500  $\mu\text{g/ml}$  DNA solution. The steady state fluorescent measurement was performed on a

spectrofluorometer (RF-1501, Shimadzu, Tokyo, Japan) at an excitation wavelength of 560 and an emission wavelength of 605 nm. An aliquot CS solution (1 mg/ml of SD-CS in sterile water) was then titrated into the DNA/EtBr solution to the varied N/P ratios of CS/DNA complexes. The fluorescent intensity calculated based on the fluorescent intensity of the DNA/EtBr solution is shown in Equation 2. The recorded fluorescent intensity (FI) was expressed relative to the fluorescent intensity of the DNA/EtBr solution in the absence of SD-CS ( $FI_0$ ), after subtracting the fluorescence of EtBr in the absence of DNA under the same buffer conditions ( $FI_{buff}$ ). Data are presented as mean $\pm$ SD. The assay was performed in triplicate.

$$FI (\%) = [(FI - FI_{buff}) / (FI_0 - FI_{buff})] \times 100 \quad (2)$$

### 5.3 Size and zeta potential measurements

The particle size and surface charge of CS/DNA complexes were assessed using a laser Doppler anemometry using a Zetasizer 3000 (Malvern Instruments, Southborough, MA, USA). CS/DNA complexes were prepared in sterile water (500  $\mu$ l) at various N/P ratios of 1, 2, 4, 6, 8, 12, 20 and 28. The measurements were performed using the aqueous flow cell in the automatic mode at 25  $^{\circ}$ C. Data are presented as mean $\pm$ SD. The assay was performed in triplicate.

### 5.4 Surface morphology

Morphological examination of CS/DNA complexes was performed using transmission electron microscopy (TEM) and atomic force microscopy (AFM).

#### 5.4.1 Transmission electron microscopy (TEM)

5  $\mu$ l of the complex solution was deposited on the copper grid and left to dry for 5 min, then rinsed with distilled water. The grid was stained with one drop of filtered solution containing 1% uranyl acetate for 2 min, and the excess of uranyl acetate was removed with filter paper. The grid was allowed to dry for further 10 min and then examined with a transmission electron microscope (JEOL JEM-1230 electromicroscope, Japan).

#### **5.4.2 Atomic force microscopy (AFM)**

5  $\mu$ l of the complex solution was deposited onto freshly cleaved mica disk. The deposited solution was dried at room temperature. Imaging was conducted on an AFM (SPI4000-SPA400, Seiko Instruments, Chiba, Japan) in tapping mode, with 512 x 512 data acquisition at a scan of approximately 1.5 Hz at ambient condition.

### **6. *In vitro* transfection study in COS-1 cells**

#### **6.1 Transfection of SD-CS/DNA complexes**

COS-1 cells were seeded 24 h into 24-well plates at a density of  $5 \times 10^4$  cells/cm<sup>2</sup> in 1 ml of Dulbecco's modified Eagle's medium (DMEM). Prior to transfection, the medium was removed and the cells were rinsed with PBS, and then supplied with 900  $\mu$ l of low serum media, Opti-MEM (Gibco-Invitrogen, Carlsbad, CA, USA). The cells were incubated with 100  $\mu$ l of CS/DNA complexes (N/P ratios of 4, 12, 20 and 28) containing 5  $\mu$ g of pSV $\beta$ -gal for 4 h at 37 °C under 5% CO<sub>2</sub> atmosphere. Non-treated cells and cells transfected with naked plasmid and PEI/DNA complexes at an N/P ratio of 4 were used as controls. After transfection, the medium was replaced with 1 ml of fresh growth medium, and the cells were incubated for 24 h at 37 °C under 5% CO<sub>2</sub> atmosphere. The experiment was performed from two separate experiments in triplicate.

#### **6.2 $\beta$ -galactosidase activity assay**

$\beta$ -galactosidase activity was determined using the  $\beta$ -galactosidase kit according to the manufacturer's instructions (Promega, Madison, USA). The cells were lysed with Report Lysis Buffer (Promega, Madison, USA), and the cell lysate was centrifuged at 10,000 rpm for 5 min, and the supernatant was collected.  $\beta$ -galactosidase expression determined as milliunit  $\beta$ -galactosidase per milligram of cellular protein (mU/mg protein). Absorbance was measured at 480 nm using a microplate reader (Universal Microplate Analyzer, AOPUS01 and AI53601, Packard Biosciences, Meriden, CT, USA). Total protein content of the samples was measured using Bradford protein assay (Li et al. 2003: 7-18). Data are presented as mean $\pm$ SD. The assay was performed in triplicate.

### **6.3 Bradford protein assay**

Bradford assay was used to determine the amount of protein in cell lysate because it is a rapid assay (Boyer 1993: 51-58). The cell lysate was centrifuged at 10,000 rpm for 5 min at 4 °C. 10 µl of supernatant of each sample was added to 100 µl of Bradford protein assay reagent (Bio-Rad Laboratories, Hercules, CA, USA) and incubated for 15 min at room temperature. Absorbance was determined at 595 nm by a microplate reader (Universal Microplate Analyzer, Model AOPUS01 and AI53601, Packard Biosciences, Meriden, CT, USA) using bovine serum albumin as a standard. Data are presented as mean±SD. The assay was performed in triplicate.

## **7. *In vitro* transfection study in CHO-K1 cells**

### **7.1 Transfection of CS/DNA complexes**

CHO-K1 cells were seeded 24 h into 24-well plates at a density of  $5 \times 10^4$  cells/cm<sup>2</sup> in 1 ml of growth medium (RPMI-1640 containing 10% FBS, supplemented with 2 mM L-glutamine, 100 U/ml penicillin and 100 µg/ml streptomycin). Prior to transfection, the medium was removed and the cells were rinsed with phosphate-buffered saline (PBS, pH 7.4), and then supplied with 150 µl of fresh culture medium without FBS. The cells were incubated with 100 µl of CS/DNA complexes (N/P ratios of 2, 4, 6, 8 and 12) containing 5 µg of pcDNA3-CMV-Luc for 24 h at 37 °C under 5% CO<sub>2</sub> atmosphere. Non-treated cells and cells transfected with naked plasmid and PEI/DNA complexes at an N/P ratio of 4 were used as controls. After transfection, the medium was replaced with 1 ml of fresh growth medium, and the cells were incubated for 24 h at 37 °C under 5% CO<sub>2</sub> atmosphere. The experiment was performed from two separate experiments in triplicate.

### **7.2 Luciferase activity assay**

Cells were harvested by removing the medium and then adding 100 µl of 1x Glo lysis buffer (Promega, Madison, IL, USA), and incubating for 5 min prior to gentle scraping of the plate. The cell lysate was centrifuged at 10,000 rpm for 3 min and the supernatant was collected. 10 µl of the supernatant was placed into a 1.5 ml-ependorf tube (Eppendorf, Hamburg, Germany) in which 50 µl of luciferase substrate (Promega, Madison, WI, USA) was added. The luminescence was measured using a Mini-Lum

luminometer (Bioscan Inc., Washington DC, USA) immediately after mixing the cell lysate with the luciferase substrate. The transfection efficiency was defined as relative light unit (RLU) standardized with a protein concentration determined by the bicinchoninic acid (BCA) protein assay (Pierce; Rockford, IL, USA) using bovine serum albumin (Sigma Chemical, St Louis, MO, USA) as a standard. Data are presented as mean $\pm$ SD. The assay was performed in triplicate.

### **7.3 Bicinchoninic acid (BCA) protein assay**

Bicinchoninic acid (BCA) protein assay was performed in order to determine the amount of protein in cell lysate lysed by Glo Lysis buffer (Romero et al. 2006: 6046-6055; Little et al. 2004: 9534-9539). Bicinchoninic acid (BCA) protein assay was used in stead of Bradford assay because Glo Lysis Buffer is a proprietary formulation developed to promote rapid lysis of cultured mammalian cells. It is compatible with Luciferase Assay reagent and yielded stable luciferase enzyme at room temperature (Promega, Madison, IL, USA 2007b). The cell lysate obtained by lysis in was centrifuged at 10,000 rpm for 5 min at 4 °C. 10  $\mu$ l of supernatant of each sample was added to 100  $\mu$ l of bicinchoninic acid protein assay reagent and incubated for 30 min at 37 °C. Absorbance was determined at 550 nm by a microplate reader (340 ATTC; SLT Lab Instruments, Salzburg, Austria). Data are presented as mean $\pm$ SD. The assay was performed in triplicate.

## **8. Evaluation of cytotoxicity**

Cytotoxicity of CS/DNA complexes was performed by the MTT-based cytotoxicity assay (Mosmann 1983: 55-63). Evaluation of cytotoxicity was performed by MTT assay. The cells were seeded in a 96-well plate at a density of  $5 \times 10^4$  cells/cm<sup>2</sup> in 100  $\mu$ l of growth medium and incubated for 24 h at 37 °C under 5% CO<sub>2</sub> atmosphere. Prior to transfection, the medium was removed and the cells were rinsed with phosphate-buffered saline (PBS, pH 7.4), and then supplied with 15  $\mu$ l of fresh culture medium without FBS. The cells were then treated with 10  $\mu$ l of a CS/DNA complex (N/P ratios of 2, 4, 6, 8, 12, 20 and 20) containing 0.5  $\mu$ g of DNA for 24 h at 37 °C under 5% CO<sub>2</sub> atmosphere. Non-treated cells and cells treated with naked plasmid and PEI at an N/P ratio of 4 were used as controls incubated for the same duration of time. After treatment, CS/DNA complexes solutions were removed and fresh cell culture

medium was added and incubated for 4 h to stabilize the cells. Finally, the cells were incubated with 20  $\mu$ l MTT containing medium (0.5 mg/ml MTT in medium) for 4 h. Then the medium was removed, the cells were rinsed with PBS, pH 7.4, and the formazan crystals formed in living cells were dissolved in 100  $\mu$ l DMSO per well. Relative viability (%) was calculated based on absorbance at 550 nm using a microplate reader (340 ATTC; SLT Lab Instruments, Salzburg, Austria). Viability of non-treated control cells was arbitrarily defined as 100%. Data are presented as mean $\pm$ SD from two separate experiments (n=6).

## **9. Statistical analysis**

Statistical significance of differences in binding affinity, transfection efficiencies and cell viability were examined using one-way analysis of variance (ANOVA) followed by an LSD *post hoc* test. The significance level was set at  $p < 0.05$ .

## **CHAPTER IV**

### **RESULTS AND DISCUSSION**

1. Characterization of SD-CS
2. Characterization of SD-CS/DNA complexes
  - 2.1 Physicochemical properties of SD-CS/DNA complexes
    - 2.1.1 Effect of N/P ratio on physicochemical properties of SD-CS/DNA complexes
    - 2.1.2 Effect of MW of chitosan on physicochemical properties of SD-CS/DNA complexes
    - 2.1.3 Effect of salt form of chitosan on physicochemical properties of SD-CS/DNA complexes
  - 2.2 Transfection efficiency of SD-CS/DNA complexes
  - 2.3 Cytotoxicity of SD-CS/DNA complexes
3. Characterization of CS/DNA complexes
  - 3.1 Physicochemical properties of CS/DNA complexes
    - 3.1.1 Effect of pH on physicochemical properties of CS/DNA complexes
    - 3.1.2 Effect of N/P ratio on physicochemical properties of CS/DNA complexes
    - 3.1.3 Effect of MW of chitosan on physicochemical properties of CS/DNA complexes
    - 3.1.4 Effect of salt form of chitosan on physicochemical properties of CS/DNA complexes
  - 3.2 Transfection efficiency of CS/DNA complexes
    - 3.2.1 Optimization of transfection condition of CS/DNA complexes
    - 3.2.2 Effect of N/P ratio on transfection efficiency
    - 3.2.3 Effect of MW of chitosan on transfection efficiency
    - 3.2.4 Effect of salt form of chitosan on transfection efficiency
  - 3.3 Cytotoxicity of CS/DNA complexes
  - 3.4 Optimal transfection efficiency condition of chitosan/DNA complexes

## 1. Characterization of SD-CS

The amount of acids used to dissolve chitosan is shown in Table 6. The CS solution was spray dried at a feed rate of 5 ml/min, inlet temperature of  $125\pm 2$  °C and outlet temperature of  $65\pm 2$  °C. The yield of SD-CS powder was about 40-50%.

Table 6 Molar ratio of D-glucosamine unit and acids.

Acid	D-glucosamine unit:acid (mol)
Aspartic acid	1:1
Glutamic acid	1:1
Lactic acid	1:1.3

The physicochemical characteristics of SD-CS were determined by FTIR spectroscopy,  $^{13}\text{C}$  NMR spectroscopy, DSC, TGA and X-ray powder diffraction. The chemical functional groups in SD-CS were identified by FTIR spectroscopy. Characterized by FTIR spectroscopy, chitosan and SD-CS exhibited OH stretching at 3450 to 3400  $\text{cm}^{-1}$ , indicating intermolecular hydrogen bonding (Figure 7). The  $\text{NH}_2$  stretching peak at 1602  $\text{cm}^{-1}$  representing the glucosamine functional group was exhibited in the spectrum of chitosan base. In SD-CS, the  $\text{NH}_2$  stretching peak was hardly observed. SD-CAs exhibited the NH bending peak at 1617  $\text{cm}^{-1}$  representing the amine group and the symmetric carboxylate anion stretching peak at 1390  $\text{cm}^{-1}$  representing the carboxylate groups, in aspartate salt. SD-CGI exhibited the NH bending peak at 1627  $\text{cm}^{-1}$  representing the amine group, and the asymmetric carboxylate anion stretching peak at 1565  $\text{cm}^{-1}$  and the symmetric carboxylate anion stretching peak at 1401  $\text{cm}^{-1}$  representing the carboxylate groups, in glutamate salt. SD-CLa exhibited the carbonyl stretching peak at 1734  $\text{cm}^{-1}$ , and the asymmetric carboxylate anion stretching peak at 1584  $\text{cm}^{-1}$  and the symmetric carboxylate anion stretching peak at 1413  $\text{cm}^{-1}$  representing the carboxylate groups, in lactate salt. (Nunthanid et al. 2004: 15-26; Brown and Foote 2002: 427-452).

$^{13}\text{C}$  NMR spectroscopy was used to identify the spectrum of sugar resonance in SD-CS. By  $^{13}\text{C}$  NMR spectroscopy of chitosan base and SD-CS, the sugar resonances at 50-110 ppm were assigned to methine/methylene carbon, which indicated the presence of glucosamine units (Figure 8). SD-CAs exhibited the resonances of 175 ppm assigned to

carbonyl carbon and at 37 ppm assigned to  $-\text{CH}-\text{CH}_2$  carbon representing aspartate functionality. SD-CGI exhibited the resonances of 175 ppm assigned to carbonyl carbon and at 28 ppm assigned to  $-\text{CH}-\text{CH}_2-\text{CH}_2$  carbon representing glutamate functionality. SD-CLa exhibited the resonances of 182 ppm assigned to carbonyl carbon and at 21 ppm assigned to  $\text{CH}_3$  carbon representing lactate functionality (Nunthanid et al. 2004: 15-26; Brown and Foote 2002: 453-498).

DSC thermogram of chitosan exhibited a broad endothermic peak around 50-148 °C. SD-CAs was 25-125 and 125-300 °C. SD-CGI was 25-126 and 125-260 °C. SD-CLa was 25-107 and 125-225 °C (Figure 9). The endothermic peaks associated with the weight loss in TGA thermograms (Figure 10). Amount of weight loss could be due to the amount of water in chitosan and SD-CS. The endothermic peak of DSC at the lower temperature could be attributed to the loss of water. The thermal behavior of SD-CS at higher temperature exhibited interaction between chitosan and its salts (Nunthanid et al. 2004: 15-26).

X-ray powder diffraction chitosan was found sharp peaks at  $10.05^\circ$  and  $19.10^\circ$  ( $2\theta$ ) indicating the crystalline state of chitosan. SD-CAs, SD-CGI and SD-CLa showed halo diffractions indicating amorphous state of SD-CS (Figure 11) (Nunthanid et al. 2004: 15-26).

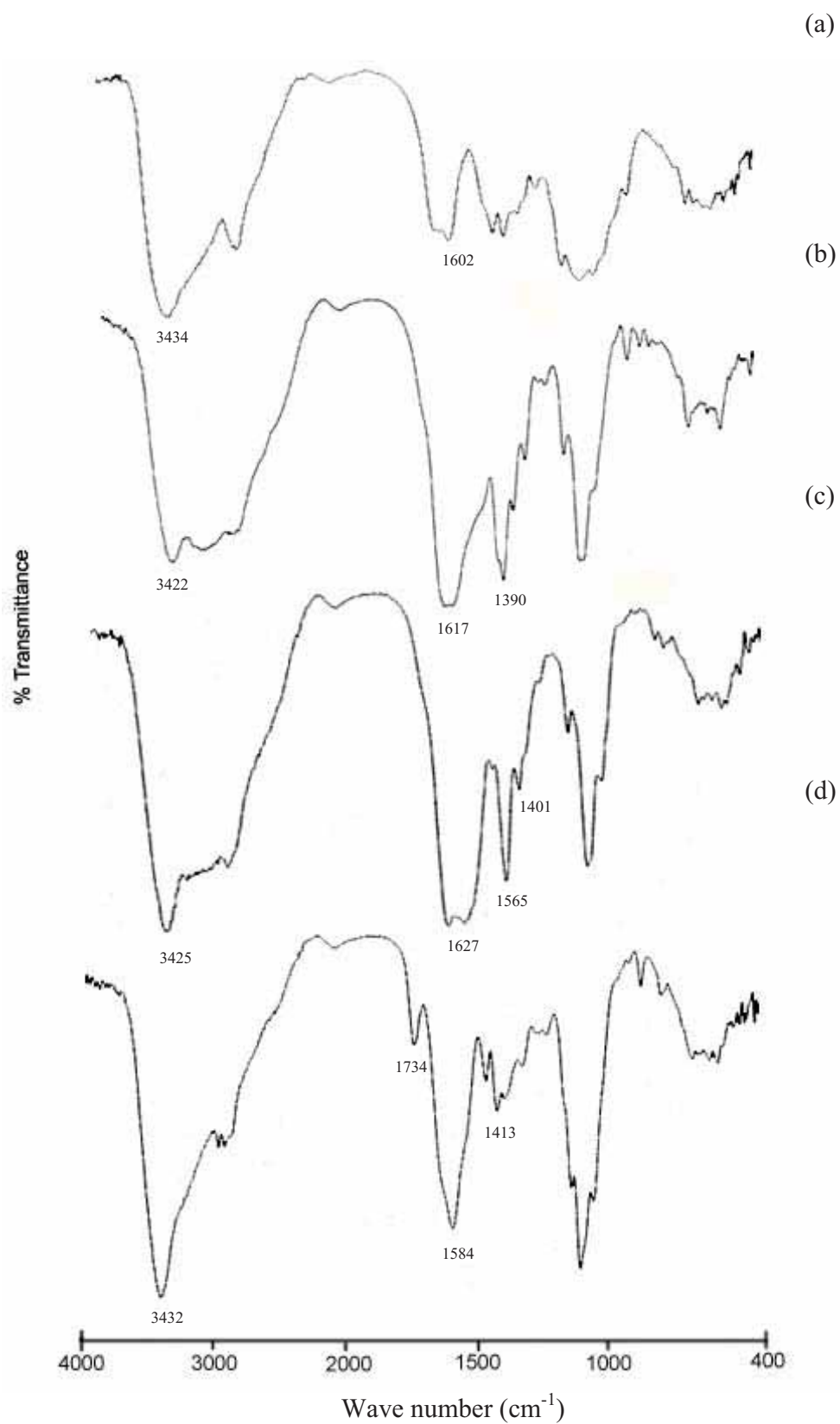


Figure 7 Transmission infrared spectrum of (a) chitosan base, (b) SD-CAs, (c) SD-CGI and (d) SD-CLa.

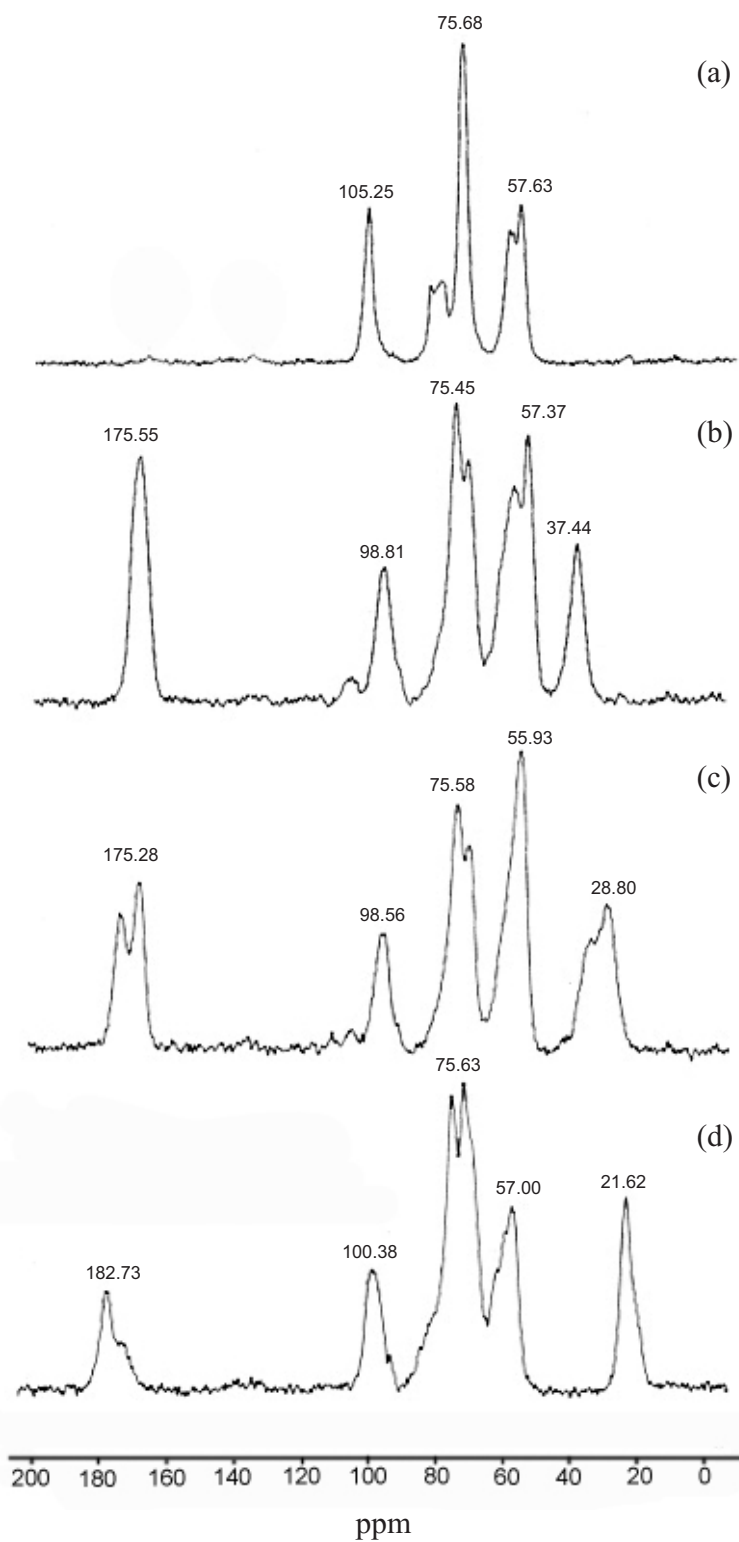


Figure 8 Solid-state  $^{13}\text{C}$ -NMR spectrum of (a) chitosan base, (b) SD-CAs, (c) SD-CGI and (d) SD-CLa.

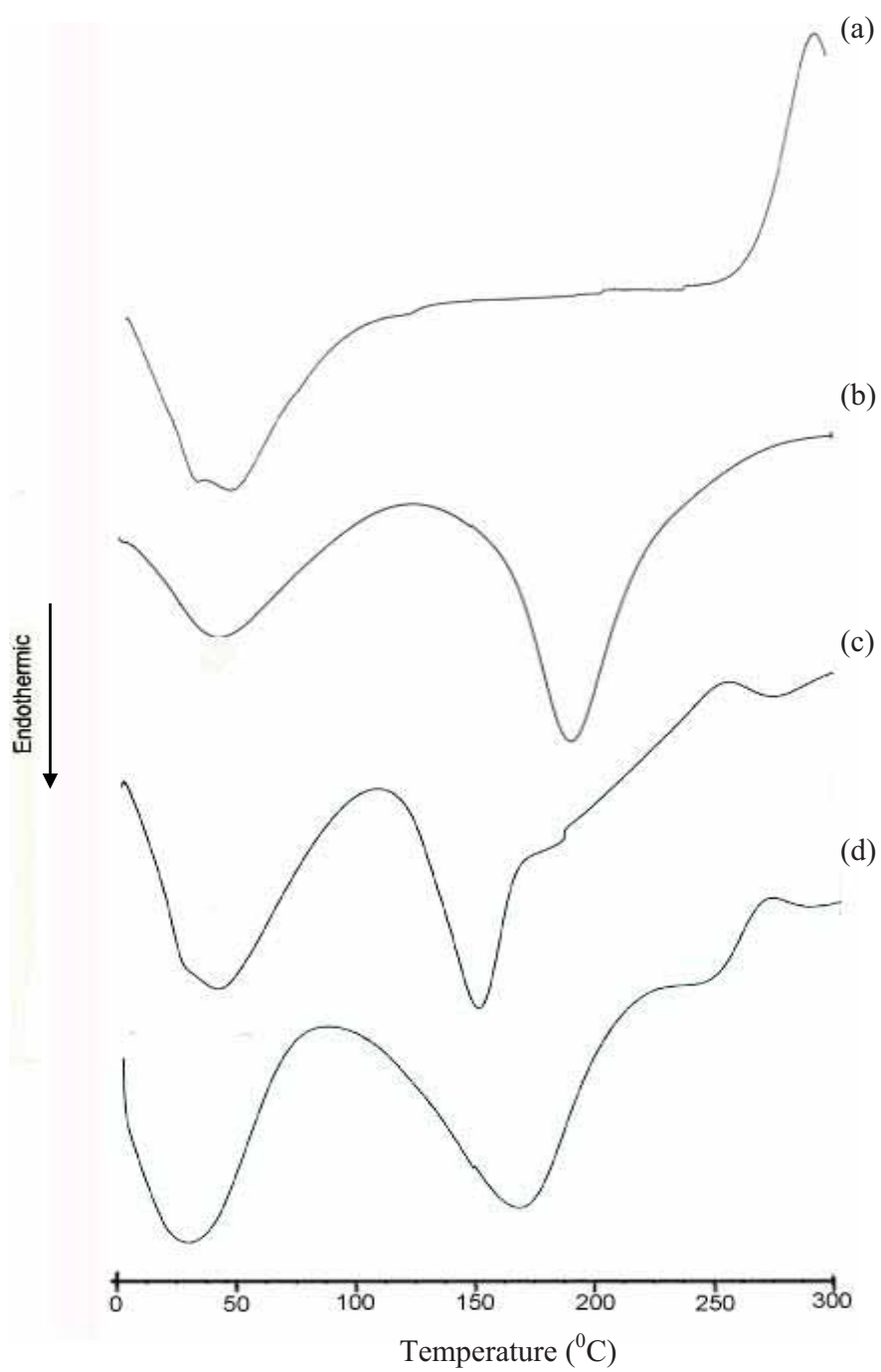


Figure 9 DSC thermogram of (a) chitosan base, (b) SD-CAs, (c) SD-CGI and (d) SD-CLa.

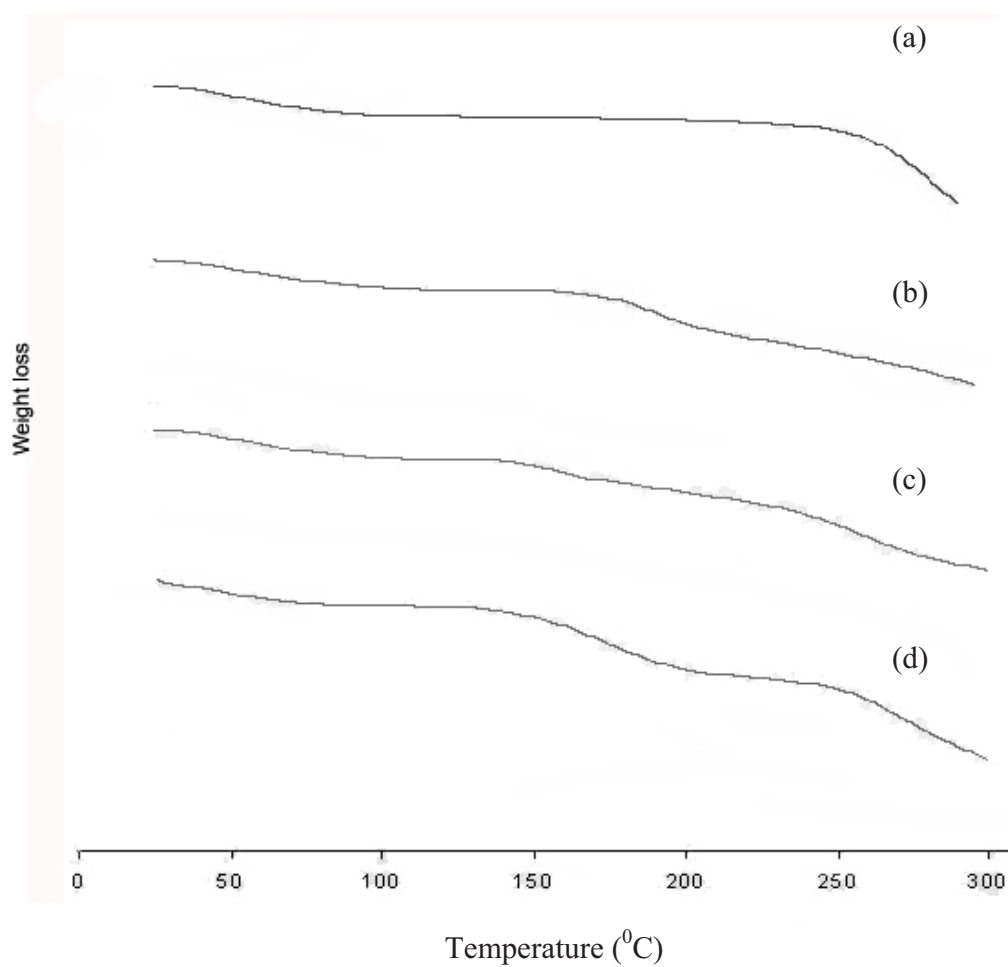


Figure 10 TGA thermogram of (a) chitosan base, (b) SD-CAs, (c) SD-CGI and (d) SD-CLa.

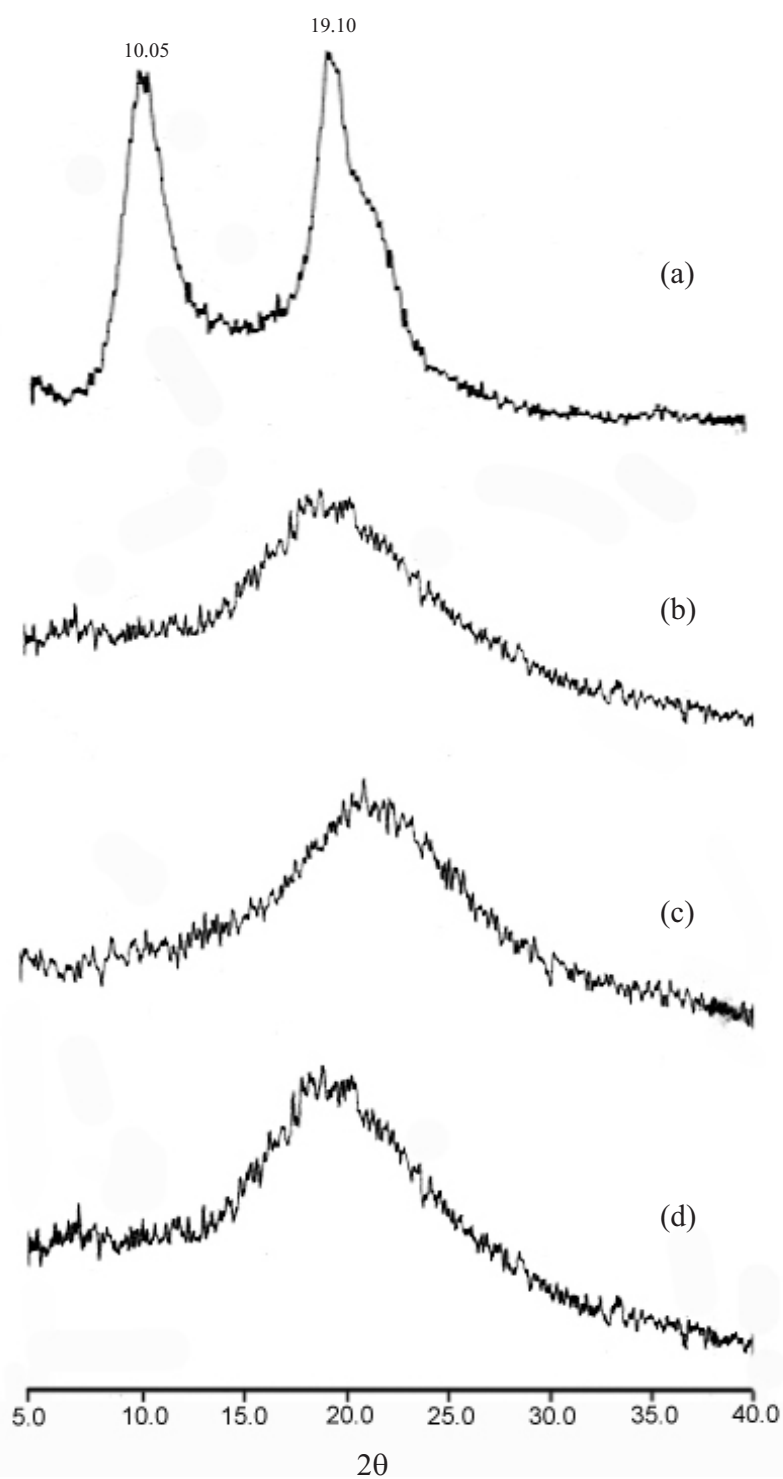


Figure 11 Powder X-ray diffraction pattern of (a) chitosan base, (b) SD-CAs, (c) SD-CGI and (d) SD-CLa.

## **2. Characterization of SD-CS/DNA complexes**

### **2.1 Physicochemical properties of SD-CS/DNA complexes**

Physicochemical properties of SD-CS/DNA complexes including complex formation, binding affinity, particle size and zeta potential were characterized because these properties might affect the transfection efficiency.

#### **2.1.1 Effect of N/P ratio on physicochemical properties of SD-CS/DNA complexes**

N/P ratio is one of formulation parameters that affect the physicochemical properties of chitosan/DNA complexes. By using an agarose gel electrophoresis technique, the ability of chitosan to interact with DNA was investigated. When the concentration of chitosan was changed and the DNA concentration kept constant, the N/P ratio of the complex was varied. The complex formation between chitosan and DNA was dependent on the N/P ratio (Figure 12). When the concentration of chitosan gradually increased, the DNA was gradually retained within the gel loading well. Migration of DNA on an agarose gel was retarded because of the charge neutralization of the complexes. The complete complexes were formed as the DNA was totally retained within the well.

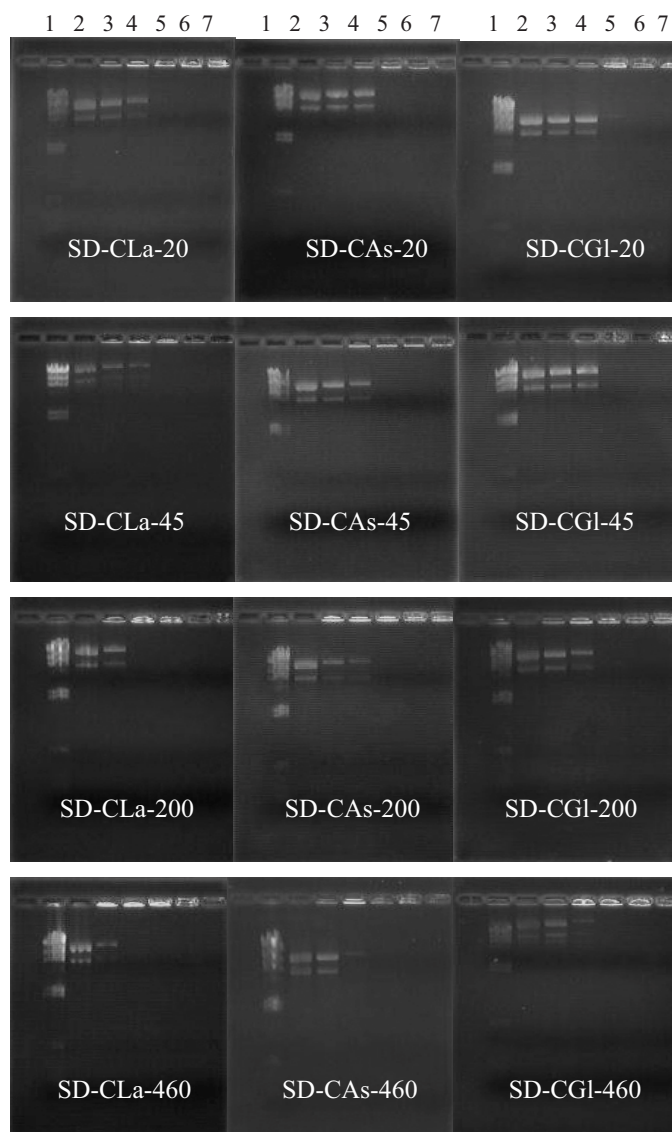


Figure 12 Gel electrophoresis of SD-CS/DNA complexes with different chitosan salts and MW. Lane 1,  $\lambda$ HindIII DNA marker; lanes 2, pSV $\beta$ -gal; lanes 3-7, SD-CS/DNA complexes at N/P ratios of 2, 4, 12, 20 and 28, respectively.

The binding affinity of SD-CS/DNA complexes was studied by ethidium bromide (EtBr) displacement assay. EtBr intercalates between the base pairs of the DNA double helix, yielding a highly fluorescent DNA/EtBr complex. Upon SD-CS binding to DNA, EtBr is expelled from the DNA/EtBr complex, resulting in a decrease in fluorescence. The degree of displacement of EtBr by SD-CS illustrates the binding affinity, indicating the relative strength of the interaction between SD-CS and DNA.

Figure 13 shows relative fluorescent intensity of SD-CS/DNA complexes with various ratios of chitosan. DNA/EtBr complex without titration of SD-CS was considered as a control with a relative fluorescent intensity of 100%. With the increase in the amount of SD-CS, the intensity of fluorescence showed a decreasing trend, indicating EtBr was replaced by the added SD-CS, that is, SD-CS bound selectively to DNA. This could be the increase in the interaction of SD-CS and DNA when the amount of SD-CS increased. The result agreed with that of Liu et al. (2005: 2705-2711) and Strand et al. (2005: 3357-3366). They found that the binding affinity of chitosan to DNA increased with increasing the N/P ratio. In addition, the binding affinity reached a plateau at high N/P ratio.

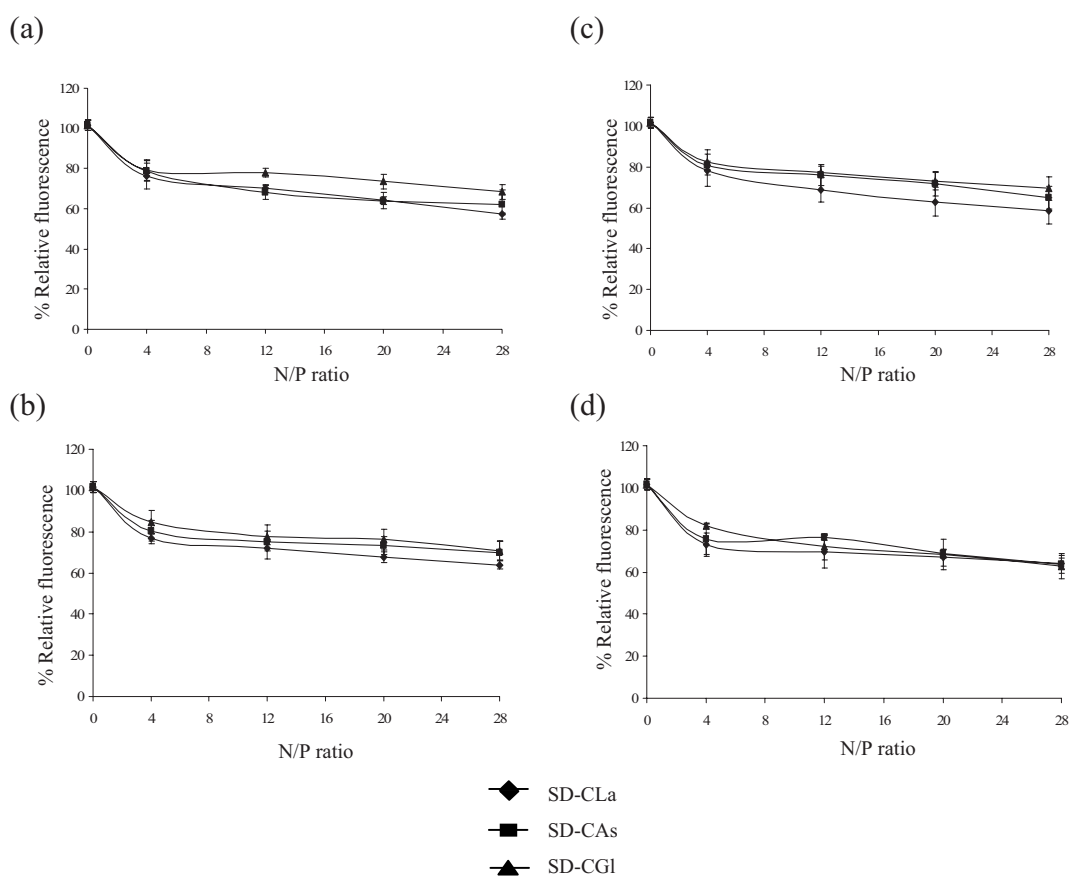


Figure 13 Relative fluorescent intensity of DNA/EtBr complex at varying N/P ratios of SD-CS at MW (a) 20 kDa, (b) 45 kDa, (c) 200 kDa and (d) 460 kDa.

The particle size was dependent on the N/P ratio. At an N/P of 4, the particle size of the complexes was microsized (630 to 6,000 nm), confirming that complete complexes were not formed. At N/P ratios above 4, the complexes were nanosized (200 to 600 nm), showing that complete complexes were formed (Figure 14-17). At N/P ratios above 12, the particle size of all SD-CS/DNA complexes increased with increasing N/P ratio. This was due to the intermolecular cross-linking between DNA strands by self-aggregates with an excess amount of SD-CS. The increase in particle size of chitosan/DNA complexes with increasing N/P ratio was also observed by Ishii, Okahata and Sato (2001: 51-64) and Özgel and Akbuğa (2006: 44-51).

The N/P ratio could affect the zeta potential. At an N/P ratio of 4, the zeta potential was approximately neutral (Figure 14-17). The zeta potential increased when the N/P ratio increased from 4 to 12 and increased to reach a plateau of about +32 to +49 mV at N/P ratios greater than 12. The zeta potential appeared to reach a maximum at high N/P ratios also observed by Strand et al. (2005: 3357-3366), Kiang et al. (2004: 5293-5301) and Lavertu et al. (2006: 4815-4824). The zeta potential increased when the N/P ratio increased could be due to their higher density of protonated amines in the chitosan backbone. At high N/P ratios, the zeta potential reached a maximum. It was attributed to the excess of amines available from particle formation (Kiang et al. 2004: 5293-5301).

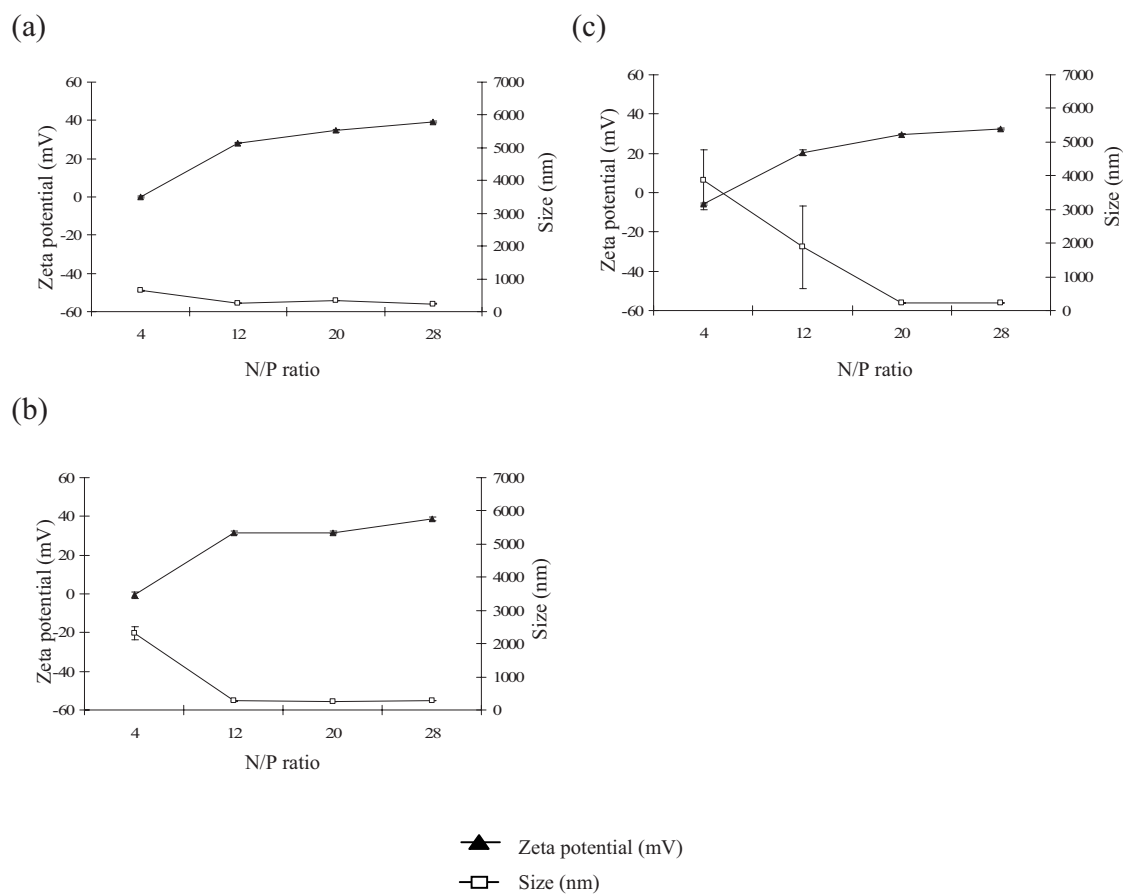


Figure 14 Zeta potential and particle size at varying N/P ratios of SD-CS-20kDa/DNA complexes (a) SD-CLa, (b) SD-CAs and (c) SD-CGL.

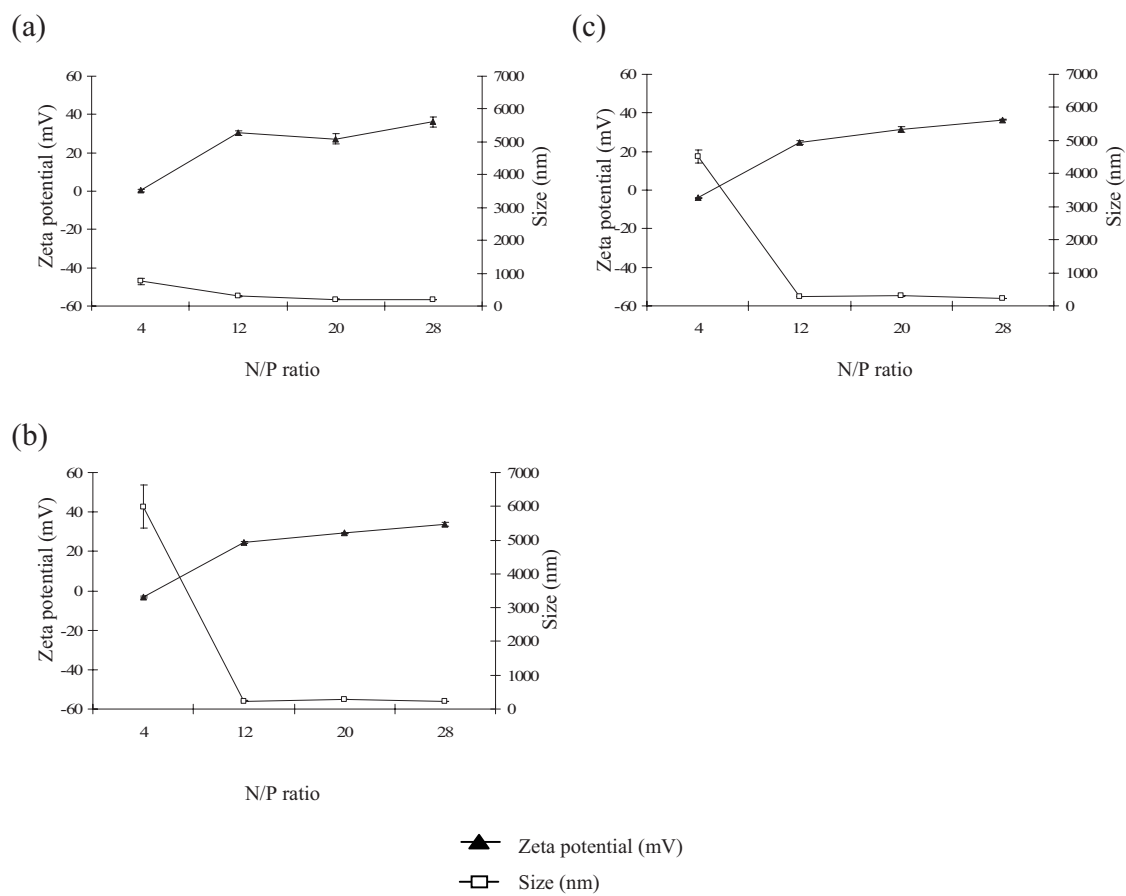


Figure 15 Zeta potential and particle size at varying N/P ratios of SD-CS-45kDa /DNA complexes (a) SD-CLa, (b) SD-CAs and (c) SD-CGL.

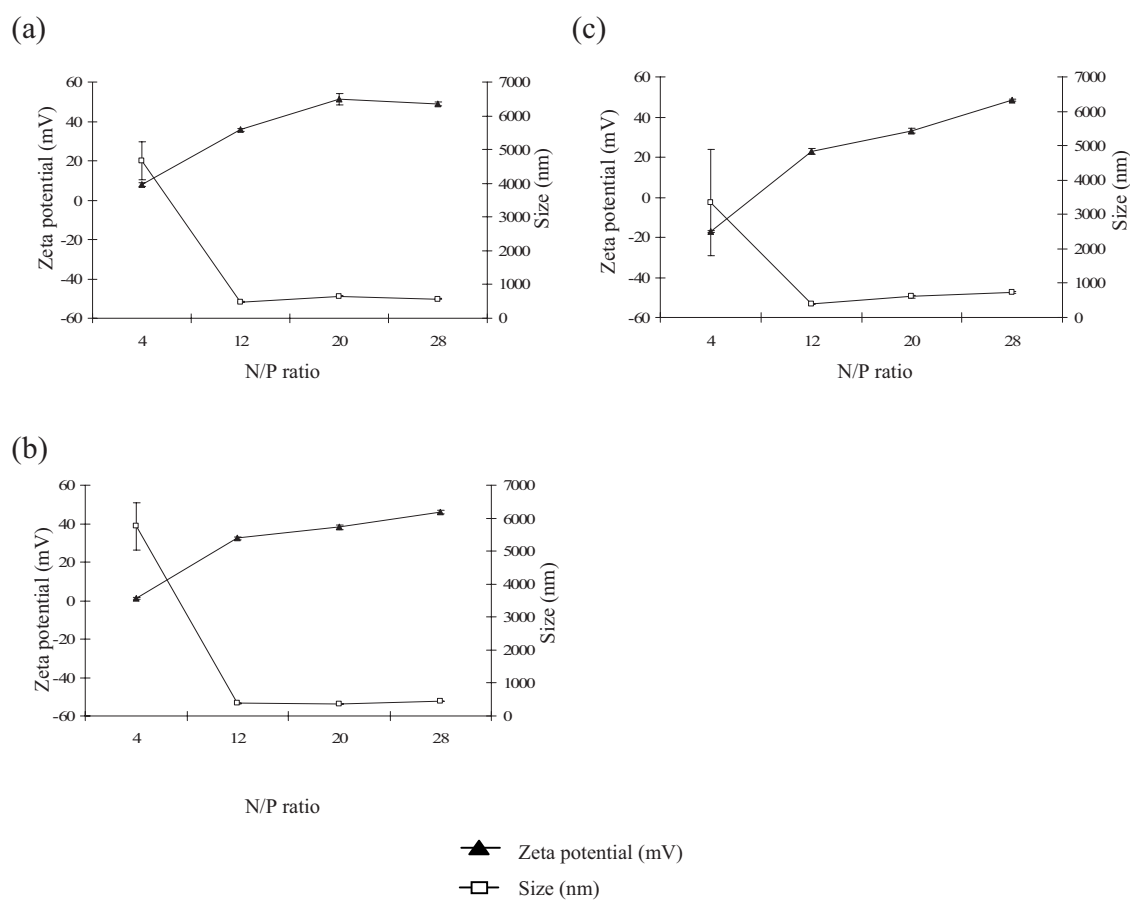


Figure 16 Zeta potential and particle size at varying N/P ratios of SD-CS-200kDa/DNA complexes (a) SD-CLa, (b) SD-CAs and (c) SD-CGL.

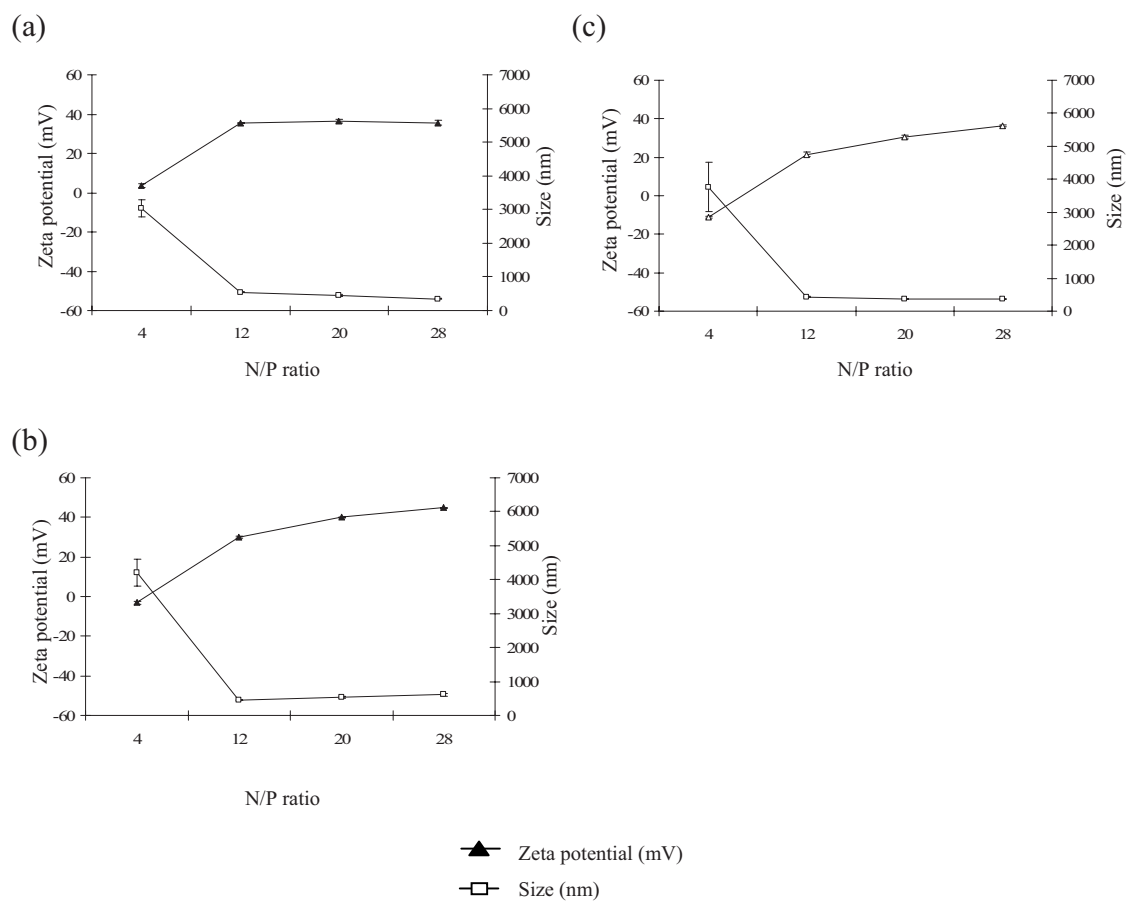


Figure 17 Zeta potential and particle size at varying N/P ratios of SD-CS-460kDa/DNA complexes (a) SD-CLa, (b) SD-CAs and (c) SD-CG1.

The morphology of SD-CLA/DNA complex imaging by TEM is shown in Figure 18. Their shape appeared spherical with mean diameter about 100 nm. The particle size of the complexes at an N/P ratio of 20 was slightly larger than at an N/P ratio of 12 as analyzed by dynamic light scattering.

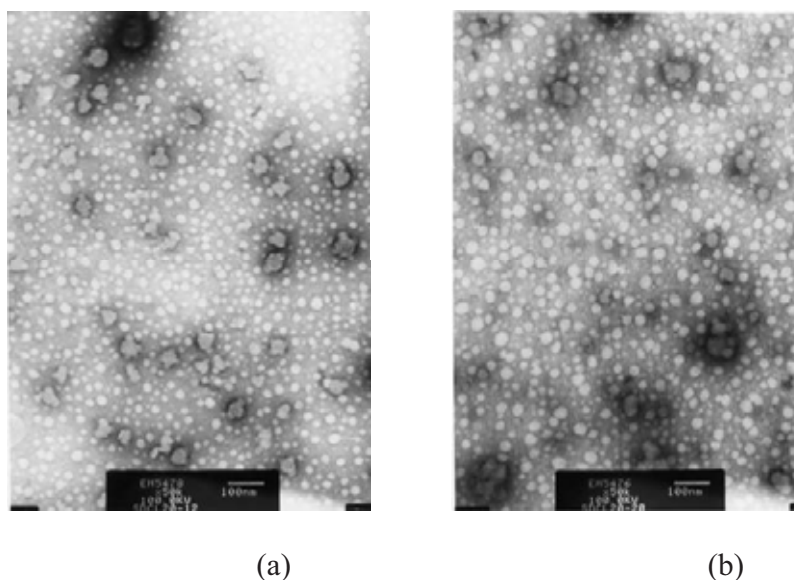


Figure 18 Transmission electron microscope images of SD-CLA-20kDa/DNA complex at N/P ratios of (a) 12 and (b) 20.

### 2.1.2 Effect of MW of chitosan on physicochemical properties of SD-CS/DNA complexes

The MW used to form complex with DNA can be classified in two groups; low MW (20, 45 kDa) and high MW (200, 460 kDa). MW of chitosan affected the binding properties of SD-CS/DNA complexes. At the same SD-CS, low MW chitosan required higher N/P ratios to completely bind the DNA compared to high MW chitosan (Figure 12). The binding affinity of SD-CS increased with increasing chitosan MW (Figure 19). The influence of MW in complex formation and binding affinity could be attributed to a chain entanglement effect. Chain entanglement contributes less to complex formation as the MW of chitosan decreases. An increase in the number of chitosan chains is required to achieve the same N/P ratio compared to higher MW chitosan. Longer chitosan chains in high MW chitosan more easily entangle and trap free DNA once the initial electrostatic interaction has occurred. The need for more

chitosan chains with low MW chitosan/DNA binding may not be energetically favorable for complex formation (Kiang et al., 2004: 5293-5301).

Particle size of SD-CS/DNA complexes formulated with high MW chitosan had higher particle size than low MW chitosan (Figure 14-17). This could be because the higher viscosity of high MW chitosan compared to low MW chitosan leading to larger particle size. The particle size of CS/DNA complexes increased with an increasing chitosan molecular weight was consistent with Maclaughlin et al. (1998: 259-272). They found that larger particle size of high MW chitosan complexes compared to low MW complexes probably due to high MW chitosan being less soluble. As a result, an increase in particle diameter or aggregation could occur.

The zeta potential of SD-CS/DNA complexes was also dependent on the MW of chitosan. The zeta potential of SD-CS/DNA complexes formulated with high MW chitosan was higher than those formulated with low MW chitosan (Figure 14-17). This could be due to the higher valency of high MW chitosan, resulting in the higher zeta potential. The increase in zeta potential in high MW chitosan was also observed by Huang et al. (2005: 391-406).

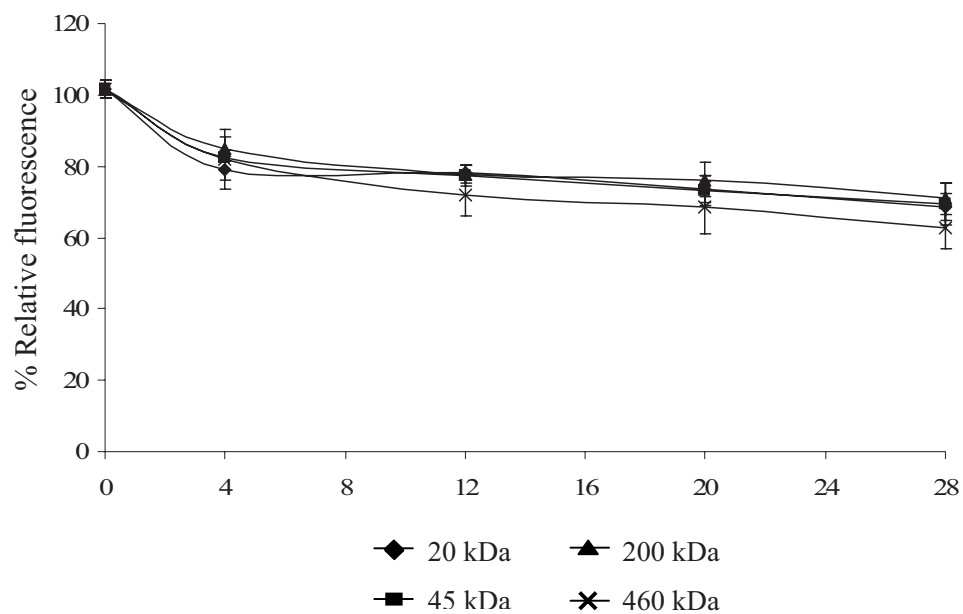


Figure 19 Relative fluorescent intensity of DNA/EtBr complex at varying N/P ratios of SD-CGI at MW (a) 20 kDa, (b) 45 kDa, (c) 200 kDa and (d) 460 kDa.

### 2.1.3 Effect of salt form of chitosan on physicochemical properties of SD-CS/DNA complexes

The complex formation between SD-CS and DNA was checked by agarose gel electrophoresis (Figure 12). The counter ions from SD-CS can be classified into two groups; amino acid counter ion (aspartic and glutamic counter ions) and non-amino acid counter ion (lactate counter ion). At low MW, all SD-CS/DNA complexes did not exhibit significantly different ability to form complex with DNA. The complete complexes were formed at N/P ratios of 4. At high MW, non-amino acid had higher ability to form complex than amino acid. The complete complexes were formed at N/P ratios above 2 and 4 for non-amino acid and amino acid, respectively. The different complex formation would be due to the different counter ions and pH present in the complex solution that could interact with chitosan. Because the size of an aspartate or glutamate counter ion is larger than lactate counter ion, a larger counter ion might partially hinder the complex formation between chitosan and DNA. In addition, a factor that can affect the complex formation between chitosan and DNA is the pH of chitosan solution. Because the pH of SD-CLa solution (pH 4.2-4.3) was lower than SD-CAs (pH 4.6-4.7) and SD-CGI solutions (pH 4.7-4.8) (Table 7). The higher degree of protonation of the amine groups in chitosan can more interact with the DNA at a lower pH. As a result, in SD-CAs/DNA and SD-CGI/DNA solution, more chitosan was required to maintain a positive charge for complete interaction with DNA.

Table 7 pH of SD-CS in various solutions.

SD-CS	pH		
	Water	Complex solution	Transfection medium
SD-CLa	4.2-4.3	6.8-6.9	7.3-7.4
SD-CAs	4.6-4.7	7.1-7.2	7.3-7.4
SD-CGI	4.7-4.8	7.1-7.2	7.3-7.4

The result of EtBr displacement by different SD-CS at various N/P ratios showed that the relative fluorescent intensity of SD-CLa solution was lower than SD-CAs and SD-CGI solutions, confirming that the binding affinity of chitosan in SD-CLa

solution (pH 4.2-4.3) was higher than SD-CAs (pH 4.6-4.7) and SD-CGI solutions (pH 4.7-4.8) (Figure 13), as analyzed in gel electrophoresis. Strand et al. (2005: 3357-3366) and Liu et al. 2005: 2705-2711) studied the interaction between chitosan and DNA at a varied pH. They found that chitosan lost their ability to displace intercalated EtBr from DNA at high pH because the protonation of the amine groups is suppressed and the charge density of chitosan is thus substantially reduced.

The zeta potential was approximately neutral at an N/P ratio of 4 where the complexes almost were completely formed (Figure 14-17). At neutral zeta potential, the particle size of SD-CAs/DNA (pH 7.1-7.2) and SD-CGI/DNA solutions (pH 7.1-7.2) was larger than SD-CLa/DNA solution (pH 6.8-6.9) (Figure 14-17). This difference would be the effect from different counter ions and pH of complex solution. The counter ion with larger size might hinder the interaction between chitosan and DNA. The pH of complex solution also could play an important role on the particle size. The larger particle size of the complexes in SD-CAs/DNA and SD-CGI/DNA solutions compared to SD-CLa/DNA solution might be the loosely formed complexes in a higher pH. This result showed that pH is an important factor that affects the physicochemical properties of chitosan/DNA complexes. Therefore, in order to study the effect of salt form of chitosan on the physicochemical properties and transfection efficiency of chitosan/DNA complexes, it is very necessary to control the pH of complex solution/transfection medium to be the same.

## **2.2 Transfection efficiency of SD-CS/DNA complexes**

SD-CS/DNA complexes were transfected in COS-1 and CHO-K1 cells. The transfected cells were detected by  $\beta$ -galactosidase and luciferase activity assays. The transfection efficiency of PEI/DNA complexes as a control was 2.84 mU/mg protein and  $2.59 \times 10^5$  RLU/mg protein in COS-1 and CHO-K1, respectively. The pH of SD-CS/DNA complex solutions had different values (SD-CLa/DNA, 6.8-6.9; SD-CAs/DNA, 7.1-7.2; SD-CGI/DNA, 7.1-7.2) (Table 7). When they were diluted in pH 7.3-7.4 transfection medium (Opti-MEM or RPMI), the pH of all SD-CS was the same (pH 7.3-7.4) at all N/P ratios (Table 7). The transfection efficiency of all complex solutions was not different from the naked DNA in both COS-1 and CHO-K1 cells (Figure 20, 21). This could be because SD-CS/DNA formation did not produce effective complexes that be able to transfect the cells at this pH of transfection medium. At high

pH value (pH 7.3-7.4), the amine groups of chitosan could be deprotonated, and the interaction between chitosan and DNA was decreased, thereby decreasing the stability of the complex in the transfection medium. In addition, the complexes might have low charge density to be able to associate the cell surface and subsequent uptake. Previous studies suggested that pH of transfection medium is very important to achieve transfection efficiency because chitosan/DNA complexes are positively charged, and can bind with the negatively charged cells through electrostatic interaction at pH below 7.0. When pH of transfection medium is above 7.4, transfection efficiency drastically decreased (Sato, Ishii, and Okahata 2001: 2075-2080; Lavertu et al. 2006: 4815-4824; Zhao et al. 2006 223-228).

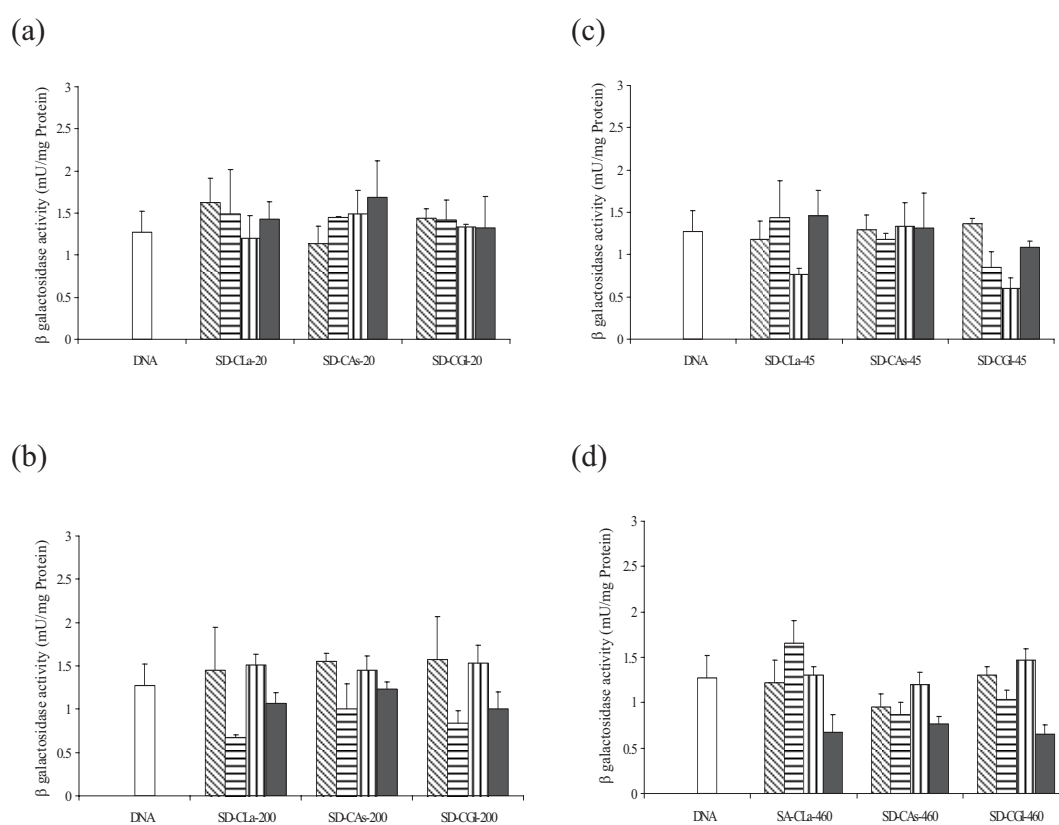


Figure 20 Transfection efficiency of SD-CS/pSV $\beta$ -gal complexes, MW (a) 20 kDa, (b) 45 kDa, (c) 200 kDa, and (d) 460 kDa in COS-1 cells. (▨ = N/P ratio of 4; ▩ = N/P ratio of 12; ▪ = N/P ratio of 20; ■ = N/P ratio of 28)

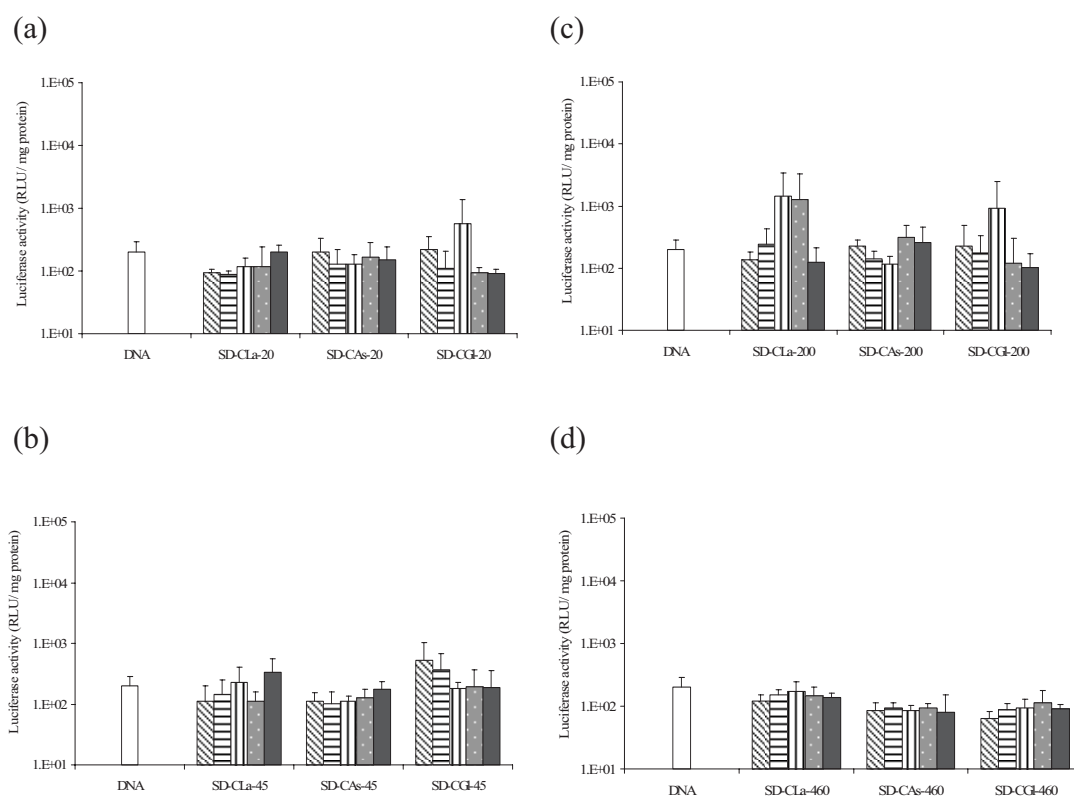


Figure 21 Transfection efficiency of SD-CS/pcDNA3-CMV-Luc complexes, MW

(a) 20 kDa, (b) 45 kDa, (c) 200 kDa, and (d) 460 kDa in CHO-K1 cells.

(▨ = N/P ratio of 2; ▩ = N/P ratio of 4; ▪ = N/P ratio of 6; ▧ = N/P ratio of 8; ▣ = N/P ratio of 12)

### 2.3 Cytotoxicity of SD-CS/DNA complexes

Although SD-CS had low transfection efficiency in both COS-1 and CHO-K1 cells, it was interesting to investigate the cytotoxicity of SD-CS. Cytotoxicity assay was performed in COS-1 cells. The viability of COS-1 cells was examined in the presence of SD-CS/DNA complexes at various N/P ratios as studied in the transfection experiment. Cells without treatment of SD-CS/DNA complexes were considered as a positive control with a cell viability of 100%. SD-CS/DNA complexes formulated with various SD-CS had low cytotoxicity level (Figure 22). The average cell viability was over 90%. PEI was used as a control because it is a cationic polymer commercially available. The average cell viability of PEI/DNA complexes was about 50%.

A required characteristic of a gene delivery system is that it is not cytotoxic. The cytotoxicity of chitosan/DNA complexes was found to be low compared to other

cationic complexes such as poly(L-lysine), DOSPA and DOTAP (Lee et al. 2001: 427-431; Thanou et al. 2002: 153-159; Corsi et al. 2003: 1255-1264). The cytotoxicity of chitosan has been reported in B16F10 cells (Carreño-Gómez and Duncan 1997: 231-240). However, there was no report of cytotoxicity available on COS-1 cells. The cell viability was monitored using the MTT assay after 4 h incubation with SD-CS/DNA complexes. The SD-CS/DNA complexes did not affect the viability of COS-1 cells. This showed that SD-CS/DNA complexes formulated with SD-CAC, SD-CAs, SD-CGI and SD-CLa were safe at N/P ratios between 4 to 28.

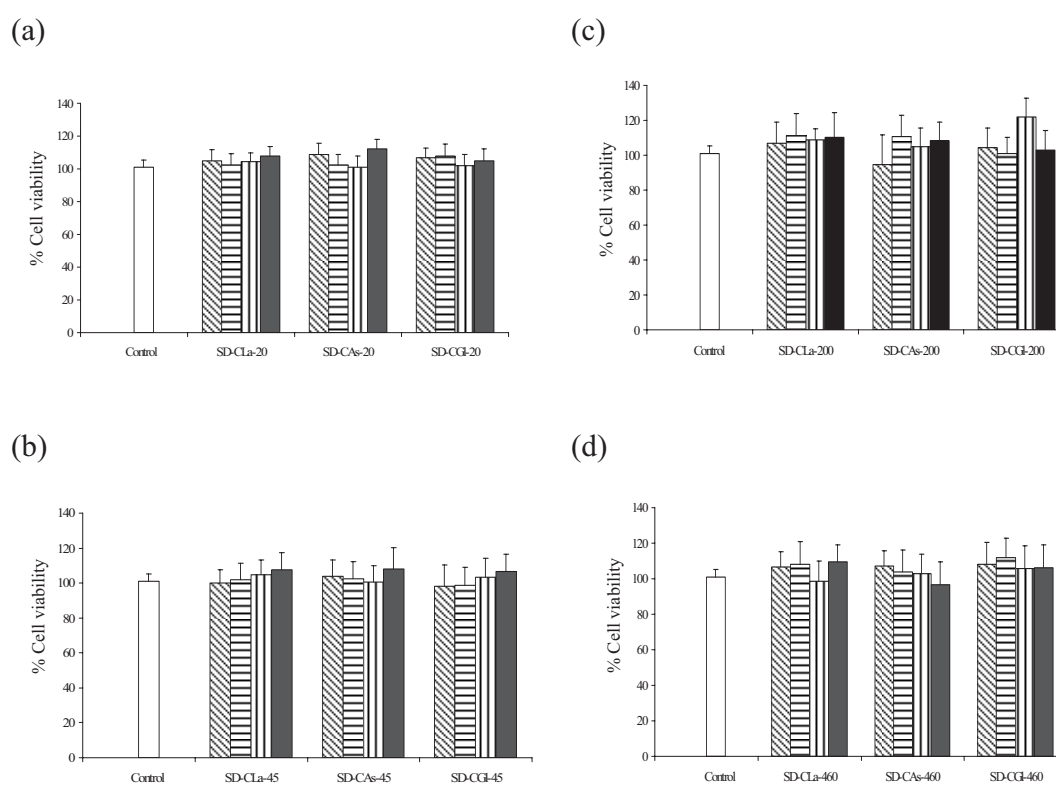


Figure 22 Effect of SD-CS/DNA complexes formulated with SD-CS of MW (a) 20 kDa, (b) 45 kDa, (c) 200 kDa, and (d) 460 kDa on COS-1 cell viability. (▨ = N/P ratio of 4; ▤ = N/P ratio of 12; ▥ = N/P ratio of 20; ■ = N/P ratio of 28).

### **3. Characterization of CS/DNA complexes**

#### **3.1 Physicochemical properties of CS/DNA complexes**

From the study of SD-CS/DNA complexes, the physicochemical properties and the transfection efficiency of the complexes could be resulted from the effect of salt form of chitosan and pH of complex solution. In addition, it has been reported that the biological activities of the transfection reagents highly associate with their physicochemical properties (Pedroso de Lima et al. 2001: 277-294; Thomas and Klibanov 2003: 27-34). The variable MW of chitosan, N/P ratio and pH of transfection medium influenced the physicochemical properties and transfection efficiency of chitosan/DNA complexes (Sato et al., 2001: 2075-2080; Rómoren et al. 2003: 115-127; Ishii, Okahata and Sato 2001: 51-64; Haung et al. 2005: 391-406; Lavertu et al. 2006: 4815-4824; Zhao, Yu, et al., 2006: 223-228) Therefore, the complex formation, particle size and zeta potential of CS/DNA complexes were investigated with the complex solution of different pH, N/P ratios, salt forms and MW of chitosan.

##### **3.1.1 Effect of pH on physicochemical properties of CS/DNA complexes**

The effect of pH on the formation of CS/DNA complexes was carried out in the complex solution at pH 3.0, 5.0 and 6.5. The gel electrophoresis shows that, at the pH 3.0, a complete complex was formed at an N/P of 1. When the pH of complex solution increased to 5.0 and 6.5, N/P ratios at which the complete complexes were formed, increased to 2 and 4, respectively (Figure 23). This showed that the DNA binding was dependent on the pH of complex solution. The higher pH of complex solution required a higher charge ratio to completely bind the DNA. The different complexing ability could be due to the different level of protonated amine in chitosan backbone, resulting from the different pH.

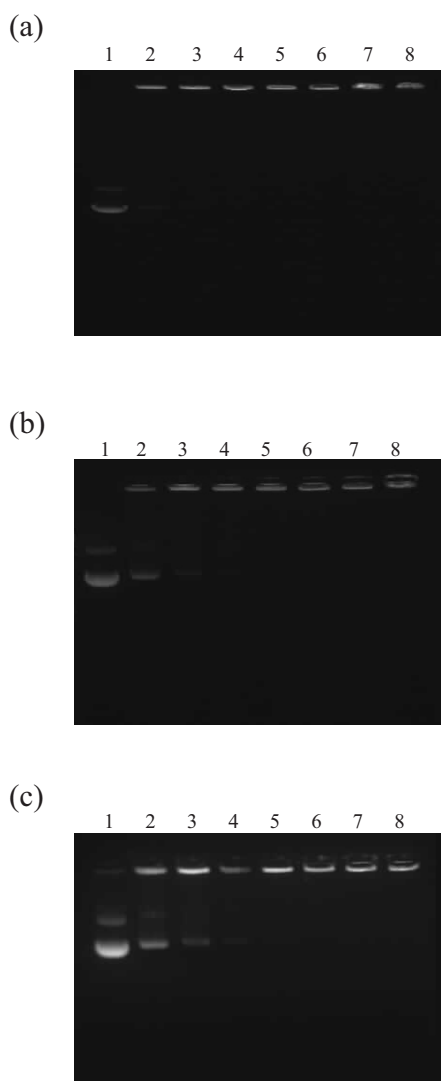


Figure 23 Gel electrophoresis of CAC-45kDa/DNA complexes at pH (a) 3.0, (b) 5.0 and (c) 6.5. Lane 1, pcDNA3-CMV-Luc plasmid; lanes 2-8, CAC/DNA complexes at N/P ratios of 0.5, 1, 2, 4, 6, 8 and 12, respectively.

Chitosan is a weak base with a  $pK_a$  value of about 6.2-7.0. When it presents in acidic solution, the amine groups in chitosan backbone can be protonated and more in lower pH of solution, resulting in a higher level of protonated amine in its backbone. The level of protonated amine in chitosan in high pH solution is less than that in low pH solution; therefore, more chitosan was required to maintain a positive charge for complete interaction with DNA. The protonated amine and unprotonated amine of

chitosan in the complex solution at various pH calculated from Henderson-Hasselbalch equation (3) is shown in Table 8. The  $pK_a$  of chitosan used to calculate was 6.6.

$$pH = pK_a + \log \frac{[\text{base}]}{[\text{acid}]} \quad (3)$$

Table 8 Protonated amine and unprotonated amine of chitosan in the complex solution at various pH of complex solution at  $pK_a$  of chitosan of 6.6.

pH	Protonated amine in chitosan (%)	Unpronated amine in chitosan (%)
3.0	99.97	0.03
5.0	97.55	2.45
6.5	55.55	44.45
7.4	20	80

Lee et al. (1998: 213-220) studied the effect of pH on the formation between a chitosan derivative and a plasmid DNA. They found that free DNA dissociated from chitosan/DNA complex observed by gel electrophoresis at pH above 8.0. They suggested that this observation could be due to the unionized form of amino groups in chitosan, resulting in the decrease of association between chitosan and DNA.

The effect of pH on the size of CS/DNA complexes was investigated in a different pH of complex solution, 3.0 and 6.5. At an N/P of 2, the particle size of the complexes at pH 6.5 was larger than those at pH 3.0 (Figure 24). This could be due to incompletely formed complexes at high pH. As a result, the interaction between chitosan and DNA was low and the particle size of the complexes become larger.

The charge density of chitosan is reduced when the pH of the chitosan solution increases from low to high pH. Due to the reduced charge density of chitosan at high pH, a weaker interaction between the DNA and chitosan is expected. As a consequence, the size of the complex increases as the pH increases (Romóren et al. 2003: 115-127).

When the N/P ratio was greater than 2, the particle size of the complexes was almost the same at both pH 3.0 and 6.5, confirming that complete CS/DNA complexes were formed. High MW chitosan showed the same particle size at both pH 3.0 and 6.5 (Figure 25). This could be due to high DNA binding affinity with high MW chitosan. Thus, it can effectively bind the DNA at both pH levels.

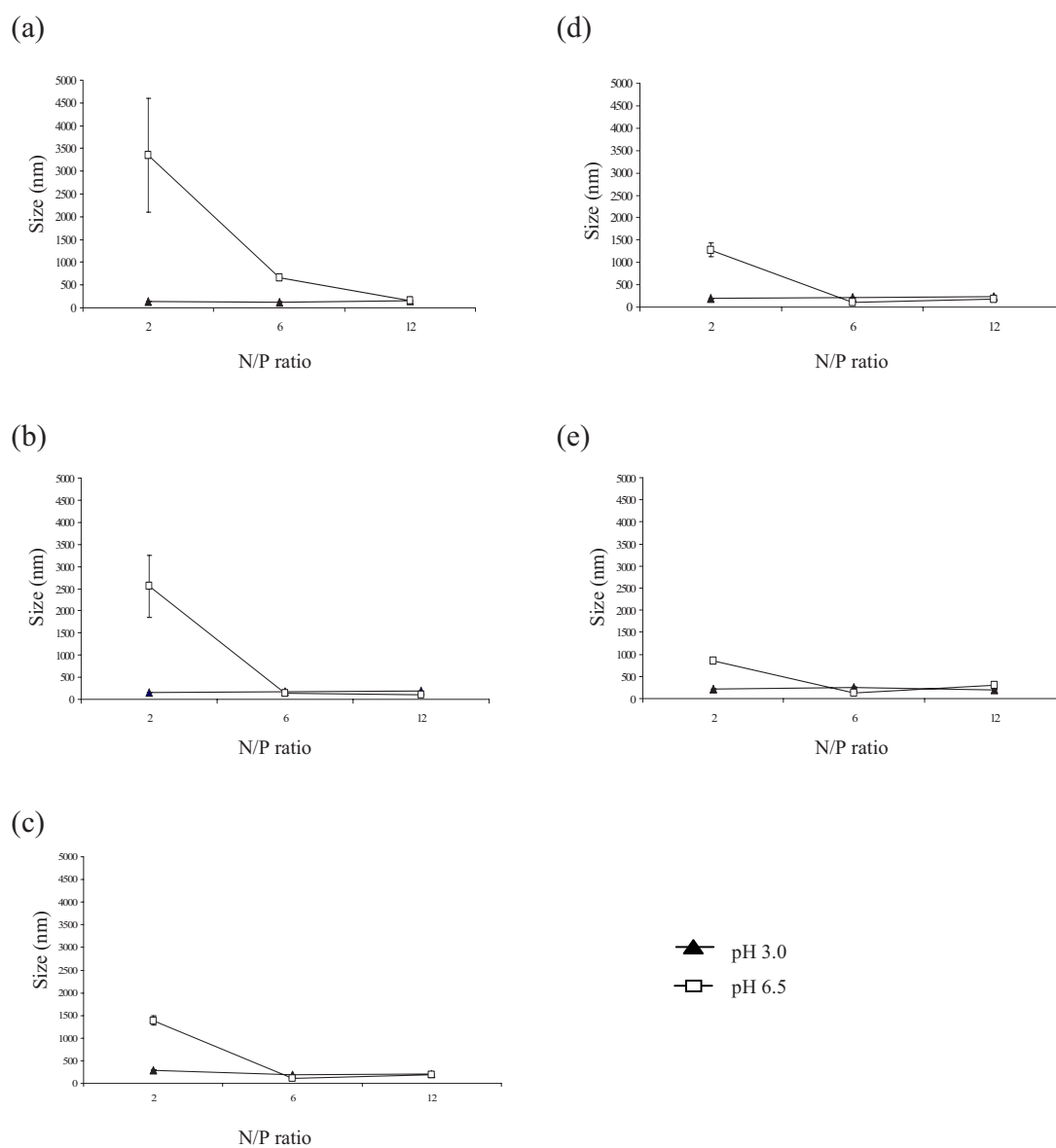


Figure 24 Particle size at varying N/P ratios of CS-45kDa/DNA complexes with different chitosan salts (a) CHy, (b) CLa, (c) CAc, (d) CAs and (e) CGl at pH 3.0 and 6.5.

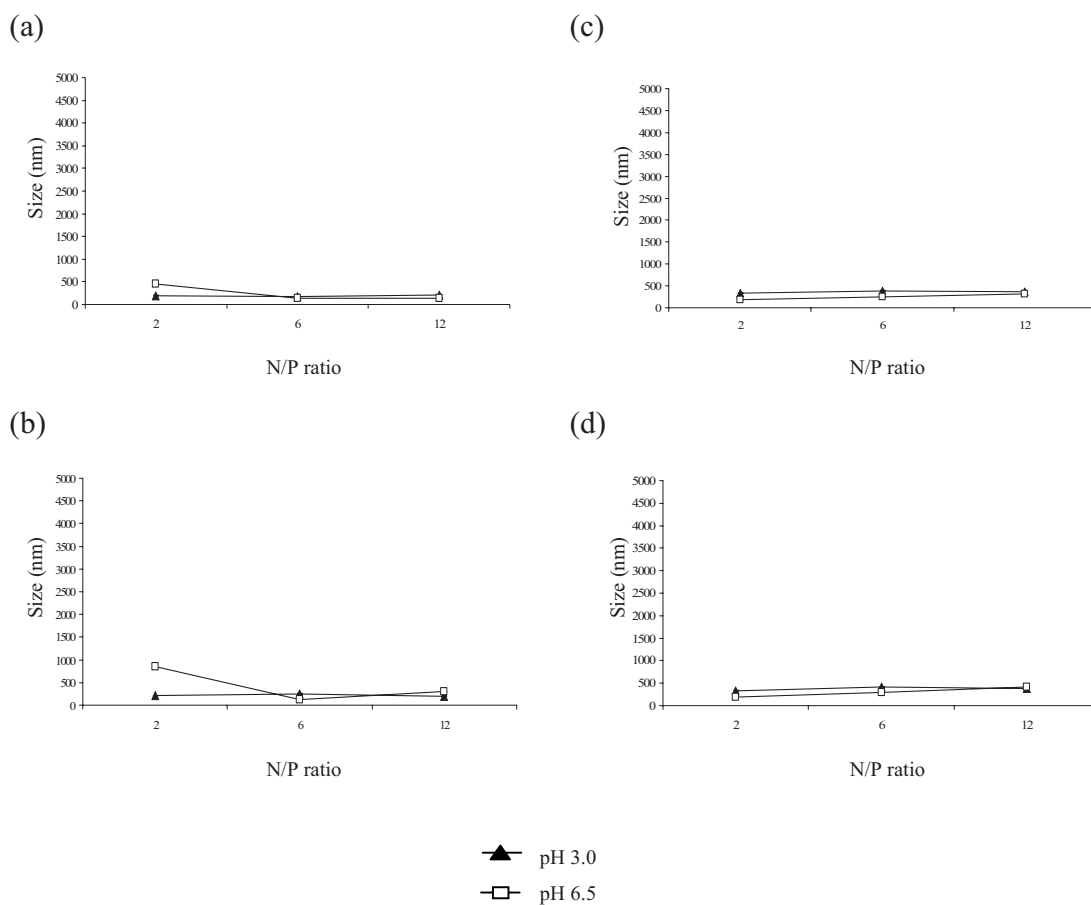


Figure 25 Particle size at varying N/P ratios of of CGI/DNA complexes with different chitosan MW (a) 20 kDa, (b) 45 kDa, (c) 200 kDa and (d) 460 kDa at pH 3.0 and 6.5.

The effect of pH on the zeta potential of CS/DNA complexes was carried out in complex solution at pH 3.0 and 6.5. It was clearly observed that the different pH value resulted in different surface charge of the complexes. The zeta potential of the complexes at pH 3.0 was extremely higher than those at pH 6.5 (Figure 26-27), illustrating that higher level of protonated amine in chitosan backbone was obtained at lower pH. This result is similar to that of chitosan/DNA complexes in which the protonation of chitosan drastically occurred when pH of medium altered from high to low pH (Ishii, Okahata and Sato 2001: 51-64; Zhao et al. 2006: 223-228). Mao et al. (2001: 399-421) demonstrated that the pH of buffer, in which chitosan is dissolved, affects the charge of its complex. At pH 5.5-5.7, about 90% of the amino groups are protonated. At a neutral pH the degree of protonation is reduced, meaning that the actual

charge of the complex is different from the charge of a complex of the same charge ratio made at pH 5.5. As a consequence, the zeta potential of chitosan/DNA complex is reduced with an increased pH (Mao et al. 2001: 399-421).

Since the physicochemical properties of CS/DNA complexes depended on the pH of complex solution; therefore, the pH of complex solution was adjusted to 6.5 in all complex formulations.

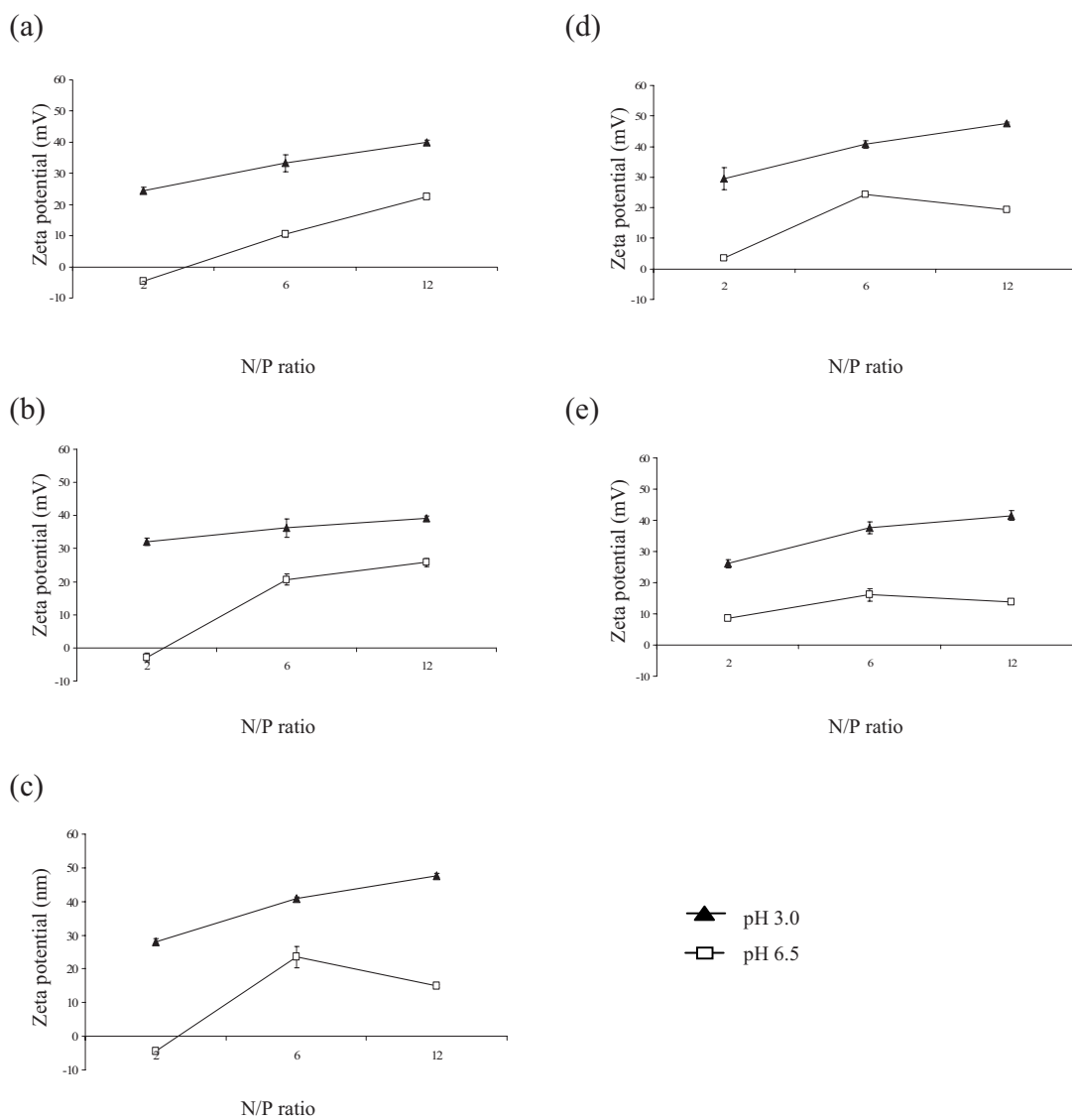


Figure 26 Zeta potential at varying N/P ratios of CS-45kDa/DNA complexes with different chitosan salts (a) CHy, (b) CLa, (c) CAc, (d) CAs and (e) CGl at pH 3.0 and 6.5.

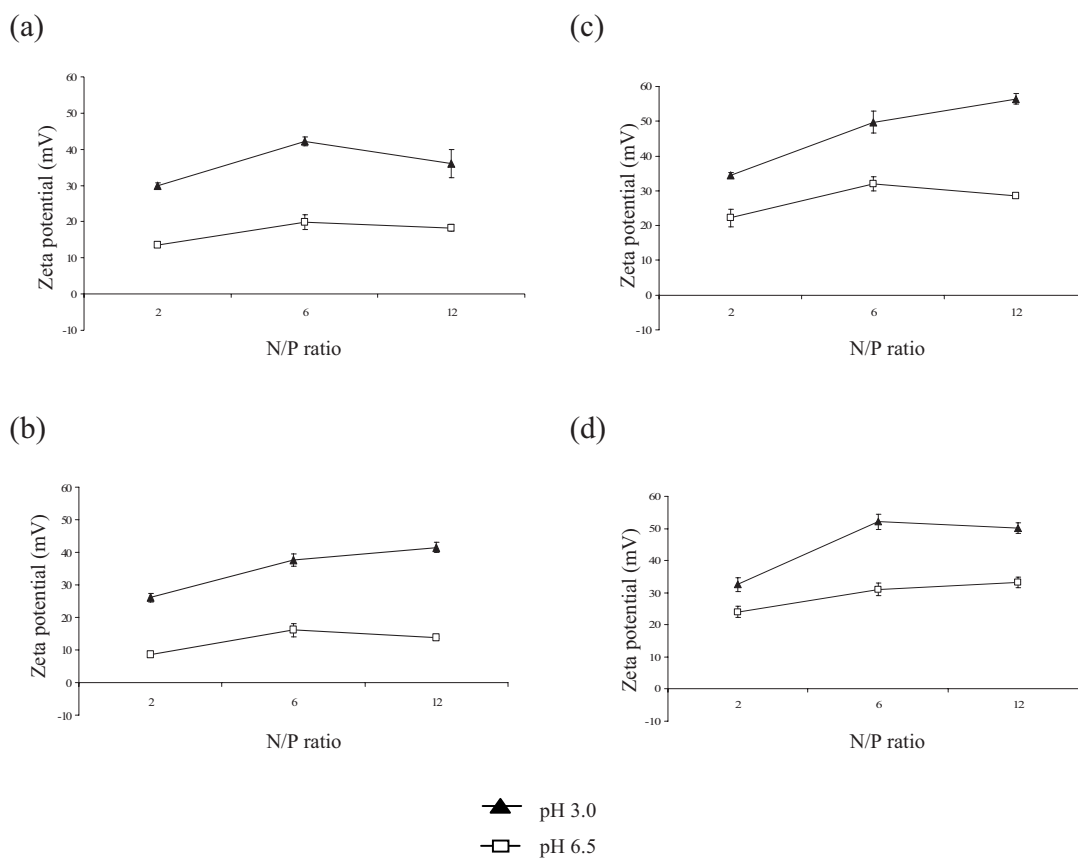


Figure 27 Zeta potential at varying N/P ratios of CGI/DNA complexes with different chitosan MW (a) 20 kDa, (b) 45 kDa, (c) 200 kDa and (d) 460 kDa at pH 3.0 and 6.5.

### 3.1.2 Effect of N/P ratio on physicochemical properties of CS/DNA complexes

At the same pH (pH 6.5), the gel electrophoresis showed that the extent of DNA retardation in the gel loading well increased with increasing ratio of CS/DNA (Figure 28). When the complete complexes were formed, the DNA was totally retained in the gel loading well. This was because the gradual increase in amount of chitosan gradually bound the DNA. When the amount of chitosan was sufficient, complete complexes were formed.

It has been previously reported that complexes having a particle size of 100-500 nm have successfully transfected the cells (Maclaughlin et al. 1998: 259–272; Li et al. 2003: 7-18; Özgel and Akbuğa 2006: 44-51; Lavertu et al. 2006: 4815-4824). The average particle size of CS/DNA complexes formulated with various CS and MW in these studies was in the range of 120-400 nm.

At the same pH (pH 6.5), the particle size of CS/DNA complexes depended on the N/P ratio. The particle size of CS/DNA complexes formulated with chitosan MW 45 kDa increased with an increasing N/P ratio from 1 to 2 and decreased to constant value in the range of 101 to 299 nm after a charge ratio of 2 (Figure 29). The complexes were nanosize particles at all N/P ratios whereas they were microsized at an N/P ratio of 2 (850 to 3,400 nm). A larger particle size may result from the loosely formed complexes. This finding was in compliance with a study performed with chitosan/DNA complex, showing that the particle size of nearly complete complex was microsized (Özgel and Akbuğa 2006: 44-51). At N/P ratios above 2, the particle size of all CS/DNA complexes increased with increasing N/P ratio. This was due to the intermolecular cross-linking between DNA strands by self-aggregates with an excess amount of CS.

The zeta potential of CS/DNA complexes was also dependent on the N/P ratio (Figure 29). At an N/P ratio lower than 2, the CS/DNA complex had a negative value of zeta potential (-35 to -60 mV). This was due to the amount of chitosan not sufficient to form complex with DNA. At an N/P ratio of 2, where complete complexes were almost formed, the zeta potential was nearly zero (-4 to +3 mV). At N/P ratios higher than 2, where complete complexes were formed, the zeta potential was positive (+15 to +28 mV). The zeta potential of the complexes increased with an increase in N/P ratio could be due to their higher density of protonated amines in the chitosan backbone. A similar result was observed in previous studies (Kiang et al. 2004: 5293-5301; Lavertu et al. 2006: 4815-4824). At N/P ratios higher than 2, an excess of amine groups

is available from complex formation, and the final zeta potentials plateau to almost equivalent levels (+15 to +28 mV) for all CS compounds studied.

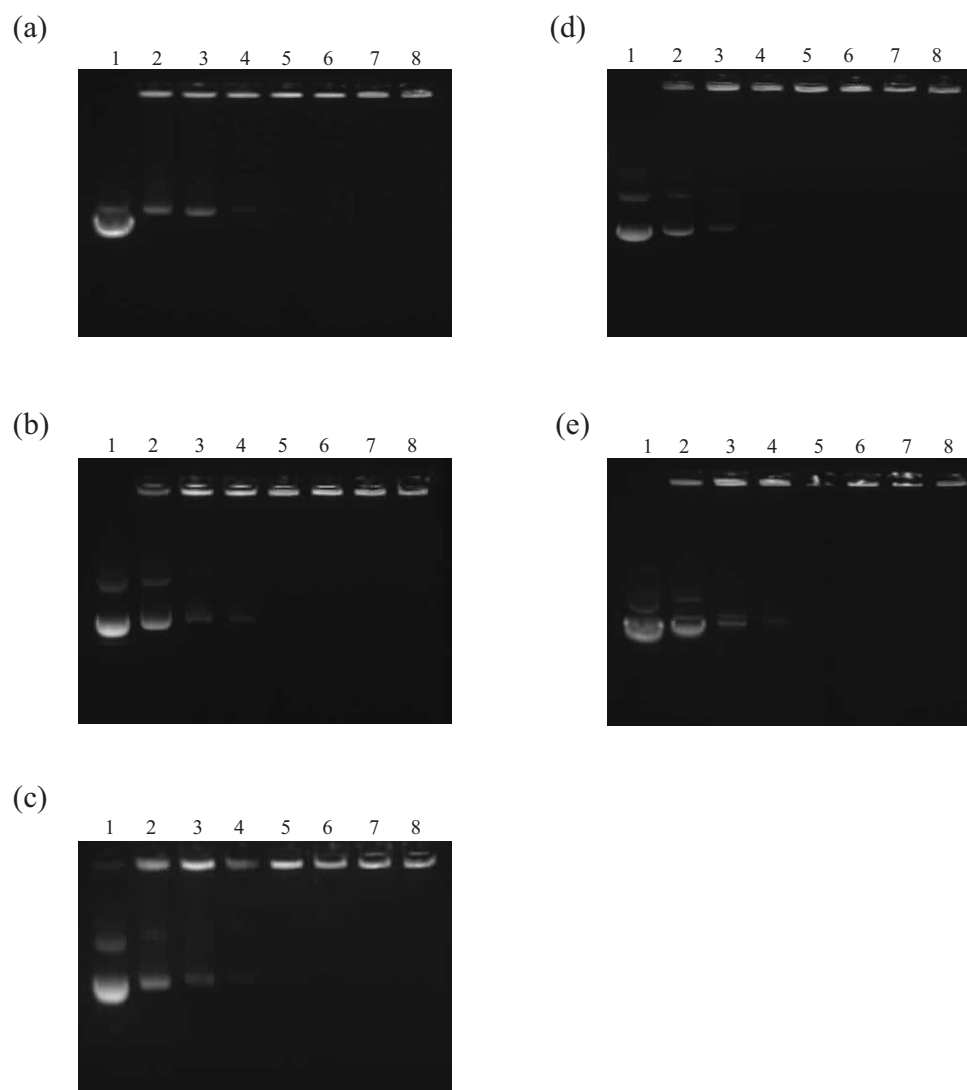


Figure 28 Gel electrophoresis of CS-45kDa/DNA complexes with chitosan different salts (a) CHy, (b) CLa, (c) CAc, (d) CAs and (e) CGI. Lane 1, pcDNA3-CMV-Luc plasmid; lanes 2-8, CS/DNA complexes at N/P ratios of 0.5, 1, 2, 4, 6, 8 and 12, respectively.

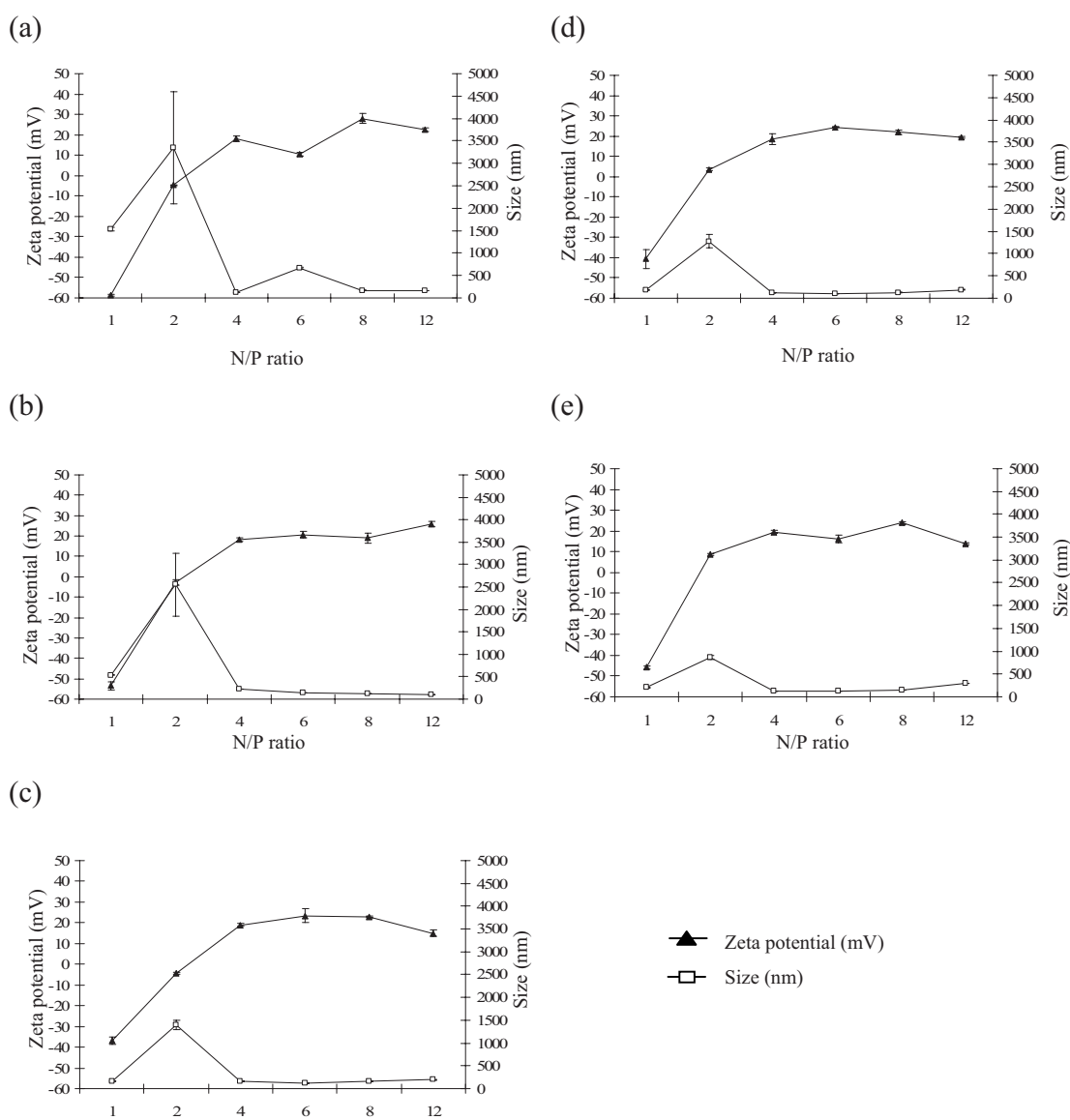


Figure 29 Zeta potential and particle size at varying N/P ratios of CS-45kDa/DNA complexes (a) CHy, (b) CLa, (c) CAC, (d) CAs and (e) CGL.

### **3.1.3 Effect of MW of chitosan on physicochemical properties of CS/DNA complexes**

In order to investigate the effect of MW on the complex formation, CGI/DNA complexes with chitosan of different MW (20, 45, 200 and 460 kDa) were formulated. CGI was used to study because it is one of CS that has been used for gene delivery (Li et al. 2003: 7-18). Figure 30 shows that the complexes were completely formed at N/P ratios above 1 for chitosan MW 200 and 460 kDa, whereas complete complexes for chitosan MW 20 and 45 kDa were formed at N/P ratios above 2. The low MW chitosan required higher N/P ratio to completely form complexes compared to high MW chitosan. This could be due to the different binding ability of chitosan MW. High MW chitosan has longer chitosan chain that can efficiently entangle and trap the DNA than low MW chitosan. Therefore, low MW chitosan needs more chitosan to form complete complex with DNA. The complex formation depending on chitosan MW was also observed by Kiang et al. (2004: 5293-5301) and Haung et al. (2005: 391-406).

The particle size of the complexes had a trend that showed an increase in the particle size as the MW was increased (Figure 31). Although it may be expected that a higher MW chitosan can interact with and thus condense the DNA more efficiently than low MW chitosan, as analyzed by electrophoresis (Figure 30), the particle size of the complex with higher MW should be smaller. This is outweighed by the fact that higher MW chitosan is less soluble, and as a result, an increase in particle diameter or aggregation may result (Maclaughlin et al. 1998: 259–272).

The zeta potential of CS/DNA complexes was dependent on the MW of chitosan. The zeta potential of CS/DNA complexes formulated with high MW chitosan was higher than those formulated with low chitosan MW (Figure 31). This difference could be due to the high valency of high MW chitosan. The long chain of high MW chitosan can effectively entangle and trap the DNA, and leaves unbound protonated amines available on the complex surface, thereby resulting in its highly positive charge density. Haung et al. (2005: 391-406) reported that highly positive charge density of high MW chitosan enhances the cellular uptake and transfection efficiency of their complexes.

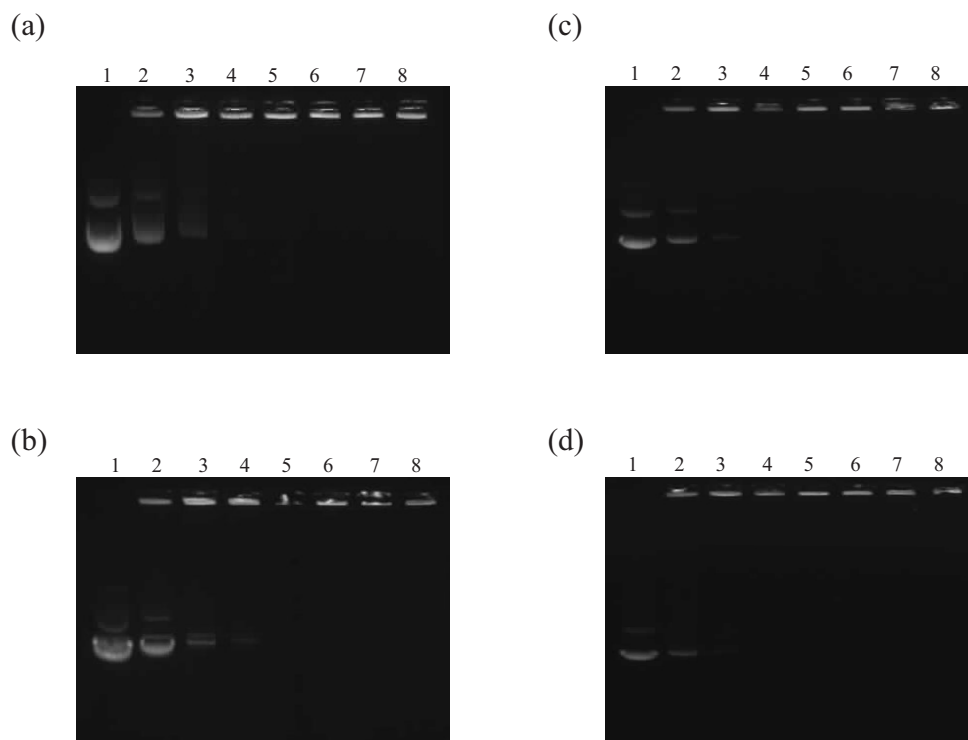


Figure 30 Gel electrophoresis of CGI/DNA complexes complexes with different chitosan MW (a) 20 kDa, (b) 45 kDa, (c) 200 kDa, and (d) 460 kDa. Lane 1, pcDNA3-CMV-Luc plasmid; lanes 2-8, CGI/DNA complexes at N/P ratios of 0.5, 1, 2, 4, 6, 8 and 12, respectively.

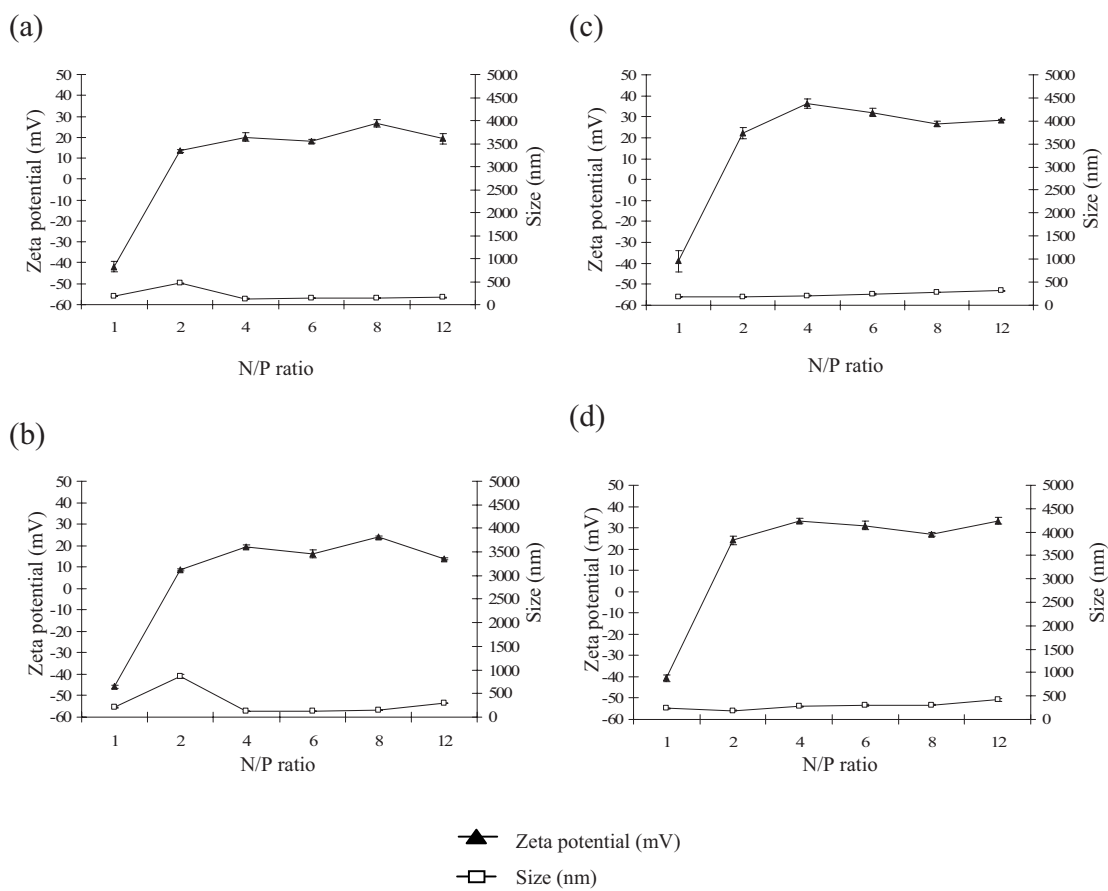


Figure 31 Zeta potential and particle size at varying N/P ratios of CGI/DNA complexes with different MW (a) 20 kDa, (b) 45 kDa, (c) 200 kDa, and (d) 460 kDa.

### 3.1.4 Effect of salt form of chitosan on physicochemical properties of CS/DNA complexes

Low MW chitosan (45 kDa) was used to study the effect of the salt forms of chitosan on the physicochemical properties and transfection efficiency of their CS/DNA complexes because low MW chitosan had a promise gene transfection investigated in preliminary study.

At a constant chitosan MW of 45 kDa, the CS/DNA complexes formulated with CHy, CLa, CAc, CAs and CGI was formed at N/P ratios above 2, showing that all CS appeared similar abilities to form complexes with DNA (Figure 28).

The particle size of CS/DNA complexes formulated with different salts depended on the type of salt (counter ions) of chitosan. At neutral zeta potential (N/P ratio 2), all CS formulated with chitosan MW 45 kDa showed the largest particle size and the size rank of the complexes was CHy (3346 nm) > CLa (2553 nm) > CAc (1390 nm) > CAs (1276 nm) > CGI (856 nm) (Figure 29). This variation could be the effect from different counter ions formed from acids with different  $pK_a$  values. At the same pH, acids with lower  $pK_a$  dissociate to yield a greater amount of anions than those with higher  $pK_a$ . These ions could neutralize the positive charge of CS, thereby decreasing the interaction between CS and DNA. As a result, the binding of chitosan and DNA is loose and the size of the complex likely becomes larger. The acids used to form CS in this study can be classified into two groups; amino acids (aspartic acid:  $pK_a = 3.65$  and glutamic acid:  $pK_a = 4.25$ ), and non-amino acids (hydrochloric acid: 100% dissociation, lactic acid:  $pK_a = 3.86$  and acetic acid:  $pK_a = 4.75$ ). The size of the complexes decreased in the order of CHy > CLa > CAc for non-amino acids and CAs > CGI for amino acids, which corresponds to the increasing order of  $pK_a$ .

From the variation in particle size of the complexes with different CS, it can be observed that, at the same complete complexes, gel electrophoresis could not reflect the different particle size of the complexes.

AFM was used to assess the size and morphology of chitosan/DNA complexes at N/P ratios of 2 and 12. From the AFM images of CS/DNA complexes at the neutral zeta potential, the morphology of the complexes was spherical of shape in all CS. The particle size of the complexes formulated with non amino acid was in the range of 1,500-5,000 nm, whereas those formulated with amino acid was in the range of 500-1,000 nm (Figure 32). At an N/P ratio of 12, where a complete complex was formed and

the DNA was completely condensed, the shape of the complex was spherical with mean diameter about 100 nm (Figure 33). This morphology is also typical when DNA is complexed with other MW chitosan (Liu et al, 2005, Danielsen, Varum and Stokke 2004: 928-936) or other condensing reagents, i.e., PLL (Kwoh et al. 1999: 171-190) and PEI (Dunlop et al. 1997: 3095-3101).

The zeta potential of CS/DNA complexes was dependent on the type of the salts (counter ions). At N/P ratio of 2 (nearly completely-formed complex), the zeta potential of CHy/DNA, CLa/DNA, CAc/DNA, CAs/DNA and CGI/DNA complexes was -4.64, -2.93, -4.35, +3.64 and +8.63 mV, respectively (Figure 29). The zeta potential of CS/DNA complexes formulated with CAs/DNA and CGI/DNA complexes (amino acids) was slightly positive value, whereas those formulated with CHy/DNA CLa/DNA and CAc/DNA complexes (non amino acids) was slightly negative value. This might be due to the amine existing in the aspartate and glutamate counter ions that was protonated in the medium, subsequently increasing the level of positive charge of their complexes.

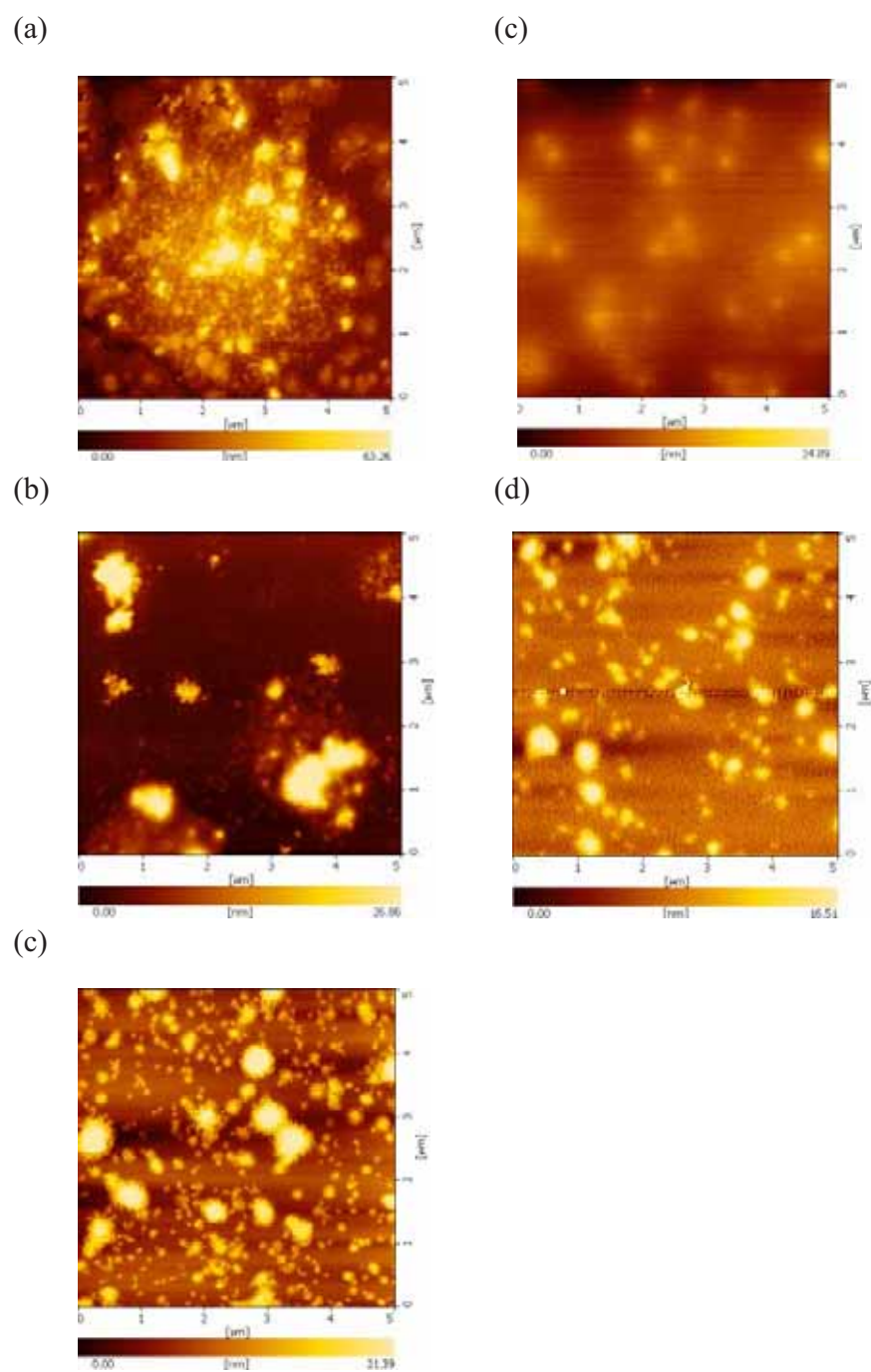


Figure 32 Topological image of atomic force microscopy of CS-45kDa/DNA complexes (a) CHy, (b) CLa, (c) CAc, (d) CAs and (e) CGI at an N/P of 2.

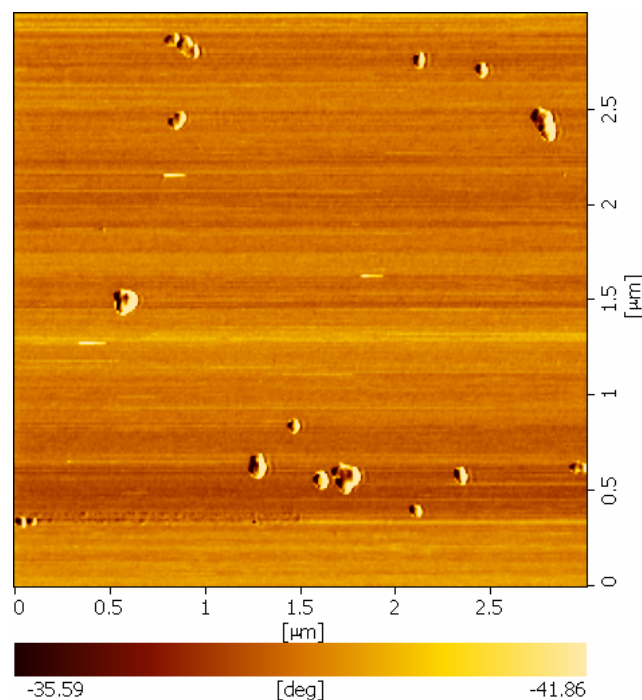


Figure 33 Phase contrast image of atomic force microscopy of CLa-20/DNA complexes at an N/P of 12.

### 3.2 Transfection efficiency of CS/DNA complexes

#### 3.2.1 Optimization of transfection condition of CS/DNA complexes

Because the physicochemical properties of the complexes directly connect with their bioactivities, investigating the transfection in different conditions in order to obtain the best transfection efficiency is necessary. Previous studies demonstrated that the gene delivery potential of chitosan in mammalian cells depends on several factors such as chitosan MW, N/P ratio, pH of transfection medium/complex solution and cell type (Sato, Ishii, and Okahata 2001: 2075-2080; Ishii, Okahata and Sato 2001: 51-64; Rómoren et al. 2003: 115-127; Haung et al. 2005: 391-406; Lavertu et al. 2006: 4815-4824; Zhao et al., 2006: 223-228). Therefore, following studies including amount of acid, pH of transfection medium, and incubation time of the complex with the cells, transfection efficiency in these different conditions were investigated to find an optimal transfection condition and gene expression level.

In order to study the different amounts of the acid in CS solution on transfection efficiency, transfection of CHO-K1 cells using CAC/DNA complexes as a model of CS/DNA complexes. CAC/DNA complexes were formulated at N/P ratios of 2, 4, 6, 8 and 12 and carried out the transfection in RPMI. The amount of acetic acid in

CAC solution was varied from 0.1%, 0.2% and 0.6% w/v. The transfection efficiency increased when the amount of acetic acid in CAC solution increased. 0.6% w/v acetic acid in CAC solution yielded significantly higher transfection efficiency than 0.1%, 0.2% w/v acetic acid ( $p < 0.05$ ) (Figure 34). The high transfection efficiency at high amount of acid could be due to the successful transfected cells obtaining from highly protonated chitosan/DNA complexes. An increase in amounts of the acid could increase in the positive charge on the complex, thereby promoting the interaction with the negatively charged cell surface and an association of the complex with the cell surface. The maximum transfection efficiency achieved at N/P ratios of 6 and 8. At N/P ratios of 2 and 4, the transfection efficiency of CAC/DNA complexes was not different from the naked DNA. This could be due to the amount of chitosan was too low to transfect the cells. At an N/P ratio of 12, the transfection efficiency of CAC/DNA complexes decreased. This could be due to the high binding between chitosan and DNA when the amount of chitosan increased. The reduced transfection efficiency when the N/P ratio was too high also demonstrated by Rómoren et al. (2003: 115-127). They transfected chitosan/DNA complexes into *Epithelioma papulosum cyprinid* cells at N/P ratios of 0.5, 1, 2, 3, 4, 5 and 10.

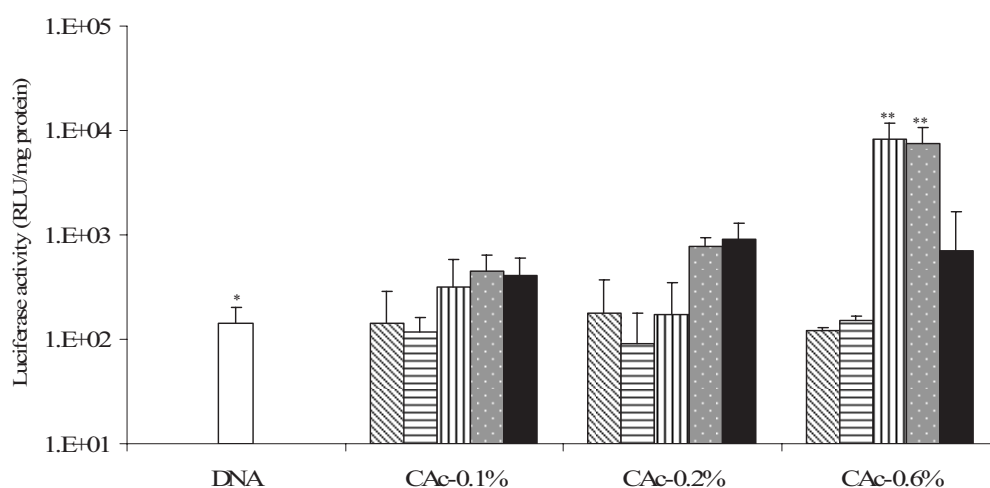


Figure 34 Transfection efficiency of CAC-45kDa/DNA complexes at 0.1%, 0.2% and 0.6% acetic acid solution in CHO-K1 cells. (▨ = N/P ratio of 2; ▤ = N/P ratio of 4; ▥ = N/P ratio of 6; ▦ = N/P ratio of 8; ▧ = N/P ratio of 12). Differences values \* vs \*\* were statistically significant ( $P < 0.05$ , ANOVA, LSD).

The transfection efficiency decreased when the pH of transfection medium increased (Figure 35). The highest transfection efficiency was obtained at pH 6.0. When the pH of transfection medium increased to 7.4, the transfection efficiency significantly decreased. The low transfection efficiency was similar to the transfection of SD-CS/DNA complexes when the transfection medium pH of 7.4 was used. This could be attributed to the low degree of protonation of the amine groups at pH 7.4, resulting in the loosely formed complex that can not effectively associate with the cell surface and subsequent uptake. Zhao et al. (2006: 223-228) suggested that the transfection efficiency of chitosan/DNA complexes dramatically decreased when the pH of transfection medium increased, attributing to the dissociation of free plasmid from the complexes at higher pH. Strand et al. (2005: 3357-3366) studied the stability of chitosan/DNA complexes at a varied pH of buffer solution. They showed that chitosan/DNA complexes rapidly dissociated at high pH. At low pH value, the amine groups of chitosan could be highly protonated, and the interaction between chitosan and DNA was increased, thereby increasing the stability of the complex in the transfection medium. In addition, the complexes had high charge density that could be able to associate the cell surface and subsequent uptake. These results illustrated that there is the extreme importance of pH of transfection medium to gene transfer mediated by chitosan, which is a unique property of this vector. Previous studies reported that pH condition of transfection medium is very important to achieve high transfection efficiency (Sato, Ishii, and Okahata 2001: 2075-2080; Ishii, Okahata and Sato 2001: 51-64; Lavertu et al. 2006: 4815-4824).

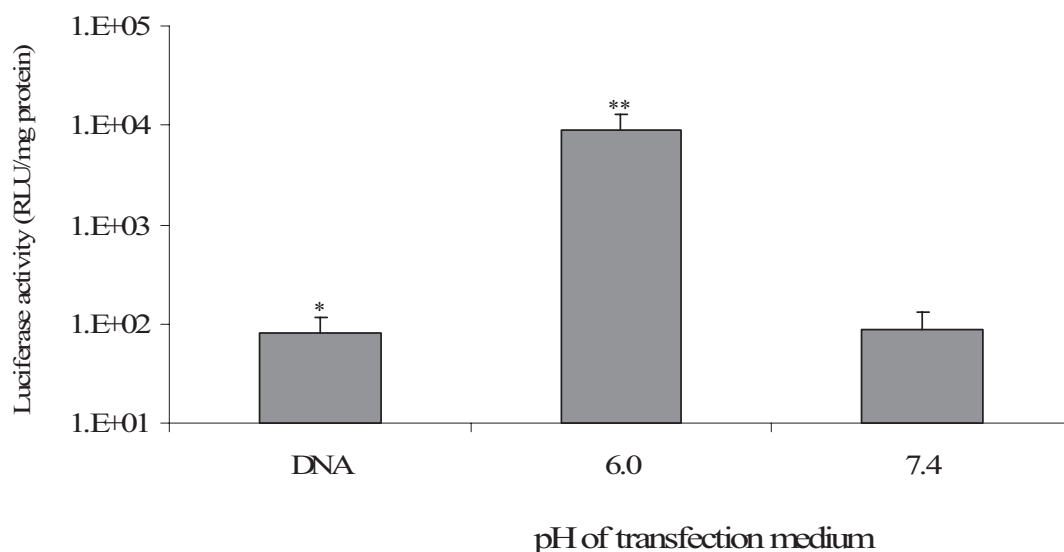


Figure 35 Transfection efficiency of CAc-45kDa/DNA complexes at pH of transfection medium 6.0 and 7.4 in CHO-K1 cells. Differences values \* vs \*\* were statistically significant ( $P < 0.05$ , ANOVA, LSD).

The effect of incubation time of the complex with the cells was investigated on the transfection of CAc/DNA complexes for 1, 2, 4, 6 and 24 hours (Figure 36). The transfection efficiency of CAc/DNA complexes at the incubation time of 1, 2, 4 and 6 hours was not significantly different from the naked DNA. When the incubation time increased to 24 hours, the transfection efficiency of the complexes significantly increased ( $p < 0.05$ ). The increase in transfection efficiency could be due to the increase in cellular uptake of the complexes when the exposure time was extended.

From these results, next investigation was then carried out at 0.6% acetic acid, pH 6.5 and 24 h incubation time.

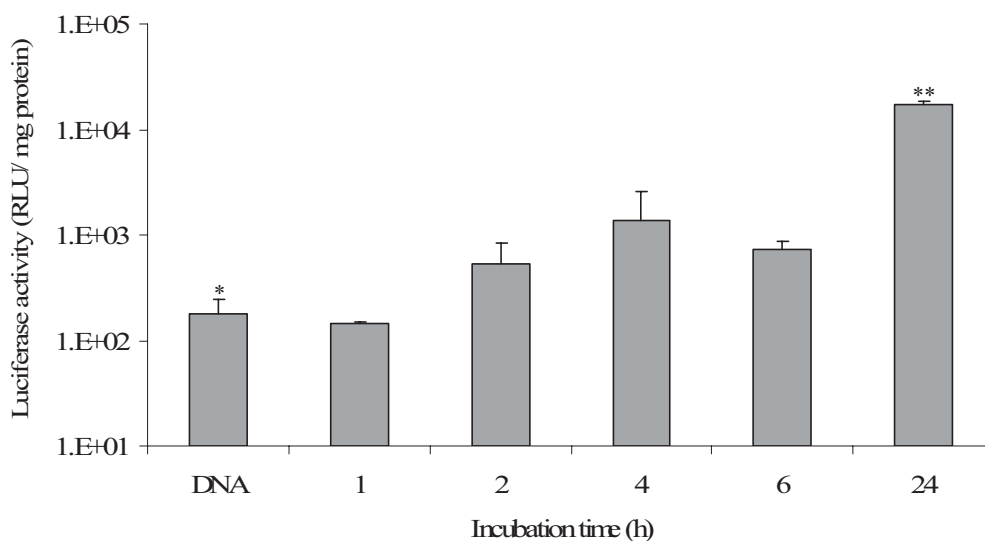


Figure 36 Transfection efficiency of CAC-45kDa/DNA complexes at incubation time 1, 2, 4, 6 and 24 hours in CHO-K1 cells. Differences values \* vs \*\* were statistically significant ( $P < 0.05$ , ANOVA, LSD).

### 3.2.2 Effect of N/P ratio on transfection efficiency

The transfection of CS/DNA complexes was fixed at the pH 6.5, 0.6% acetic acid and 24 h incubation time. Polyethylenimine (PEI, 25 kDa) was used as a positive control. The sufficient transfection efficiency of PEI/DNA complexes at an N/P ratio of 4 was  $2.59 \times 10^5$  RLU/mg protein.

The transfection efficiency had a tendency to increase as the N/P ratio increased (Figure 37). At N/P ratios of 2 and 4, the transfection efficiencies of all MW of CS/DNA complexes were not significant different from the naked DNA ( $P > 0.05$ ). At N/P ratios higher than 4, the transfection efficiency of all MW of CS/DNA complexes was higher than for the naked DNA. At a low N/P ratio, the transfection efficiency of all CS/DNA complexes was not different from the naked DNA. This might be because the amount of positively charged amines in chitosan in the chitosan/DNA complexes was not sufficient to transfect cells. The CS/DNA complexes achieved sufficient transfection efficiencies at higher N/P ratios (N/P ratio of above 4). This could be because an increase in the concentration of chitosan at higher N/P ratios could yield a higher amount of positively charged complexes to successfully transfect cells. The increase in

transfection ability with an increase in chitosan concentration in chitosan/DNA complexes was also demonstrated by Lavertu et al. (2006: 4815-4824).

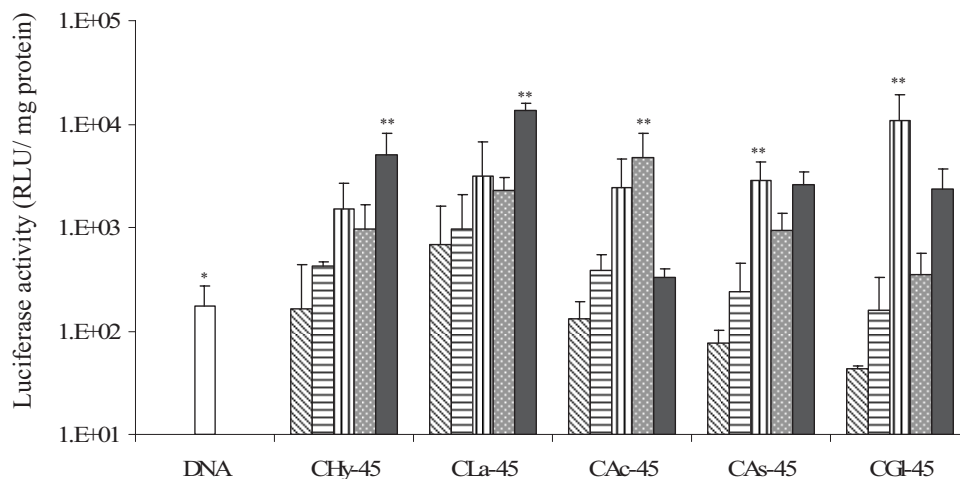


Figure 37 Transfection efficiency of CS-45kDa/DNA complexes with chitosan salts in CHO-K1 cells. (▨ = N/P ratio of 2; ▩ = N/P ratio of 4; ▧ = N/P ratio of 6; ▦ = N/P ratio of 8; ■ = N/P ratio of 12). Differences values \* vs \*\* were statistically significant ( $P < 0.05$ , ANOVA, LSD).

### 3.2.3 Effect of MW of chitosan on transfection efficiency

CGI/DNA complexes were formulated with chitosan of various MWs (20, 45, 200 and 460 kDa) in order to investigate the effect of MW on transfection efficiency. CGI was used to study because it is one of CS that has been used for gene delivery (Li et al. 2003: 7-18). The transfection efficiencies of CGI/DNA complexes are shown in Figure 38. The transfection efficiency had a tendency to increase as the N/P ratio increased. At N/P ratios of 2 and 4, the transfection efficiencies of all MW of CS/DNA complexes were not significant different from the naked DNA ( $P > 0.05$ ). At N/P ratios higher than 4, the transfection efficiency of all MW of CS/DNA complexes was higher than for naked DNA. However, in different MW of CS, the maximum transfection efficiency was found in different N/P ratios. CGI/DNA complexes of MW 20, 45, 200 and 460 kDa showed maximum transfection efficiency at N/P ratios of 12, 6, 6, and 6, respectively. The MW of chitosan in the range studied affected the transfection

efficiency. Chitosan MW 20 and 45 kDa had effective transfection efficiencies ( $P < 0.05$ ), whereas MW 200 and 460 kDa had slightly higher transfection efficiency than naked DNA. This could be due to the high association between chitosan and DNA that prevented dissociation once inside the cells. The high association between chitosan and DNA in high MW chitosan was due to high complexing ability observed by gel electrophoresis (Figure 30) and high binding affinity observed by ethidium bromide (EtBr) displacement assay (Figure 19). Köping-Höggård et al. (2004: 1441-1452) demonstrated that the high transfection efficiency of chitosan/DNA complexes formulated with low MW chitosan compared to that of high MW chitosan was attributed to the high association between high MW chitosan and DNA. This observation was also in agreement with previous studies (Maclaughlin et al. 1998: 259–272; Ishii, Okahata and Sato 2001: 51-64; Sato et al., 2001: 2075-2080). On the other hand, high transfection efficiency of chitosan/DNA complexes formulated with high MW chitosan was observed by Zhao et al. (2006: 223-228) and Haung et al. (2005: 391-406). Haung et al. (2005: 391-406) suggested that high transfection efficiency of high MW chitosan was attributed to the highly-positive charge chitosan/DNA complexes that be able to be uptaked by the cells.

The MW of chitosan and N/P ratio of chitosan/DNA complexes is one of the important formulation parameters that affect transfection efficiency. In chitosan/DNA complexes, there was an interaction between both the MW and the N/P ratio, where a high MW chitosan gave a higher transfecton efficiency at a low N/P ratio, and a low MW chitosan required a higher N/P ratio. This event was in agreement with previous studies (Rómoren et al., 2003; Lavertu et al., 2006). They suggested that the optimal association and dissociation between chitosan and DNA in chitosan/DNA complexes with an optimal MW of chitosan and N/P ratio of chitosan/DNA complexes that resulted in a high transfection efficiency.

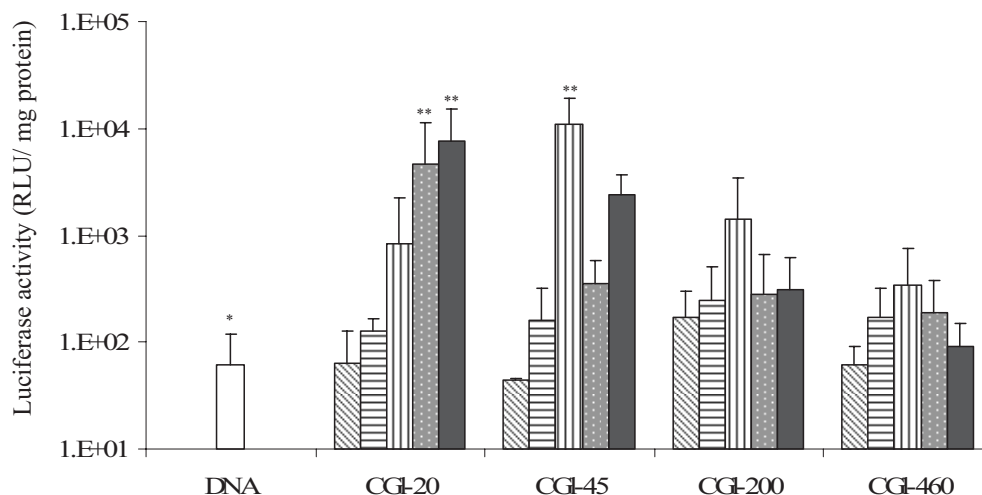


Figure 38 Transfection efficiency of CGI/DNA complexes with different chitosan MW in CHO-K1 cells. (▨ = N/P ratio of 2; ▩ = N/P ratio of 4; ▪ = N/P ratio of 6; ▫ = N/P ratio of 8; ▬ = N/P ratio of 12). Differences values \* vs \*\* were statistically significant ( $P < 0.05$ , ANOVA, LSD).

### 3.2.4 Effect of salt form of chitosan on transfection efficiency

CS/DNA complexes were formulated with chitosan MW of 45 kDa in order to investigate the effect of salt form of chitosan on the transfection efficiency at the same pH of transfection medium (pH 6.5). Figure 37 shows the transfection efficiency of CS/DNA complexes formulated with chitosan MW of 45 kDa at N/P ratios of 2, 4, 6, 8 and 12. All CS/DNA complexes had effective transfection efficiency. However, the maximum transfection efficiency was found at different N/P ratios. CHy/DNA, CLa/DNA, CAc/DNA, CAs/DNA and CGI/DNA complexes showed the maximum transfection efficiency at an N/P ratio of 12, 12, 8, 6, and 6 ( $P < 0.05$ ), respectively. The transfection efficiency was affected by salt form (counter ion) of chitosan. Of the different CS, the maximum transfection efficiency was dependent on different N/P ratios. This discrepancy could be due to the effect of counter ions that hinder the interaction between chitosan and DNA. In the case of hydrochloride which highly dissociate into anionic chloride ion, more chitosan was required to maintain a positive charge for a complete interaction with DNA. The maximum transfection efficiency of the CHy/DNA complex was achieved at an N/P ratio of 12. The N/P ratio at which the transfection efficiency was maximum for CLa/DNA was also higher than for CAc/DNA

because lactic acid can more ionize than acetic acid. However, those differences could not be observed in CAs/DNA and CGI/DNA. These might be due to other factors such as solubility, molecular size and charge.

CLa had higher transfection efficiency than CAc and CHy. This might be because the molecule of lactate counter ion is larger than that of acetate and chloride counter ion. The larger counter ion may aid the dissociation of the complexes, resulting in higher transfection efficiency. Similar result was obtained in CAs and CGI. CGI had higher transfection efficiency than CAs. The molecule of glutamate counter ion is also larger than that of aspartate counter ion.

### **3.3 Cytotoxicity of CS/DNA complexes**

The viability of CHO-K1 cells was tested in the presence of CS/DNA complexes at various N/P ratios as studied in the transfection experiment. Cells without treatment of the CS/DNA complexes were considered as a positive control with a cell viability of 100%. The results are shown in Figure 39 and 40. Thereby they are shown that CS/DNA complexes formulated with various CS had low cytotoxicity level. The average cell viability was over 90%.

CS/DNA complexes were investigated for a possible cytotoxic effect. The cell viability was monitored using the MTT assay after 24 h incubation with CS/DNA complexes. CS/DNA complexes did not affect the viability of CHO-K1 cells. It was clear that CS/DNA complexes formulated with CAc, CAs, CGI, CHy and CLa were safe at N/P ratios between 2 to 12.

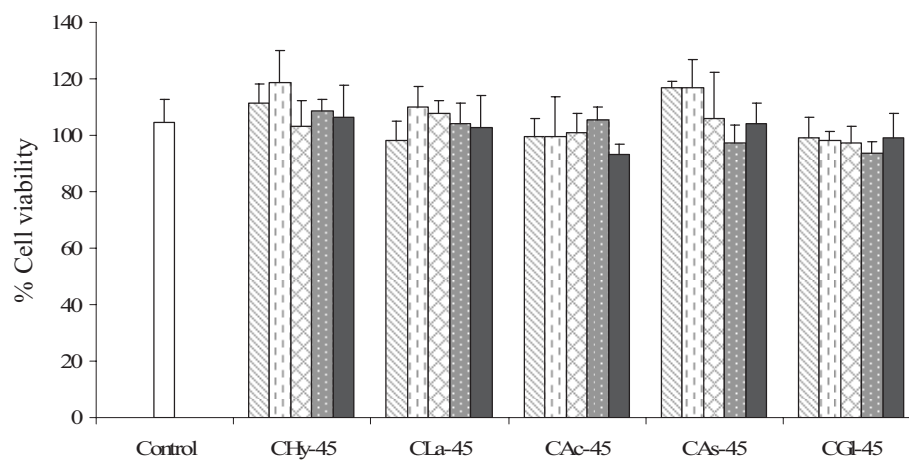


Figure 39 Effect of CS-45kDa/DNA complexes with different chitosan salts on CHO-K1 cell viability. (▨ = N/P ratio of 2; ▩ = N/P ratio of 4; ▪ = N/P ratio of 6; ▫ = N/P ratio of 8; ■ = N/P ratio of 12).

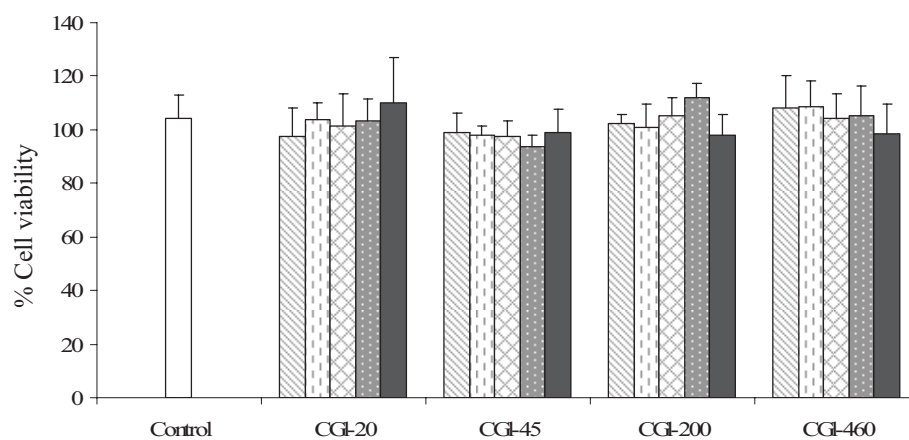


Figure 40 Effect of CGI-45kDa/pcDNA3-CMV-Luc complexes with different chitosan MW on CHO-K1 cell viability. (▨ = N/P ratio of 2; ▩ = N/P ratio of 4; ▪ = N/P ratio of 6; ▫ = N/P ratio of 8; ■ = N/P ratio of 12).

### 3.4 Optimal transfection efficiency condition of chitosan/DNA complexes

The mixing technique of chitosan and plasmid DNA used to prepare complexes in these study was by adding chitosan solution over plasmid DNA solution, pipetting up and down for about 5 times, and vortexing for 3-5 sec. The incubation time between chitosan/DNA complexes and the cells was found to be not different in the range of 1-6 h. The effective incubation time was 24 h. The pH of complex solution in the transfection medium was in the range of 6.0-7.0 depending on the N/P ratio.

Different pH of transfection medium, in the range of 6.0-7.4, and the amount of the acetic acid used in CAc solution in the range of 0.1-0.6% were tested as a model complex. The effective transfection efficiency was found to be at the amount of acid of 0.6% with the pH of transfection medium of 6.0-6.5 at N/P ratios of 6 and 8.

The pH of transfection medium was adjusted to the same at 6.5 in order to study the effect of the salt form and MW of chitosan on the transfection efficiency. At the same pH, different CS had maximum transfection efficiency at different N/P ratios. CHy/DNA, CLa/DNA, CAc/DNA, CAs/DNA and CGI/DNA complexes showed the maximum transfection efficiency at an N/P ratio of 12, 12, 8, 6, and 6, respectively. Transfection efficiency was also dependent on the MW. Low MW chitosan (20 and 40 kDa) had higher transfection efficiency than high MW chitosan (200 and 460 kDa). Different MW of chitosan had maximum transfection efficiency at different N/P ratios. CGI-20kDa/DNA, CGI-45kDa/ DNA, CGI-200kDa/DNA and CGI-460kDa/DNA complexes had maximum transfection efficiency at an N/P ratio of 12, 6, 6, and 6, respectively. Effective transfection efficiency achieved at N/P ratios of 6 to 12 with particle size range of 100 to 200 nm and zeta potential range of +15 to +25 mV.

## CHAPTER V

### CONCLUSION

This present study had an attempt to investigate the different salt forms (counter ions) of chitosan on their transfection efficiencies. Physicochemical properties of the complex such as complexing ability, binding affinity, particle size and zeta potential, and cytotoxicity were investigated.

#### 1. SD-CS/DNA complexes

1.1 Complexing ability and binding affinity between SD-CS and DNA were found to depend on:

##### 1.1.1 MW of chitosan

The ranking order was MW of chitosan 460  $\approx$  200 > 45  $\approx$  20 kDa.

##### 1.1.2 Salt form of chitosan and pH of chitosan solution

The ranking order was SD-CLa (pH 4.2-4.3) > SD-CAs (pH 4.6-4.7)  $\approx$  SD-CGI (pH 4.7-4.8).

1.2 Particle size and zeta potential depended on:

##### 1.2.1 N/P ratio

At an N/P of 4, the particle size of the complexes was microsized (630-6,000 nm). At N/P ratios above 4, the complexes were nanosized (200-600 nm). At N/P ratios above 12, the particle size of all SD-CS/DNA complexes increased with increasing N/P ratio. The ranking order was N/P ratio of 28 > 20 > 12.

Zeta potential increased when the N/P ratio increased from 4 to 12 and reached a plateau of about +32 to +49 mV at N/P ratios above 12.

##### 1.2.2 MW of chitosan

Particle size and zeta potential of the complexes formulated with high MW chitosan had higher particle size than low MW chitosan. The ranking order was MW of chitosan 460  $\approx$  200 > 45  $\approx$  20 kDa.

##### 1.2.3 Salt form of chitosan and pH of chitosan solution

At neutral zeta potential, the particle size rank was SD-CAs/DNA (pH 7.1-7.2)  $\approx$  SD-CGI (pH 7.1-7.2) > SD-CLa (pH 6.8-6.9).

### 1.3 Transfection efficiency:

Transfection efficiency was affected by the pH of transfection medium. Effective transfection efficiency of SD-CS/DNA complexes could not be achieved in both COS-1 and CHO-K1 cells at the transfection medium pH of 7.3-7.4.

### 1.4 Cytotoxicity:

All SD-CS/DNA complexes had low cytotoxicity in COS-1 cells at N/P ratios between 4 to 28. The average cell viability was over 90%.

## 2. CS/DNA complexes

### 2.1 Complexing ability depended on:

#### 2.1.1 MW of chitosan

The ranking order was MW of chitosan 460  $\approx$  200 > 45  $\approx$  20 kDa.

#### 2.1.2 pH of complex solution

The ranking order was pH 3.0 > 5.0 > 6.5.

#### 2.1.3 Salt form of chitosan

All CS had similar complexing ability. The complete complexes were formed at N/P ratios above 2.

### 2.2 Particle size and zeta potential depended on:

#### 2.2.1 N/P ratio

At the same pH (6.5), the particle size increased with an increasing N/P ratio from 1 to 2 and decreased to constant value in the range of 101 to 299 nm after a charge ratio of 2. The zeta potential was nearly zero at an N/P ratio of 2 (-4 to +3 mV). The zeta potential was a negative value at an N/P ratio lower than 2 (-35 to -60 mV). At N/P ratios above 2, the zeta potential was positive (+15 to +28 mV).

#### 2.2.2 MW of chitosan

Particle size and zeta potential had a trend to increase when the MW increased. The ranking order was MW of chitosan 460  $\approx$  200 > 45  $\approx$  20 kDa.

#### 2.2.3 pH of complex solution

The particle size increased with an increase in the pH of complex solution. The ranking order was pH 6.5 > 3.0. The zeta potential increased with a decrease in the pH of complex solution. The ranking order was pH 3.0 > 6.5.

#### 2.2.4 Salt form of chitosan.

The size rank was hydrochloride > lactate > acetate > aspartate > glutamate.

### 2.3 Transfection efficiency was found to depend on:

### 2.3.1 N/P ratio

Effective transfection efficiency achieved at N/P ratios of 6 to 12.

### 2.3.2 Amount of the acid in CS solution

Transfection efficiency increased with an increase in the amount of the acid in CS solution. The ranking order was 0.6% > 0.2%  $\approx$  0.1% w/v acid solution.

### 2.3.3 pH of transfection medium.

Effective transfection efficiency was in the pH range of 6.0-6.5.

### 2.3.4 Incubation time

Effective transfection efficiency was achieved at the incubation time of 24 h.

### 2.3.5 MW of chitosan

Low MW chitosan had higher effective transfection efficiency than high MW chitosan. The ranking order was MW of chitosan 20  $\approx$  45  $\gg$  200 > 460 kDa.

### 2.3.6 Salt form of chitosan

Different salt forms had different maximum transfection efficiencies at different N/P ratios at the same pH (6.5). CHy/DNA, CLa/DNA, CAc/DNA, CAs/DNA and CGI/DNA complexes had the maximum transfection efficiency at an N/P ratio of 12, 12, 8, 6, and 6, respectively.

## 2.4 Cytotoxicity

All CS/DNA complexes had low cytotoxicity in CHO-K1 cells at N/P ratios between 2 to 12. The average cell viability was over 90%.

In conclusion, this study demonstrated that the variables of formulation affected the physicochemical properties and transfection efficiency of chitosan/DNA complexes. At an optimal condition of transfection, CS can have the potential to be used as safe gene delivery vectors.

**BIBLIOGRAPHY**

- Akbuğa, J. et al. "Plasmid-DNA loaded chitosan microspheres for in vitro IL-2 Expression." European Journal of Pharmaceutics and Biopharmaceutics 58 (2004) 501-507.
- Aldevron, Fargo, ND, USA. gWIZ™ reporter plasmids [Online]. Accessed 3 May 2007. Available from [http://www.aldevron.com/gene\\_therapy/reporter\\_plasmids](http://www.aldevron.com/gene_therapy/reporter_plasmids)
- Appleby, C.E. et al. "A novel combination of promoter and enhancers increases transgene expression in vascular smooth muscle cells in vitro and coronary arteries in vivo after adenovirus-mediated gene transfer." Gene Therapy 10 (2003): 1616-1622.
- Ausubel F.M. "Analysis of proteins." In Short Protocols in Molecular Biology, 277-284. New York, USA: John Wiley and Sons, Inc., 2002.
- Bandyopadhyay, P. et al. "Enhanced gene transfer into HuH-7 cells and primary rat hepatocytes using targeted liposomes and polyethylenimine." Biotechniques 25 (1998): 282-284, 286-292.
- Blaese, R.M. et al. "T-lymphocyte-directed gene therapy for ADA-SCID: initial trial results after 4 years." Science 270 (1995): 475-480.
- Blankinship, M.J. et al. "Efficient transduction of skeletal muscle using vectors based on adeno-associated virus serotype." Molecular therapy 10 (2004): 671-678.
- Bolsover, S.R. et al. "Transcription and the control of gene expression." In From Genes to Cells, 148-151. New York, USA: John Wiley and Sons, Inc., 1997.
- Bonini, C. et al. "HSV-TK gene transfer into donor lymphocytes for control of allogeneic graft-versus-leukemia." Science 276 (1997): 1719-1724.
- Bouragaize, D., T.R. Jewell and R.G. Buiser. "Genetic disease and gene therapy." In Biotechnology, 224-230. California, USA: Addison Wesley Longman, Inc., 2000.
- Bouragaize, D., T.R. Jewell and R.G. Buiser. "Genetic engineering: tools and techniques." In Biotechnology, 138-169. California, USA: Addison Wesley Longman, Inc., 2000.
- Boyer, R.F. "Measurement of protein solution." In Modern Experimental Biochemistry, 51-58, CA, USA: The Benjamin/Cummings Publishing Company, Inc., 1993.

- Bradford, M. "A rapid and sensitive method for the quantitation of microgram quantities of protein utilizing the principle of protein-dye binding." Analytical Biochemistry 72 (1976): 248-254.
- Brown, W.H. and C.S. Foote. "Infrared spectroscopy." In Organic Chemistry, 427-452. New York, USA: Harcourt College Publishers, 2002.
- Brown, W.H. and C.S. Foote. "Nuclear magnetic resonance Spectroscopy." In Organic Chemistry, 453-498. New York, USA: Harcourt College Publishers, 2002.
- Brunner, S. et al. "Cell cycle dependence of gene transfer by lipoplex, polyplex and recombinant adenovirus." Gene Therapy 7 (2000): 401-407.
- Buttgereit, P. et al. "Efficient gene transfer into lymphoma cells using adenoviral vectors combined with lipofection." Cancer Gene Therapy 7 (2000): 1145-1155.
- Caprette, D.R. Absorbance assay (280 nm) [Online]. Accessed 2 May 2006. Available from <http://www.ruf.rice.edu/~bioslabs/methods/protein/abs280.html>
- Carberry, D. Atomic force microscopy [Online]. Accessed 28 May 2007. Available from <http://spm.phy.bris.ac.uk/techniques/AFM/>
- Carreño-Gómez, B. and R. Duncan. "Evaluation of the biological properties of soluble chitosan and chitosan microsphere." International Journal of Pharmaceutics 148 (1997): 231-240.
- Cassaday, R.D. et al. "A phase I study of immunization using particle-mediated epidermal delivery of genes for gp100 and GM-CSF into uninvolved skin of melanoma patients." Clinical Cancer Research 13 (2007): 540-549.
- Chae, S.Y. et al. "Deoxycholic acid-conjugated chitosan oligosaccharide nanoparticles for efficient gene carrier." Journal of Controlled Release 109 (2005): 330-344.
- Chang, D.C. "Structure and dynamics of electric field-induced membrane pores as revealed by rapid-freezing electron microscopy." In Guide to Electroporation and Electrofusion, 9-27. Edited by Chang, D.C. et al., San Diego, USA: Academic Press, Inc., 1992.
- Chirmule, N. et al. "Immune responses to adenovirus and adeno-associated virus in humans." Gene Therapy 6 (1999): 1574-1583.
- Choi, J.S. et al. "Enhanced transfection efficiency of PAMAM dendrimer by surface modification with L-arginine." Journal of Controlled Release 99 (2004): 445-456.

- Choi, Y.H. et al. "Polyethylene glycol-grafted poly-L-lysine as polymeric gene carrier." Journal of Controlled Release 54 (1998): 39-48.
- Congiu, A. et al. "Correlation between structure and transfection efficiency: a study of DC-Chol--DOPE/DNA complexes." Colloids and Surfaces B Biointerfaces 36 (2004): 43-48.
- Corsi, K. et al. "Mesenchymal stem cells, MG 63 and HEK293 transfection using chitosan-DNA nanoparticles." Biomaterials 24 (2003): 1255-1264.
- Cui, Z. "DNA vaccine." In Non-viral Vectors for Gene Therapy part II, 258-289. Edited by Haung, L., M. Hung and E. Wagner., California, USA: Elsevier Academic Press, 2005.
- Cui Z. and R.J. Mumper "Chitosan based nanoparticles for genetic immunization." Journal of Controlled Release 75 (2001): 409-419.
- da Cruz, M.T., S. Simões and M.C. de Lima. "Improving lipoplex-mediated gene transfer into C6 glioma cells and primary neurons." Experimental Neurology 187 (2004): 65-75.
- Danielsen, S., K.M. Varum and B.T. Stokke. "Structural analysis of chitosan mediated DNA condensation by AFM: Influence of chitosan molecular parameters." Biomacromolecules 5 (2004): 928-936.
- Dass, C.R. "Chitosan microparticles encapsulating PEDF plasmid demonstrate efficacy in an orthotopic metastatic model of osteosarcoma." Biomaterials 28 (2007): 3026-3033.
- Davidoff, A.M. et al. "Comparison of the ability of adeno-associated viral vectors pseudotyped with serotype 2, 5, and 8 capsid proteins to mediate efficient transduction of the liver in murine and nonhuman primate models." Molecular therapy 11 (2005): 875-888.
- Dickson, G. "DNA-based immunization." In Molecular and Cell Biology of Human Gene Therapeutics, 368-372. London, UK: Chapman and Hall, 1995.
- Dunachis, S.J. et al. "A DNA prime-modified vaccinia virus ankara boost vaccine encoding thrombospondin-related adhesion protein but not circumsporozoite protein partially protects healthy malaria-naive adults against Plasmodium falciparum sporozoite challenge." Infection and Immunity 74 (2006): 5933-5942.

- Dunlop, D.D. et al. "Nanoscopic structure of DNA condensed for gene delivery." Nucleic Acids Research 25 (1997): 3095-3101.
- Dunn, M. J. "Protein determination of total protein concentration." In Protein Purification Methods Edited by Harris, E.L.V. and S. Angal. Swansea, UK: Oxford IRL Press, 1992.
- Ellen, H., J. Bentz and F.C. Szoka. "Fusion of phosphatidylethanolamine-containing liposomes and mechanism of La-HII phase transition." Biochemistry 25 (1986): 4141-4147.
- Evans, C.H. et al. "Gene therapeutic approach hes-transfer in vivo." Advanced Drug Delivery Reviews 58 (2006): 243-258.
- Ewert, K. et al. "Efficient synthesis and cell-transfection properties of a new multivalent cationic lipid for nonviral gene delivery." Journal of Medicinal Chemistry 45 (2002): 5023-5029.
- Faneca, H., S. Simoes and M.C. Pedroso de Lima. "Association of albumin or protamine to lipoplexes: enhancement of transfection and resistance to serum." Journal of Gene Medicine 6 (2004): 681-692.
- Farhood, H., N. Serbini and L. Huang. "The role of dioleoyl phosphatidylethanolamine in cationic liposome mediated gene transfer." Biochimica et Biophysica Acta 1235 (1995): 289-295.
- Felgner, J.H. et al. "Enhanced gene delivery and mechanism studies with a novel series of cationic lipid formulations." Journal of Biological Chemistry 269 (1994): 2550-2561.
- Felgner, P.L. et al. "Lipofection: a highly efficient, lipid-mediated DNA-transfection procedure." Proceedings of the National Academy of Sciences USA 4 (1987): 7413-7417.
- Felgner, P.L. et al. "Nomenclature for synthetic gene delivery systems." Human Gene Therapy 8 (1997): 511-512.
- Ferber, D. "Gene therapy: safer and virus-free?." Science 294 (2001): 1638-1642.
- Ferdous, A. et al. "Comb-type copolymer:Stabilization of triplex DNA and possible application in antigene strategy." Journal of Pharmaceutical Sciences 87 (1998): 1400-1405.

- Floch, V. et al. "New biocompatible cationic amphiphiles derivative from glycine betaine: a novel family of efficient nonviral gene transfer agents." Biochemical and Biophysical Research Communications 25 (1998): 360-365.
- Florea, B.I. et al. "Enhancement of bronchial octreotide absorption by chitosan and N-trimethyl chitosan shows linear in vitro/in vivo correlation." Journal of Controlled Release 110 (2006): 353-361.
- Fominaya, J., C. Uherek and W. Wels. "A chimeric fusion protein containing transforming growth factor- $\alpha$  mediates gene transfer via binding to the EGF receptor." Gene Therapy 5 (1998): 521-530.
- Forrest, M. L, N. Gabrielson and D.W. Pack. "Cyclodextrin-polyethyleneimine conjugates for targeted in vitro gene delivery." Biotechnology and Bioengineering 89 (2005): 416-423.
- Friend, D.S., D. Papahadjopoulos and R.J. Debs. "Endocytosis and intracellular processing accompanying transfection mediated by cationic liposomes." Biochimica et Biophysica Acta 1278 (1996): 41-50.
- Fynan, E.F. et al. "DNA vaccines: Protective immunizations by parenteral, mucosal, and gene-gun inoculations." Proceedings of the National Academy of Sciences USA 90 (1993): 11478-11482.
- Gabriel, B.L. "Transmission electron microscope instrument." In Biological Electron Microscopy, 1-12, New York, USA: Van Nostrand Reinhold Company, Inc., 1982.
- Gabrielson, N.P. and D.W. Pack. "Acetylation of polyethyleneimine enhances gene delivery via weakened polymer/DNA interactions." Biomacromolecules 7 (2006): 2427-2435.
- Gao, H. and K.M. Hui. "Synthesis of a novel series of cationic lipids that can act as efficient gene delivery vehicles through systemic heterocyclic substitution of cholesterol derivatives." Gene therapy 8 (2001): 855-863.
- Gao, X. and L. Huang. "A novel cationic liposome reagent for efficient transfection of mammalian cells. Biochemical and Biophysical Research Communications 179 (1991): 280-285.
- Gao, S. et al. "Galactosylated low molecular weight chitosan as DNA carrier for hepatocyte-targeting." International Journal of Pharmaceutics 255 (2003): 57-68.

- Garnett, M.C. "Gene-delivery systems using cationic polymers." Critical Reviews in Therapeutic Drug Carrier Systems 16 (1999): 147-207.
- Genlantis, CA, USA. How to choose optimal gene delivery method [Online]. Accessed 25 November 2006. Available from [http://www.genlantis.com/commerce/staticwebpage.jsp?param=transfection\\_articles\\_3](http://www.genlantis.com/commerce/staticwebpage.jsp?param=transfection_articles_3)
- Guliyeva et al. "Chitosan microparticles containing plasmid DNA as potential oral gene delivery system." European Journal of Pharmaceutics and Biopharmaceutics 62 (2006): 17-25.
- Guo, T. et al. "Porous chitosan-gelatin scaffold containing plasmid DNA encoding transforming growth factor- $\beta$ 1 for chondrocytes proliferation." Biomaterials 27 (2006): 1095-1103.
- Hartl, D.L. and E.W. Jones. Molecular biology of gene expression." In Genetics, 2000, 452-456. Massachusetts, USA: Jones and Bartlett Publisher, Inc., 2000.
- Hartl, A. et al. "Characterization of the protective and therapeutic efficiency of a DNA vaccine encoding the major birch pollen allergen Bet v 1a." Allergy 59 (2004): 65-73.
- Hasimoto, M. et al. "Lactosylated chitosan for DNA delivery into hepatocytes: the effect of lactosylation on the physicochemical properties and intracellular trafficking of pDNA/chitosan complexes." Bioconjugate Chemistry 17 (2006): 309-316.
- Hejazi, R. and M. Amiji. "Chitosan-based gastrointestinal delivery systems." Journal of Controlled Release 89 (2003): 151-165.
- Heyes, J.A. et al. "Synthesis of novel cationic lipids: effect of structural modification on the efficiency of gene transfer." Journal of Medical Chemistry 45 (2002): 99-114.
- Hidber, H.R. and Tonin, A. Principle of AFM-imaging [Online]. Accessed 28 May 2007. Available from [http://monet.unibas.ch/famars/afm\\_prin.htm](http://monet.unibas.ch/famars/afm_prin.htm)
- Hill, I.R.C. et al. "In vitro cytotoxicity of poly(amidoamine)s: relevance to DNA delivery." Biochimica et Biophysica Acta 1427 (1999): 161-174.
- Hino, T. et al. "Drug release from w/o/w emulsions prepared with different chitosan salts and concomitant creaming up." Journal of Controlled Release 69 (2000): 413-419.

- Hong, C.S. et al. "Herpes simplex virus RNAi and neprilysin gene transfer vectors reduce accumulation of Alzheimer's disease-related amyloid-beta peptide in vivo." Gene Therapy 13 (2006):1068-1079.
- Hu, F. et al. "A novel chitosan oligosaccharide-stearic acid micelles for gene delivery:properties and in vitro transfection studies." International Journal of Pharmaceutics 315 (2006): 158-166.
- Huang, M. et al. "Transfection efficiency of chitosan vectors: effect of polymer molecular weight and degree of deacetylation." Journal of Controlled Release 106 (2005): 391-406.
- Igarashi, S., Y. Hattori and Y. Maitani. "Biosurfactant MEL-A enhances cellular association and gene transfection by cationic liposome Journal of Controlled Release 112 (2006): 362-368.
- Ishii, T., Y. Okahata and T. Sato. "Mechanism of cell transfection with plasmid/chitosan complexes." Biochimica et Biophysica Acta 1514 (2001): 51-64.
- Jeong, G.J. et al. "Biodistribution and tissue expression kinetics of plasmid DNA complexed with polyethylenimines of different molecular weight and structure." Journal of Controlled Release 118 (2007): 118-125.
- Jewis, R. "Gene action and expression." In Human Genetics, 193-194. New York, USA: The McGrawHill, 2003.
- Jiang, X. et al. "Chitosan-g-PEG/DNA complexes deliver gene to the rat liver via intrabiliary and intraportal infusions." The Journal of Gene Medicine 8 (2006): 477-487.
- Kang, K.K. et al. "Safety evaluation of GX-12, a new HIV therapeutic vaccine: investigation of integration into the host genome and expression in the reproductive organs." Intervirology 46 (2003): 270-276.
- Kiang, T. et al. "The effect of the degree of chitosan deacetylation on the efficiency of gene transfection." Biomaterials 25 (2004): 5293-5301.
- Kichler, A.C. et al. "Polyethylenimine-mediated gene delivery: a mechanistic study." The Journal of Gene medicine 3 (2001): 135-144.
- Kilk, K. et al. "Evaluation of transportan 10 in PEI mediated plasmid delivery assay, Journal of Controlled Release 103 (2005): 511-523.

- Kim, J.B. et al. "Enhanced transfection efficiency of primary cortical cultures using arginine-grafted PAMAM dendrimer, PAMAM-Arg." Journal of Controlled Release 114 (2006): 110-117.
- Kim, J.J and D.B. Weiner "DNA vaccines." Gene Therapy: Therapeutic mechanisms and Strategies, 551-559. Edited by Templeton, N.S., New York, USA: Marcel Dekker, Inc., 2000.
- Kim, T.H. et al. "Efficient gene delivery by urocanic acid-modified chitosan." Journal of Controlled Release 93 (2003): 389-402.
- Kim, T.H. et al. "Synergistic effect of poly(ethylenimine) on the transfection efficiency of galactosylated chitosan/DNA complexes." Journal of Controlled Release 105 (2005): 354-366.
- Kircheis, R. et al. "Tumor-targeted gene delivery of tumor necrosis factor-alpha induces tumor necrosis and tumor regression without systemic toxicity." Cancer Gene Therapy 9 (2002): 673-80.
- Klenchin, V.A. et al. "Electrically induced DNA uptake by cells is a fast process involving DNA electrophoresis." Biophysical Journal 60 (1991): 804-811.
- Kok, M.R. et al. Immune responses following salivary gland administration of recombinant adeno-associated virus serotype 2 vectors." Journal of Gene Medicine 7 (2005): 432-441.
- Köping-Höggård, M. et al. "Chitosan as a nonviral gene delivery system. Structural-property relations and characteristics compared with polyethylenimine in vitro and after lung administration in vivo." Gene Therapy 8 (2001): 1108-1121.
- Köping-Höggård, M. et al. "Improved chitosan-mediated gene delivery based on easily dissociated chitosan polyplexes of highly defined chitosan oligomers." Gene Therapy 11 (2004): 1441-1452.
- Kranykh, V.N. et al. "Generation of recombinant adenovirus vectors with modified fibers for altering viral tropism." Journal of Virology 70 (1996): 6839-6846.
- Kumar, M. et al. "Chitosan IFN-gamma-pDNA nanoparticle (CIN) therapy for allergic asthma." Genetic Vaccines Therapy 1 (2003): 3.
- Kwoh, D.Y. et al. "Stabilization of poly-L-lysine/DNA polyplexes for in vivo gene delivery to the liver." Biochimica et Biophysica Acta 1444 (1999): 171-190.
- Labat-Moleur, F. et al. "An electron microscopy study into the mechanism of gene transfer with lipopolyamines." Gene Therapy 3 (1996): 1010-1017.

- Lampela, P. et al. "The use of low-molecular-weight PEIs as gene carriers in the monkey fibroblastoma and rabbit smooth muscle cell cultures." The Journal of Gene Medecine 4 (2002): 205-214.
- Lavertu, M. et al. "High efficiency gene transfer using chitosan/DNA nanoparticles with specific combinations of molecular weight and degree of deacetylation." Biomaterials 27 (2006): 4815-4824.
- Laxmi, A.A. et al. "Novel non-glycerol-based cytofectins with lactic acid-derived head groups." Biochemical and Biophysical Research Communications 289 (2001):1057-1062.
- Lee, C.H. et al. "Synergistic effect of polyethylenimine and cationic liposomes in nucleic acid delivery to human cancer cells." Biochimica et Biophysica Acta 1611 (2003): 55-62.
- Lee, H., J.H. Jeong and T.G. Park. "PEG grafted polylysine with fusogenic peptide for gene delivery: high transfection efficiency with low cytotoxicity." Journal of Controlled Release 79 (2002): 283-291.
- Lee, K.Y. et al. "Preparation of chitosan self-aggregates as a gene delivery system." Journal of Controlled Release 51 (1998): 213-220.
- Lee, M. et al. "Water-soluble and low molecular weight chitosan-based plasmid DNA delivery." Pharmaceutical Research 18 (2001): 427-431.
- Li, H. and J. Birchall "Chitosan-modified dry powder formulation for pulmonary gene delivery." Pharmaceutical Research 23 (2006): 941-950.
- Li, X.W. et al. "Sustained expression in mammalian cells with DNA complexed with chitosan nanoparticles." Biochimica et Biophysica Acta 1630 (2003): 7-18.
- Li, Y. et al. "Nanoparticles bearing polyethyleneglycol-coupled transferrin as gene carriers: preparation and in vitro evaluation." International Journal of Pharmaceutics 259 (2003): 93-101.
- Liang, D.C. et al. "Pre-deliver chitosanase to cells: a novel strategy to improve gene expression by endocellular degradation-induced vector unpacking." International Journal of Pharmaceutics 314 (2006): 63-71.
- Little S.R. et al. "Poly- amino ester-containing microparticles enhance the activity of nonviral genetic vaccines." Proceedings of the National Academy of Sciences USA 101 (2004): 9534-9539.

- Liu, W. et al. "An investigation on the physicochemical properties of chitosan/DNA complexes" Biomaterials 26 (2005): 2705-2711.
- Lodish, H. et al. "Molecular genetic techniques and genomics." In Molecular Cell Biology 378-380, New York, USA: W.H. Freeman and Company, 2004.
- Luangtana-anan, M. et al. "Effect of chitosan salts and molecular weight on a nanoparticulate carrier for therapeutic protein." Pharmaceutical Development and Technology 10 (2005): 189-196.
- MacLaughlin, F.C. et al. "Chitosan and depolymerized chitosan oligomers as condensing carriers for in vivo plasmid delivery." Journal of Controlled Release 6 (1998): 259-272.
- Mady, M.M. et al. "Efficient gene delivery with serum into human cancer cells using targeted anionic liposomes." Journal of Drug Targeting 12 (2004):11-8.
- Maestrelli, F. et al. "Influence of chitosan and its glutamate and hydrochloride salts on naproxen dissolution rate and permeation across Caco-2 cells." International Journal of Pharmaceutics 271 (2004): 257-267.
- Mao, H.Q. et al. "Chitosan-DNA nanoparticles as gene carriers: synthesis, characterization and transfection efficiency." Journal of Controlled Release 6 (2001): 399-421).
- Maruyama, A. et al. "Characterization of interpolyelectrolyte complexes between double-strand DNA and polylysine comb-type copolymers having hydrophilic side chains." Bioconjugate Chemistry 9 (1998): 292-299.
- Maruyama, K. et al. "Immunoliposomes bearing polyethyleneglycol-couple Fab' fragment show prolonged circulation time and high extravasation into targeted solid tumor in vivo." Federation of European Biochemical Societies Letters 413 (1997): 177-180.
- Maruyama, K. et al. "Novel receptor-mediated gene delivery system comprising plasmid/protamine/sugar-containing polyanion ternary complex." Biomaterials 25 (2004): 3267-3273.
- Matsuura, M. et al. "Polycation liposome-mediated gene transfer in vivo." Biochimica et Biophysica Acta 1612 (2003): 136-143.
- Mehier-Humbert, S. and R.H. Guy. "Physical methods for gene transfer: Improving the kinetics of gene delivery into cells." Advanced Drug Delivery Reviews 57 (2005): 733-753.

- Mislick, K.A. and J.D. Baldeschwieler. "Evidence for the role proteoglycans in cation-mediated gene transfer." Proceedings of the National Academy of Sciences USA 93 (1996): 12349–12354.
- Mislick, K.A. et al. "Transfection of folate-polylysine DNA complexes: evidence for lysosomal delivery." Bioconjugate Chemistry 6 (1995): 512-515.
- Mohamed, M.I. "Targeted gene delivery with trisaccharide-substituted chitosan oligomers in vitro and after lung administration in vivo." Journal of Controlled Release 115 (2006): 103-112.
- Mosmann, T. "Rapid colorimetric assay for cellular growth and survival: application to proliferation and cytotoxicity assay" Journal of Immunological Methods 65 (1983): 55-63.
- Mumper, R.J. et al. "Novel polymeric condensing carriers for gene delivery." Proceedings of the International Symposium Controlled Release Bioactive Materials 22 (1995): 178-179.
- Murata, J., Y. Ohya and T. Ouchi. "Design of quaternary chitosan conjugate having antennary galactose residues as a gene delivery tool." Carbohydrate Polymers 32 (1997): 105-109.
- Nathwani, A.C., J. McIntosh and A.M. Davidoff. "An update on gene therapy for hemophilia." Current Hematology Reports 4 (2005): 287-293.
- Neuman, E. et al. "Calcium-mediated DNA adsorption to yeast cells and kinetics of cell transformation by electroporation." Biophysical Journal 71 (1996): 868-877.
- Nicolau, C. and C. Sene. "Liposome-mediated DNA transfer in eukaryotic cells. Dependence of the transfer efficiency upon the type of liposomes used and the host cell cycle stage." Biochimica et Biophysica Acta 721 (1982): 185-190.
- Nicolau, C. et al. "In vivo expression of rat insulin after intravenous administration of the liposome-entrapped gene for rat insulin I." Proceedings of the National Academy of Sciences USA 80 (1983): 1068-1072.
- Nunthanid, J. et al. "Characterization of chitosan acetate as a binder for sustained release tablets." Journal of Controlled Release 99 (2004): 15-26.
- Ogris, M. et al. "PEGylated DNA/transferring-PEI complexes: Reduced interaction with blood and potential for systemic gene delivery." Gene Therapy 6 (1999): 595-605.

- Okamoto, H. et al. "Stability of chitosan-pDNA complex powder prepared by Supercritical carbon dioxide process." International Journal of Pharmaceutics 290 (2005): 73-81.
- Özgel, G. and J. Akbuğa. "In vitro characterization and transfection of IL-2 gene complexes." International Journal of Pharmaceutics 315 (2006): 44-51.
- Park, Y.J. et al. "Low molecular weight protamine as an efficient and nontoxic gene carrier: in vitro study." Journal of Gene Medicine 5 (2003): 700-711.
- Pedroso de Lima, M.C. et al. "Cationic lipid-DNA complexes in gene delivery: from biophysics to biological applications." Advanced Drug Delivery Reviews 47 (2001): 277-294.
- Peterson, G.L. "Dermination of total protein." Methods in Enzymology 91 (1983): 95.
- Perricone, M.A. et al. "Aerosol and lobar administration of a recombinant adenovirus to individuals with cystic fibrosis. II. Transfection efficiency in airway epithelium." Human Gene Therapy 12 (2001):1383-1394.
- Pouton, C.W. and L.W. Seymour. "Key issues in non-viral gene delivery." Advanced Drug Delivery Reviews 46 (2001): 187-203.
- Promega, Madison, IL, USA. Technical resources: complete vector list [Online]. Accessed 3 May 2007. Available from <http://www.promega.com/vectors/allvectors.htm>
- \_\_\_\_\_. .b Glo lysis buffer, 1x [Online]. Accessed 24 May 2007. Available from [http://www.promega.com/vectors/Glo lysis buffer, 1x.mht](http://www.promega.com/vectors/Glo%20lysis%20buffer%201x.mht)
- Qiagen, Santa Clarita, CA, USA. Qiagen plasmid purification [Online]. Accessed 28 November 2005. Available from <http://www.qiagen.com>
- Rebedea, I. et al. "Comparison of thiomersal-free and thiomersal-containing formulations of a recombinant hepatitis B vaccine (Hepavax-Gene) in healthy adults." Vaccine 24 (2006): 5320-5326.
- Rabinowitz, J.E. et al. "Cross-packaging of a single adeno-associated virus (AAV) type 2 vector genome into multiple AAV serotypes enables transduction with broad specificity." Journal of Virology 1 76 (2002): 791-801.
- Rejimen, J., A. et al. "Characterization and transfection properties of lipoplexes stabilized with novel exchangeable polyethylene glycol-lipid conjugates." Biochimica et Biophysica Acta 1660 (2004): 41-52.

- Richardson, S.C., H.V. Kolbe and R. Duncan. "Potential of low molecular mass chitosan as a DNA delivery system: biocompatibility, body distribution and ability to complex and protect DNA." International Journal of Pharmaceutics 178 (1999): 231-243.
- Robbins, P.D. and S.C. Ghivizzani. "Viral vectors for gene therapy." Pharmacology and Therapeutics 80 (1998): 35-47.
- Romero, D.G. et al. "Angiotensin II-Mediated Protein Kinase D Activation Stimulates Aldosterone and Cortisol Secretion in H295R Human Adrenocortical Cells." Endocrinology 147 (2006): 6046-6055.
- Romóren, K. et al. "The influence of formulation variables on in vitro transfection efficiency and physicochemical properties of chitosan-based polyplexes." International Journal of Pharmaceutics 26 (2003): 115-127.
- Roy, K. et al. "Oral gene delivery with chitosan-DNA nanoparticles generates immunologic protection in a murine model of peanut allergy." Nature Medicine 5 (1999): 387-391.
- Salvati, A., et al. "Physico-chemical characterization and transfection efficacy of cationic liposomes containing the pEGFP plasmid." Biophysical Chemistry 121 (2005): 21-29.
- Sato, T., T. Ishii and Y. Okahata. "In vitro gene delivery mediated by chitosan: effect of pH, serum, and molecular mass of chitosan on the transfection efficiency." Biomaterials 22 (2001): 2075-2080.
- Satoh et al. "6-Amino-6-deoxy-chitosan. Sequential chemical modifications at the C-6 positions of N-phthaloyl-chitosan and evaluation as a gene carrier." Carbohydrate Research 341 (2006): 2406-2413.
- Schakowski, F. et al. "Novel non-viral method for transfection of primary leukemia cells and cell lines." Genetic Vaccines and Therapy 12 (2004): 1.
- Schiedner, G. et al. "Genomic DNA transfer with a high-capacity adenovirus vector results in improved in vivo gene expression and decreased toxicity." Nature Genetics 18 (1998): 180-183.
- Schmitz, T. et al. "Development and in vitro evaluation of a thiomers-based nanoparticulate gene delivery system." Biomaterials 3 (2007): 524-531.

- Seville, P.C., I.W. Kellaway and J.C. Birchall. "Preparation of dry powder dispersions for non-viral gene delivery by freeze-drying and spray-drying." Journal of Gene Medicine 4 (2002): 428-437.
- Shenk, T.E. "Adenoviridae: the viruses and their replication." In Fields Virology, 2265-2300. Edited by Fields, B.N. and D.M. Knipe, Pennsylvania, USA: Lippincott Williams & Wilkins, 2001.
- Simon, R.H. et al. "Adenovirus-mediated gene transfer of the CFTR gene to the lung of non-human primates: a toxicity study." Human Gene Therapy 4 (1993): 771-780.
- Song, L.Y. et al. "Characterization of the inhibitory effect of PEG-lipid conjugates on the intracellular delivery of plasmid and antisense DNA mediated by cationic lipid liposomes." Biochimica et Biophysica Acta 1558 (2002): 1-13.
- Somia, N. and I.M. Verma. "Gene therapy: trials and tribulations." Nature Review Genetics 1 (2000): 91-99.
- Somiari, S. et al. "Theory and in vivo application of electroporative gene delivery." Molecular Therapy 2 (2000): 178-187.
- Smrekar, B. et al. "Tissue-dependent factors affect gene delivery to tumors in vivo." Gene Therapy 13 (2003): 1079-1088.
- Snustud, D.P. and M.J. Simmons "Molecular genetics: applications." In Principles of Genetics, 492-523. Asia: John Wiley and Sons Ltd., 2006.
- Stenesh, J. "Transcription-the synthesis of RNA." In Biochemistry, 454-455. New York, USA: Plenum Press, 1998.
- Stoscheck, C.M. "Quantitation of Protein." Methods in Enzymology 182 (1990): 50-69.
- Stracham, T. and A.P. Read. "New approaches to treating disease." In Human Molecular Genetics, 616. New York, USA: Garland Publishing, 2004.
- Strand, S.P. et al. "Influence of chitosan structure on the formation and stability of DNA-chitosan polyelectrolyte complexes." Biomacromolecules 6 (2005): 3357-3366.
- Suh, J. et al. "Ionization of poly(ethylenimine) and poly(allylamine) at various pH's." Bioorganic Chemistry 22 (1994): 318-327.
- Summerford, C. and R.J. Samulski. "Membrane-associated heparin sulfate proteoglycan is a receptor for adeno-associated virus type 2 virions." Journal of Virology 72 (1998): 1438-1445.

- Summerford, C., J.S. Bartlett and R.J. Samulski. "Alpha V beta 5 integrin: a co-receptor for adeno-associated virus type 2 infection." Nature Medicine 5 (1999): 78-82.
- Sun, M. et al. "Comparison of the capability of GDNF, BDNF, or both, to protect nigrostriatal neurons in a rat model of Parkinson's disease." Brain Research 1052 (2005): 119-129.
- Sun, X. and Z. Zhang. "Optimizing the novel formulation of liposome-polycation-DNA complexes (LPD) by central composite design." Archives of Pharmacal Research 27 (2004): 797-805.
- Todorova, K. et al. "Biochemical nature and mapping of PSMA epitopes recognized by human antibodies induced after immunization with gene-based vaccines." Anticancer Research 2005 (25): 4727-4732.
- Tang, D.C., M. DeVit and S.A. Johnston. "Genetic immunization is a simple method for eliciting an immune response." Nature 356 (1992): 152-154.
- Tang, M.X., C.T. Redemann and F.C. Szoka. "In vitro gene delivery by degraded polyamidoamine dendrimers." Bioconjugate Chemistry 7 (1996): 703-714.
- Tavel, J.A. et al. "Safety and immunogenicity of a Gag-Pol candidate HIV-1 DNA vaccine administered by a needle-free device in HIV-1-seronegative subjects." The Journal of Acquired Immune Deficiency Syndromes 44 (2007): 601-605.
- Templeton, N.S. "Cationic liposome-mediated gene delivery in vivo." Bioscience Reports 22 (2002): 283-295.
- Tengamnuay, P. et al. "Chitosans as nasal absorption enhancers of peptides: comparison between free amine chitosans and soluble salts." International Journal of Pharmaceutics 197 (2000): 53-67.
- Thanou, M. et al. "Quaternized chitosan oligomers as novel gene delivery vectors in epithelial cell lines." Biomaterials 23 (2002): 153-159.
- Thomas, M. and Klibanov, A.M. "Non-viral gene therapy: polycation-mediated DNA Delivery." Applied Microbiology and Biotechnology 62 (2003): 27-34.
- Toncheva, V. et al. "Novel vectors for gene delivery formed by self-assembly of DNA with poly(L-lysine) grafted with hydrophilic polymers." Biochimica et Biophysica Acta 138 (1998): 354-368.
- Toth, I. et al. "Novel cationic lipidic peptide dendrimer vectors-in vitro gene delivery." STP Pharma Sciences 9 (1999): 93-99.

- Ulmer, J.B. "Heterologous protection against influenza by injection of DNA encoding a viral protein." Science 259 (1993): 1745-1749.
- Vanderbyl, S., N. Macdonald and G. de Jong. "A flow cytometry technique for measuring chromosome-mediated gene transfer." Cytometry 44 (2001): 100-105.
- Vidal, M. and D. Hoekstra. "In vitro fusion of reticulocyte endocytic vesicles with liposome ." Journal of Biological Chemistry 279 (1995): 17823-17829.
- Walker, G.F. et al. "Toward synthetic viruses: endosomal pH-triggered deshielding of targeted polyplexes greatly enhances gene transfer in vitro and in vivo." Molecular Therapy 11 (2005): 418-425.
- Walsh, G. "Nucleic acid therapeutics." In Biopharmaceuticals: Biochemistry and Biotechnology, 396-402. New York, USA: John Wiley and Sons, 1998.
- Wang, J. et al. "Synthesis and characterization of long chain alkyl acyl carnitine esters. Potentially biodegradable cationic lipids for use in gene delivery." Journal of Medical Chemistry 41 (1998): 2207-2215.
- Wang, X. et al. "Gene transfer to dorsal root ganglia by intrathecal injection: effects on regeneration of peripheral nerves." Molecular Therapy 12 (2005): 314-320.
- Weaver, R.F. "Molecular tools for studying genes and gene activity." In Molecular Biology, 95-134. New York, USA: Von Hoffman Press, 1999.
- Weaver, R.F. "The transcription apparatus for prokaryotes." In Molecular Biology, 141-145. New York, USA: Von Hoffman Press, 1999.
- Weecharangsan, W. et al. "Chitosan lactate as a nonviral gene delivery vector in COS-1 cells." The AAPS PharmSciTech Journal 7 (2006.): E1-E6.
- Wickham, T.J., M.E. Carrion and I. Kovesdi. "Targeting of adenovirus penton base to new receptors through replacement of its RGD motif with other receptor-specific peptide motifs." Gene Therapy 2 (1995): 750-756.
- Wickham, T.J. et al. "Targeted adenovirus gene transfer to endothelial and smooth muscle cells by using bispecific antibodies." Journal of Virology 70 (1996): 6831-6838.
- Wikipedia, FL, USA-a. Atomic force microscope [Online]. Accessed 28 May 2007. Available from [http://en.wikipedia.org/wiki/Atomic\\_force\\_microscope](http://en.wikipedia.org/wiki/Atomic_force_microscope)
- \_\_\_\_\_.b Transmission electron microscopy [Online]. Accessed 27 May 2007. Available from [http://en.wikipedia.org/wiki/Transmission\\_electron\\_Microscopy](http://en.wikipedia.org/wiki/Transmission_electron_Microscopy)

- \_\_\_\_\_. c Gene therapy [Online]. Accessed 28 May 2007. Available from [http://en.wikipedia.org/wiki/Gene\\_therapy](http://en.wikipedia.org/wiki/Gene_therapy)
- Winter, P.C., G.I. Hickey and H.L. Fletcher. "Recombinant DNA technology." In Genetics, 255-294. Guildford, UK: Biddles Ltd., 2002.
- Woodle, M.C. "Controlling liposome blood clearance by surface-grafted polymers." Advanced Drug Delivery Reviews 32 (1998): 139-152.
- Wu, G.Y. and C.H. Wu. "Receptor-mediated in vitro gene transformation by a soluble DNA carrier system." Journal of Biological Chemistry 262 (1987): 4429-4432.
- Xu, W. et al. "Intranasal delivery of chitosan-DNA vaccine generates mucosal SIgA and anti-CVB3 protection." Vaccine 22 (2004): 3603-3612.
- Yamagata, M. et al. "Structural advantage of dendritic poly(L-lysine) for gene delivery into cells." Bioorganic and Medicinal Chemistry 15 (2007): 526-532.
- Yamashita, A. et al. "Improved cell viability of linear polyethylenimine through  $\gamma$ -cyclodextrin inclusion for effective gene delivery." ChemBioChem 7 (2006): 297-302.
- Yang, N.S. et al. "In vivo and in vitro gene transfer to mammalian somatic cells by particle bombardment." Proceedings of the National Academy of Sciences USA 87 (1990): 9568-9572.
- Yoo, H.S. et al. "Self-assembled nanoparticles containing hydrophobically modified glycol chitosan for gene delivery." Journal of Controlled Release 103 (2005): 235-243.
- Zhang, C., P. Yadava and J. Hughes. "Polyethylenimine strategies for plasmid delivery to brain derived cells." Methods 33 (2004): 144-150.
- Zhang, S. et al. "Cationic compounds used in lipoplexes and polyplexes for gene delivery." Journal of Controlled Release 100 (2004): 165-180.
- Zhang, X. et al. "Direct chitosan-mediated gene delivery to the rabbit knee joints in vitro and in vivo." Biochemical Biophysical Research Communications 341 (2006): 202-208.
- Zhao, X. et al. "Transfection of primary chondrocytes using chitosan-pEGFP nanoparticles." Journal of Controlled Release 112 (2006): 223-228.
- Zhao Y.G. et al. "Inhibitory effect of  $\text{Ca}^{2+}$  on in vivo gene transfer by electroporation." Acta Pharmacologica Sinica 27 (2006): 307-310.

## Appendix I

### Relative fluorescent intensity data of SD-CS/DNA complexes

Table 1 Relative fluorescent intensity data of SD-CS/DNA complexes with various chitosan MW.

Complex	N/P ratio				Complex	N/P ratio			
	4	12	20	28		4	12	20	28
SD-CAs-20kDa/DNA	78.89	70.21	63.59	59.04	SD-CAs-200kDa/DNA	78.32	74.57	68.74	64.15
	83.88	64.40	60.05	56.81		86.40	83.77	77.36	75.94
	74.21	69.87	68.08	70.30		76.69	67.08	73.68	69.04
Average	78.99	68.16	63.91	62.05	Average	80.47	75.14	73.26	69.71
SD	4.84	3.26	4.03	7.23	SD	5.20	8.36	4.33	5.92
SD-CGI-20kDa/DNA	82.17	75.85	69.54	64.71	SD-CGI-200kDa/DNA	79.54	76.33	71.92	66.31
	82.35	78.14	74.19	68.80		83.72	80.56	75.26	70.98
	72.86	80.07	76.84	72.06		90.77	76.40	81.64	75.38
Average	79.13	78.02	73.52	68.52	Average	84.68	77.77	76.27	70.89
SD	5.43	2.11	3.69	3.68	SD	5.67	2.42	4.94	4.54
SD-CLa-20kDa/DNA	73.52	72.24	65.99	57.00	SD-CLa-200kDa/DNA	75.27	73.25	70.41	64.33
	71.86	69.22	62.38	57.82		75.25	70.37	64.87	61.62
	83.57	68.99	63.93	57.87		79.52	72.84	67.72	65.45
Average	76.32	70.15	64.10	57.56	Average	76.68	72.15	67.67	63.80
SD	6.34	1.82	1.81	0.49	SD	2.46	1.56	2.77	1.97
SD-CAs-45kDa/DNA	78.46	70.09	65.10	58.87	SD-CAs-460kDa/DNA	73.14	77.06	70.91	66.41
	82.09	79.73	73.05	66.93		69.82	76.84	68.12	65.71
	82.02	78.06	77.19	69.47		84.12	74.93	67.83	58.64
Average	80.86	75.96	71.78	65.09	Average	75.69	76.28	68.95	63.59
SD	2.08	5.15	6.14	5.53	SD	7.49	1.17	1.70	4.30
SD-CGI-45kDa/DNA	76.73	74.15	68.27	62.79	SD-CGI-460kDa/DNA	82.79	70.37	66.03	60.50
	81.29	79.20	76.24	72.57		81.38	66.88	62.50	58.33
	88.73	78.67	74.78	72.93		82.04	78.65	76.59	69.72
Average	82.25	77.34	73.10	69.43	Average	82.07	71.96	68.37	62.85
SD	6.05	2.78	4.24	5.75	SD	0.71	6.04	7.33	6.05
SD-CLa-45kDa/DNA	78.24	75.42	70.99	64.54	SD-CLa-460kDa/DNA	68.82	68.39	63.26	64.12
	86.21	65.95	58.15	51.69		70.77	62.77	66.30	61.46
	70.53	64.80	59.39	58.93		79.50	78.16	71.09	66.36
Average	78.33	68.72	62.84	58.39	Average	73.03	69.77	66.88	63.98
SD	7.84	5.83	7.08	6.44	SD	5.69	7.79	3.94	2.46

## Appendix II

### Particle size and zeta potential data of SD-CS/DNA complex

Table 2 Particle size and zeta potential data of SD-CS-20kDa/DNA complexes.

Complex	N/P ratio	Size (nm)	Average	SD	ZP (mV)	Average	SD
SD-CAs-20kDa/DNA	4	2538	2310.00	199.87	-0.34	-0.72	1.51
		2227			0.56		
		2165			-2.38		
	12	262	268.60	7.86	32.18	31.50	0.94
		277			30.43		
		267			31.90		
	20	252	246.83	5.63	30.98	31.54	0.66
		248			32.27		
		241			31.36		
	28	280	279.67	0.90	39.54	38.57	0.94
		279			37.66		
		281			38.52		
SD-CGI-20kDa/DNA	4	4857	3880.67	886.53	-6.04	-5.71	0.56
		3126			-6.03		
		3659			-5.06		
	12	1130	1879.67	1225.59	18.64	20.29	1.57
		3294			20.45		
		1215			21.77		
	20	234	232.90	2.26	29.86	29.64	0.35
		230			29.23		
		234			29.82		
	28	221	218.30	2.42	32.63	32.50	0.33
		217			32.13		
		217			32.75		
SD-CLa-20kDa/DNA	4	627	635.17	11.94	0.33	0.13	0.56
		630			-0.49		
		649			0.56		
	12	243	246.70	6.68	28.54	28.29	0.37
		254			27.86		
		242			28.46		
	20	236	238.43	2.26	38.49	39.14	0.56
		241			39.39		
		238			39.53		
	28	342	334.27	8.24	34.98	34.79	0.69
		325			34.03		
		336			35.37		

Table 3 Particle size and zeta potential data of SD-CS-45kDa/DNA complexes.

Complex	N/P ratio	Size (nm)	Average	SD	ZP (mV)	Average	SD
SD-CAs-45kDa/DNA	4	6370	5992.00	642.63	-3.45	-3.19	0.63
		6356			-3.65		
		5250			-2.48		
	12	241	239.33	5.94	24.83	24.58	0.63
245		25.05					
233		23.86					
20	274	283.83	9.15	29.16	29.24	0.18	
	285			29.44			
	292			29.11			
28	224	225.57	1.33	34.30	33.73	0.81	
	226			32.80			
	227			34.10			
SD-CG1-45kDa/DNA	4	4343	4515.00	191.91	-3.83	-4.08	0.21
		4480			-4.17		
		4722			-4.23		
	12	297	285.77	10.00	25.60	24.67	0.85
280		24.48					
281		23.93					
20	305	297.83	8.47	31.89	31.34	1.48	
	301			32.47			
	288			29.66			
28	229	230.10	3.11	36.47	36.51	0.23	
	227			36.76			
	234			36.31			
SD-CLa-45kDa/DNA	4	665	749.87	93.32	0.78	0.41	0.77
		736			0.93		
		850			-0.48		
	12	301	300.00	3.74	30.39	30.34	1.20
303		31.51					
296		29.12					
20	207	208.83	7.12	27.97	27.22	2.68	
	217			29.45			
	203			24.24			
28	203	201.90	1.10	32.95	36.13	2.76	
	202			37.47			
	201			37.96			

Table 4 Particle size and zeta potential data of SD-CS-200kDa/DNA complexes.

Complex	N/P ratio	Size (nm)	Average	SD	ZP (mV)	Average	SD
SD-CAs-200kDa/DNA	4	6483 5056 5710	5749.67	714.33	1.33 1.35 0.89	1.19	0.26
	12	371 405 380	385.37	17.65	32.77 31.44 32.86	32.36	0.80
	20	365 355 369	363.17	7.24	39.42 38.36 36.91	38.23	1.26
	28	449 449 459	452.53	5.86	45.98 47.26 45.45	46.23	0.93
SD-CGI-200kDa/DNA	4	2652 2246 5107	3335.00	1547.97	-17.71 -17.00 -16.41	-17.04	0.65
	12	382 401 402	394.77	11.43	23.57 21.11 23.76	22.81	1.48
	20	621 563 646	610.20	42.33	32.92 34.48 32.22	33.21	1.16
	28	720 757 724	733.90	20.18	48.01 48.70 48.96	48.56	0.49
SD-CLa-200kDa/DNA	4	4688 4111 5220	4673.00	554.65	9.28 7.74 7.34	8.12	1.02
	12	479 495 470	481.13	12.96	34.82 36.39 36.00	35.74	0.82
	20	632 671 668	657.03	21.54	48.05 52.87 52.78	51.23	2.76
	28	562 584 568	571.20	11.63	49.94 47.99 49.38	49.10	1.00

Table 5 Particle size and zeta potential data of SD-CS-460kDa/DNA complexes.

Complex	N/P ratio	Size (nm)	Average	SD	ZP (mV)	Average	SD
SD-CAs-460kDa/DNA	4	3777	4195.67	392.76	-2.37	-3.04	0.73
		4254			-2.92		
		4556			-3.83		
	12	456	459.93	4.72	30.45	30.07	0.37
		465			29.71		
		458			30.06		
	20	530	537.70	33.46	40.36	40.12	0.24
		574			39.88		
		509			40.13		
	28	621	617.37	41.84	44.96	44.78	0.38
		574			45.04		
		658			44.35		
SD-CG1-460kDa/DNA	4	4226	3767.67	745.04	-11.29	-10.94	0.53
		2908			-11.20		
		4169			-10.33		
	12	446	435.83	15.56	20.27	21.43	1.11
		444			22.48		
		418			21.53		
	20	374	368.43	5.20	31.76	30.68	0.97
		369			30.41		
		363			29.87		
	28	359	358.60	4.75	36.57	36.28	0.65
		354			36.73		
		363			35.53		
SD-CLa-460kDa/DNA	4	3036	3049.00	253.75	2.71	3.73	1.07
		3309			3.66		
		2802			4.84		
	12	545	538.90	15.09	35.58	35.46	0.11
		550			35.38		
		522			35.42		
	20	469	448.43	17.84	37.47	36.51	0.91
		437			35.65		
		439			36.40		
	28	331	351.13	17.82	36.51	35.62	1.05
		360			35.89		
		363			34.46		

### Appendix III

#### Transfection efficiency data of SD-CS/DNA complexes

Table 6 Transfection efficiency data of SD-CS/DNA complexes in COS-1 cells.

Complex	N/P ratio				Complex	N/P ratio			
	4	12	20	28		4	12	20	28
SD-CAs-20kDa/DNA	1.33	1.46	1.25	1.21	SD-CAs-200kDa/DNA	1.63	0.90	1.54	1.32
	0.92	1.43	1.78	2.07		1.58	1.34	1.45	1.21
	1.16	1.44	1.42	1.77		1.44	0.78	1.01	1.16
Average	1.14	1.45	1.48	1.68	Average	1.55	1.01	1.33	0.28
SD	0.21	0.02	0.27	0.44	SD	0.09	0.29	0.28	0.08
SD-CGI-20kDa/DNA	1.49	1.66	1.28	1.08	SD-CGI-200kDa/DNA	2.10	1.00	0.64	0.99
	1.30	1.42	1.08	1.76		1.49	0.75	0.70	1.21
	1.51	1.17	1.64	1.12		1.12	0.76	0.46	0.81
Average	1.43	1.41	1.33	1.32	Average	1.57	0.84	0.60	1.00
SD	0.12	0.24	0.28	0.38	SD	0.49	0.14	0.12	0.20
SD-CLa-20kDa/DNA	1.76	1.72	1.24	1.40	SD-CLa-200kDa/DNA	2.02	0.71	0.71	1.13
	1.82	1.87	1.17	1.23		1.22	0.64	0.85	0.93
	1.30	0.89	1.18	1.65		1.10	0.66	0.74	1.15
Average	1.63	1.49	1.20	1.42	Average	1.45	0.67	0.76	1.07
SD	0.29	0.53	0.04	0.21	SD	0.50	0.04	0.07	0.12
SD-CAs-45kDa/DNA	1.19	1.11	1.54	1.11	SD-CAs-460kDa/DNA	0.81	0.85	1.58	0.86
	1.19	1.28	1.45	1.04		0.97	0.80	1.50	0.73
	1.50	1.93	1.01	1.79		1.09	0.94	1.27	0.72
Average	1.29	1.44	1.33	1.31	Average	0.96	0.86	1.45	0.16
SD	0.18	0.43	0.28	0.41	SD	0.14	0.07	0.16	0.08
SD-CGI-45kDa/DNA	1.30	1.14	0.64	1.14	SD-CGI-460kDa/DNA	1.30	1.24	1.37	0.77
	1.44	1.26	0.70	1.01		1.20	1.02	1.47	0.63
	1.35	1.13	0.46	1.12		1.39	0.86	1.77	0.56
Average	1.36	1.18	0.60	1.09	Average	1.30	1.04	1.53	0.65
SD	0.07	0.07	0.12	0.07	SD	0.10	0.19	0.21	0.11
SD-CLa-45kDa/DNA	1.11	0.64	0.71	1.20	SD-CLa-460kDa/DNA	1.12	0.85	1.47	0.48
	1.43	0.88	0.85	1.38		1.04	0.78	1.42	0.88
	1.01	1.02	0.74	1.79		1.51	0.85	1.65	0.66
Average	1.18	0.85	0.76	1.45	Average	1.22	0.83	1.52	0.67
SD	0.22	0.19	0.07	0.30	SD	0.25	0.04	0.12	0.20

Table 7 Transfection efficiency data of SD-CS/DNA complexes in CHO-K1 cells.

Complex	N/P ratio				
	2	4	6	8	12
SD-CAs-20kDa/DNA	147.74	230.18	152.11	47.59	166.10
	346.03	112.16	164.53	288.45	232.54
	100.59	45.27	64.96	162.75	52.20
Average	198.12	129.20	127.20	166.26	150.28
SD	130.25	93.62	54.26	120.47	91.21
SD-CGI-20kDa/DNA	233.55	62.64	1511.12	79.12	82.98
	347.81	219.84	99.75	118.63	108.10
	81.07	48.55	103.92	80.36	80.19
Average	220.81	110.34	571.60	92.70	90.42
SD	133.83	95.09	813.65	22.46	15.37
SD-CLa-20kDa/DNA	109.56	79.80	168.98	17.96	263.07
	89.42	100.88	89.60	77.24	152.77
	84.73	87.22	97.00	253.42	192.46
Average	94.57	89.30	118.53	116.21	202.77
SD	13.19	10.70	43.85	122.47	55.87
SD-CAs-45kDa/DNA	115.16	35.33	100.79	172.82	123.34
	69.69	121.12	92.48	76.53	169.08
	151.20	150.20	138.74	134.52	236.74
Average	112.02	102.21	110.67	127.96	176.39
SD	40.84	59.72	24.66	48.48	57.05
SD-CGI-45kDa/DNA	87.93	586.84	130.21	1.07	64.41
	413.72	4.42	202.26	227.39	107.45
	1084.38	521.83	216.43	349.36	386.61
Average	528.68	371.03	182.97	192.61	186.16
SD	508.08	319.15	46.23	176.73	174.93
SD-CLa-45kDa/DNA	146.53	48.26	58.06	157.70	161.51
	18.77	257.22	222.24	117.74	581.71
	175.75	122.68	412.05	56.67	251.36
Average	113.68	142.72	230.78	110.70	331.53
SD	83.48	105.91	177.15	50.88	221.27

Table 7 Transfection efficiency data of SD-CS/DNA complexes in CHO-K1 cells  
(Continued).

Complex	N/P ratio				
	2	4	6	8	12
SD-CAs-200kDa/DNA	196.08	99.37	131.94	189.54	148.98
	289.53	191.08	66.43	235.78	144.16
	187.75	134.01	145.93	513.03	482.00
Average	224.45	141.49	114.77	312.78	258.38
SD	56.51	46.31	42.44	174.95	193.67
SD-CGI-200kDa/DNA	22.77	11.38	19.89	12.82	20.85
	143.88	192.57	39.33	20.47	147.23
	524.28	325.22	2721.11	327.30	137.07
Average	230.31	176.39	926.78	120.20	101.72
SD	261.69	157.54	1553.97	179.40	70.21
SD-CLa-200kDa/DNA	97.64	100.40	3706.70	3594.48	20.64
	128.96	167.26	107.29	110.04	166.20
	184.79	452.75	451.45	148.54	184.19
Average	137.13	240.14	1421.81	1284.35	123.67
SD	44.15	187.14	1986.24	2000.72	89.68
SD-CAs-460kDa/DNA	62.54	118.34	105.77	88.39	102.34
	76.33	80.26	67.80	113.70	138.86
	118.03	80.63	80.36	79.91	80.28
Average	85.63	93.08	84.65	94.00	107.16
SD	28.89	21.88	19.34	17.58	29.58
SD-CGI-460kDa/DNA	53.28	68.09	102.99	48.25	71.59
	52.33	108.99	124.56	171.41	97.60
	84.87	88.80	52.04	125.26	101.65
Average	63.49	88.63	93.20	114.97	90.28
SD	18.52	20.45	37.24	62.22	16.31
SD-CLa-460kDa/DNA	97.04	148.60	228.27	212.55	135.47
	153.87	114.79	195.86	121.41	160.44
	118.35	186.71	94.64	106.78	116.68
Average	123.09	150.04	172.92	146.91	137.53
SD	28.71	35.98	69.71	57.31	21.95

### Appendix IV

Cytotoxicity data of SD-CS/DNA complexes in COS-1 cells

Table 8 Cytotoxicity data of SD-CS-20kDa/DNA and SD-CS-45kDa/DNA complexes.

Complex	N/P ratio			
	4	12	20	28
SD-CAs-20kDa/DNA	105.31	106.55	92.48	113.81
	119.25	95.13	104.96	102.79
	99.56	103.67	101.68	120.13
	106.19	93.81	94.25	112.17
	108.05	105.19	103.27	113.81
	113.30	109.97	109.69	110.23
Average	108.61	102.39	101.05	112.16
SD	6.84	6.49	6.56	5.67
SD-CGI-20kDa/DNA	114.34	113.27	100.31	98.86
	110.75	112.79	107.96	108.63
	97.61	98.67	111.68	104.20
	109.25	110.62	96.02	109.73
	105.37	97.70	94.88	113.69
	102.56	112.72	101.79	93.61
Average	106.65	107.63	102.11	104.79
SD	6.05	7.38	6.61	7.47
SD-CLa-20kDa/DNA	98.45	99.34	104.56	107.70
	107.08	98.32	104.65	107.48
	101.11	109.73	108.41	108.10
	101.99	103.10	107.96	118.14
	117.65	92.07	93.61	99.80
	104.09	110.88	106.39	105.83
Average	105.06	102.24	104.26	107.84
SD	6.81	7.19	5.46	5.92
SD-CAs-45kDa/DNA	102.21	112.62	107.67	125.24
	119.24	106.62	113.56	113.88
	102.84	113.56	91.17	105.05
	108.52	99.37	104.73	114.79
	98.86	92.97	91.17	97.38
	91.07	90.22	95.90	90.76
Average	103.79	102.56	100.70	107.85
SD	9.49	9.93	9.33	12.62
SD-CGI-45kDa/DNA	101.58	110.73	111.55	113.85
	103.47	112.93	113.25	115.33
	109.78	93.69	113.44	114.38
	105.36	92.43	98.42	104.73
	93.38	87.29	94.01	99.68
	76.97	93.91	88.33	91.17
Average	98.42	98.50	103.17	106.52
SD	11.82	10.63	10.99	9.79
SD-CLa-45kDa/DNA	95.40	96.68	95.19	115.60
	108.31	98.47	104.35	108.18
	108.44	105.12	116.37	105.55
	95.14	94.65	95.40	101.28
	103.63	95.93	110.23	121.48
	90.79	119.44	107.42	94.63
Average	100.28	101.71	104.83	107.79
SD	7.52	9.43	8.38	9.69

Table 9 Cytotoxicity data of SD-CS-200kDa/DNA and SD-CS-460kDa/DNA complexes

Complex	N/P ratio				Control
	4	12	20	28	
SD-CAs-200kDa/DNA	76.77	93.81	114.29	104.87	96.45
	83.63	114.60	112.17	110.62	101.08
	104.42	113.05	113.94	117.70	95.11
	105.31	109.73	103.54	89.42	105.99
	118.67	130.43	99.74	117.90	102.65
	80.05	102.05	86.98	109.21	104.09
Average	94.81	110.61	105.11	108.29	100.89
SD	16.97	12.42	10.70	10.53	4.30
SD-CGI-200kDa/DNA	118.14	97.70	134.27	103.32	96.45
	101.55	89.42	123.79	117.62	101.08
	103.98	98.19	122.51	94.88	95.11
	88.27	97.12	120.72	114.50	105.99
	115.60	115.09	102.81	98.86	102.65
	98.26	108.95	128.13	89.00	104.09
Average	104.30	101.08	122.04	103.03	100.89
SD	11.14	9.27	10.60	11.18	4.30
SD-CLa-200kDa/DNA	95.35	117.65	109.07	118.14	96.45
	111.28	125.22	110.18	113.27	101.08
	115.27	100.98	118.36	102.65	95.11
	124.56	117.04	100.22	131.19	105.99
	100.77	114.83	111.00	106.39	102.65
	94.88	90.28	103.32	90.79	104.09
Average	107.02	111.00	108.69	110.41	100.89
SD	11.97	12.86	6.35	13.86	4.30
SD-CAs-460kDa/DNA	107.85	126.81	113.75	112.30	96.45
	118.30	106.94	106.94	87.07	101.08
	113.56	101.89	100.37	100.87	95.11
	107.89	98.33	115.46	105.68	105.99
	100.95	90.44	91.39	96.53	102.65
	93.50	97.07	89.72	77.60	104.09
Average	107.01	103.58	102.94	96.67	100.89
SD	8.84	12.62	11.00	12.64	4.30
SD-CGI-460kDa/DNA	116.72	122.40	110.09	107.57	96.45
	124.92	117.00	115.14	127.76	101.08
	108.52	123.03	113.66	107.57	95.11
	108.83	111.67	113.12	108.20	105.99
	90.13	98.42	99.22	90.22	102.65
	98.64	97.79	82.02	95.49	104.09
Average	107.96	111.72	105.54	106.14	100.89
SD	12.41	11.32	12.88	12.98	4.30
SD-CLa-460kDa/DNA	115.43	113.75	111.36	110.73	96.45
	113.44	122.40	113.56	108.08	101.08
	104.42	121.13	91.48	117.67	95.11
	113.34	98.74	94.01	122.40	105.99
	97.38	100.63	94.54	100.63	102.65
	96.12	91.07	85.49	98.86	104.09
Average	106.69	107.95	98.41	109.73	100.89
SD	8.60	12.96	11.37	9.25	4.30

### Appendix V

#### Particle size and zeta potential data of CS/DNA complex

Table 10 Particle size and zeta potential data of CS-45kDa/DNA complexes at pH 3.0.

Complex	N/P ratio	Size (nm)	Average	SD	ZP (mV)	Average	SD
CAc-45kDa/DNA	2	287	293.00	5.29	27.3	28.13	0.80
		297			28.2		
		295			28.9		
	6	200	196.33	4.04	41.2	40.87	0.35
		197			40.9		
		192			40.5		
	12	212	204.00	9.17	47.2	47.73	0.68
		206			48.5		
		194			47.5		
CAs-45kDa/DNA	2	200	193.67	5.69	25.4	29.50	3.57
		192			31.2		
		189			31.9		
	6	204	210.00	5.29	39.5	40.70	1.15
		214			41.8		
		212			40.8		
	12	256	240.67	13.61	47.8	47.67	0.42
		236			47.2		
		230			48.0		
CHy-45kDa/DNA	2	132	135.00	2.65	23.8	24.50	1.30
		137			23.7		
		136			26.0		
	6	135	129.67	5.03	33.7	33.27	0.40
		129			32.9		
		125			33.2		
	12	153	155.67	2.52	37.8	39.87	1.89
		156			40.3		
		158			41.5		
CLa-45kDa/DNA	2	157	153.00	3.46	32.9	32.07	1.04
		151			30.9		
		151			32.4		
	6	170	166.67	3.06	38.2	36.20	2.80
		166			33.0		
		164			37.4		
	12	188	184.33	3.21	38.4	39.10	0.75
		182			39.9		
		183			39.0		

Table 11 Particle size and zeta potential data of CGI/DNA complexes at pH 3.0.

Complex	N/P ratio	Size (nm)	Average	SD	ZP (mV)	Average	SD
CGI-20kDa/DNA	2	202	200.67	2.31	30.5	29.90	0.87
		202			28.9		
		198			30.3		
	6	163	173.00	8.72	40.8	42.23	1.29
		179			42.6		
		177			43.3		
	12	216	201.33	12.86	31.6	36.07	3.93
		192			39.0		
		196			37.6		
CGI-45kDa/DNA	2	214	215.00	1.73	26.4	26.10	1.28
		217			27.2		
		214			24.7		
	6	261	249.00	15.13	35.8	37.63	1.96
		254			37.4		
		232			39.7		
	12	205	201.67	4.16	39.7	41.47	1.54
		197			42.2		
		203			42.5		
CGI-200kDa/DNA	2	334	330.67	4.16	33.7	34.43	0.75
		332			34.4		
		326			35.2		
	6	386	388.00	8.19	52.1	49.70	3.10
		397			46.2		
		381			50.8		
	12	356	367.67	11.50	57.2	56.40	1.47
		379			57.3		
		368			54.7		
CGI-460kDa/DNA	2	306	325.00	18.08	32.6	32.53	2.10
		327			30.4		
		342			34.6		
	6	412	414.33	4.04	52.1	52.10	2.40
		412			49.7		
		419			54.5		
	12	367	376.00	21.93	50.1	50.07	1.65
		360			48.4		
		401			51.7		

Table 12 Particle size and zeta potential data of CS-45kDa/DNA complexes at pH 6.5.

Complex	N/P ratio	Size (nm)	Average	SD	ZP (mV)	Average	SD
CAc-45kDa/DNA	1	165	163.00	2.00	-38.5	-36.93	1.66
		161			-35.2		
		163			-37.1		
	2	1280	1390.00	101.49	-4.4	-4.35	0.36
		1410			-4.0		
		1480			-4.7		
	4	153	153.33	0.58	18.5	19.00	0.70
154		19.8					
153		18.7					
6	120	116.33	3.21	22.1	23.50	3.14	
	114			21.3			
	115			27.1			
8	159	156.00	2.65	23.0	22.70	1.67	
	154			20.9			
	155			24.2			
12	192	193.00	2.65	14.9	15.00	0.46	
	196			15.5			
	191			14.6			
CAs-45kDa/DNA	1	174	173.67	0.58	-43.8	-40.70	4.78
		174			-43.1		
		173			-35.2		
	2	1130	1276.67	155.67	3.2	3.64	0.46
		1260			3.5		
		1440			4.1		
	4	114	112.67	1.15	21.5	18.43	2.80
112		16.0					
112		17.8					
6	101	102.00	1.00	24.8	24.43	0.35	
	102			24.4			
	103			24.1			
8	135	127.33	6.66	21.0	21.87	1.25	
	123			21.3			
	124			23.3			
12	194	188.00	5.29	19.5	19.30	0.35	
	186			19.5			
	184			18.9			

Table 13 Particle size and zeta potential data of CS-45kDa/DNA complexes at pH 6.5  
(Continued).

Complex	N/P ratio	Size (nm)	Average	SD	ZP (mV)	Average	SD
CHy-45kDa/DNA	1	1570	1533.33	32.15	-59.1	-58.63	0.45
		1520			-58.6		
		1510			-58.2		
	2	4710	3346.67	1251.49	-4.4	-4.65	0.26
		3080			-4.9		
		2250			-4.7		
	4	119	120.67	2.08	16.7	18.20	1.37
120		19.4					
123		18.5					
6	681	660.00	22.65	9.4	10.52	1.03	
	663			10.9			
	636			11.3			
8	167	170.00	3.61	25.4	28.03	2.35	
	169			28.8			
	174			29.9			
12	154	154.67	1.15	23.5	22.60	0.85	
	156			21.8			
	154			22.5			
CLa-45kDa/DNA	1	540	538.33	18.56	-52.9	-53.50	1.87
		556			-52.0		
		519			-55.6		
	2	1820	2553.33	698.16	-4.3	-2.93	1.36
		2630			-2.9		
		3210			-1.6		
	4	218	218.67	3.06	18.2	18.30	0.75
222		19.1					
216		17.6					
6	143	141.00	1.73	20.2	20.60	1.64	
	140			22.4			
	140			19.2			
8	122	125.00	3.00	15.9	18.93	2.63	
	125			20.5			
	128			20.4			
12	102	101.33	1.15	25.8	25.87	1.20	
	100			24.7			
	102			27.1			

Table 14 Particle size and zeta potential data of CGI/DNA complexes at pH 6.5.

Complex	N/P ratio	Size (nm)	Average	SD	ZP (mV)	Average	SD
CGI-20kDa/DNA	1	189	188.33	0.58	-39.8	-41.87	2.40
		188			-44.5		
		188			-41.3		
	2	460	460.00	9.00	13.0	13.57	0.74
		469			14.4		
		451			13.3		
	4	133	132.00	3.61	17.8	19.97	2.06
135		20.2					
128		21.9					
6	136	135.00	1.00	19.3	18.33	0.91	
	135			17.5			
	134			18.2			
8	144	147.33	3.06	27.9	26.87	1.79	
	150			24.8			
	148			27.9			
12	154	153.33	1.15	21.8	19.37	2.45	
	154			19.4			
	152			16.9			
CGI-45kDa/DNA	1	203	202.67	2.52	-45.1	-45.80	0.66
		205			-46.4		
		200			-45.9		
	2	865	856.33	43.65	8.8	8.63	0.30
		809			8.8		
		895			8.3		
	4	123	122.33	0.58	18.6	19.57	0.87
122		20.3					
122		19.8					
6	120	119.33	0.58	18.1	16.13	2.06	
	119			14.0			
	119			16.3			
8	153	148.67	3.79	24.7	23.90	0.80	
	146			23.9			
	147			23.1			
12	300	299.00	1.00	14.2	13.87	0.35	
	299			13.5			
	298			13.9			

Table 14 Particle size and zeta potential data of CGI/DNA complexes at pH 6.5  
(continued).

Complex	N/P ratio	Size (nm)	Average	SD	ZP (mV)	Average	SD
CGI-200kDa/DNA	1	189	184.33	4.51	-34.0	-38.90	5.17
		184			-38.4		
		180			-44.3		
	2	180	183.33	3.06	20.7	22.17	2.45
		184			20.8		
		186			25.0		
	4	199	205.33	6.03	38.5	36.40	2.26
211		34.0					
206		36.7					
6	249	243.33	14.36	30.5	32.00	2.10	
	254			31.1			
	227			34.4			
8	291	280.67	9.29	25.4	26.63	1.37	
	273			26.4			
	278			28.1			
12	309	317.00	8.00	28.3	28.57	0.25	
	325			28.8			
	317			28.6			
CGI-460kDa/DNA	1	229	237.00	9.85	-39.1	-40.60	1.45
		234			-40.7		
		248			-42.0		
	2	193	191.33	1.53	26.1	24.07	1.84
		191			22.5		
		190			23.6		
	4	283	272.67	11.68	34.4	33.20	1.15
260		32.1					
275		33.1					
6	312	302.33	12.66	30.8	31.03	1.96	
	307			33.1			
	288			29.2			
8	314	308.67	5.51	25.8	26.93	1.00	
	303			27.7			
	309			27.3			
12	423	416.00	24.27	31.9	33.27	1.58	
	389			32.9			
	436			35.0			

### Appendix VI

Transfection efficiency data of CS/DNA complexes in CHO-K1 cells

Table 15 Transfection efficiency data of CAc-45kDa/DNA complexes at 0.1%, 0.2% and 0.6% acetic acid solution.

% Acid (w/v)	N/P ratio				
	2	4	6	8	12
0.01	309.81	163.60	625.60	243.51	371.07
	50.98	72.27	149.25	463.62	232.29
	61.60	119.37	187.96	631.19	619.75
Average	140.80	118.41	320.94	446.11	407.70
SD	146.47	45.68	264.55	194.43	196.31
0.02	178.31	81.49	416.48	904.91	533.53
	373.28	183.73	36.95	839.08	895.85
	15.14	4.10	63.30	609.13	1294.55
Average	188.91	89.78	172.24	784.37	907.98
SD	179.30	90.10	211.93	155.29	380.65
0.06	131.68	138.03	12061.40	6510.77	1839.12
	110.32	170.52	7321.67	11093.98	105.06
	118.01	141.91	5208.52	4732.01	177.83
Average	120.00	150.15	8197.20	7445.59	707.34
SD	10.82	17.74	3509.33	3282.39	980.83

Table 16 Transfection efficiency data of CAc-45kDa/DNA complexes at pH of transfection medium 6.0 and 7.4.

At N/P = 8	pH	
	6.0	7.4
	4808.31	127.32
	12704.33	98.24
	9347.32	40.92
Average	8953.32	88.83
SD	3962.73	43.97

Table 17 Transfection efficiency data of CAc-45kDa/DNA complexes at incubation time 1, 2, 4, 6 and 24 hours.

At N/P = 8	Incubation time (h)				
	1	2	4	6	24
	143.14	232.92	126.16	896.95	17626.41
	139.56	510.67	1291.04	628.54	18135.24
	147.76	849.94	2657.40	665.81	16627.98
Average	143.48	531.18	1358.20	730.43	17463.21
SD	4.11	309.02	1266.96	145.40	766.77

Table 18 Transfection efficiency data of CS-45kDa/DNA complexes with various chitosan salts.

Complex	N/P ratio				
	2	4	6	8	12
CAc-45kDa/DNA	95.91	206.84	4734.37	7826.99	290.63
	97.50	517.10	2087.15	5283.28	297.63
	200.13	426.35	591.90	1024.65	408.15
Average	131.18	383.43	2471.14	4711.64	332.14
SD	59.72	159.53	2097.77	3437.01	65.92
CAs-45kDa/DNA	77.38	137.92	4045.10	955.76	2543.62
	93.99	95.91	3254.64	1380.45	3489.55
	56.64	486.45	1303.66	475.49	1639.71
Average	76.00	240.09	2867.80	937.23	2557.63
SD	18.72	214.38	1411.06	452.77	925.00
CGI-45kDa/DNA	45.82	322.67	4994.38	243.20	1275.10
	45.94	7.41	20657.24	603.95	2016.69
	41.55	165.69	7324.73	211.98	3788.74
Average	44.44	165.26	10992.12	353.04	2360.18
SD	2.50	157.63	8450.95	217.85	1291.54
CHy-45kDa/DNA	472.68	471.77	1841.14	1495.14	3569.69
	4.11	419.49	2476.36	1246.38	8573.77
	20.99	383.17	234.73	190.08	3021.56
Average	165.93	424.81	1517.41	977.20	5055.01
SD	265.79	44.54	1155.35	692.92	3059.64
CLa-45kDa/DNA	1755.04	2220.83	313.64	2095.49	16165.56
	237.24	261.95	2184.16	1608.25	12325.49
	26.74	403.60	6991.24	3124.99	11898.23
Average	673.01	962.13	3163.02	2276.24	13463.09
SD	942.96	1092.36	3444.73	774.36	2350.14

Table 19 Transfection efficiency data of CGI/DNA complexes with various chitosan MW.

Complex	N/P ratio				
	2	4	6	8	12
CGI-20kDa/DNA	159.23	151.81	487.57	4848.04	8070.16
	4.39	163.73	869.64	16854.09	20531.46
	5.72	150.30	4276.96	13720.47	19192.81
	112.32	103.95	156.21	170.06	4256.15
	83.27	100.90	325.46	294.10	3184.74
	2.51	79.12	46.25	143.34	1822.73
	110.15	86.92	181.57	519.83	1445.27
	28.94	186.75	283.38	302.46	2194.19
Average	63.32	127.93	828.38	4606.55	7587.19
SD	60.78	39.97	1416.35	6830.08	7864.86
CGI-45kDa/DNA	39.73	232.32	10778.02	208.17	297.07
	51.60	147.90	19582.96	468.80	1429.97
	43.49	284.29	3910.96	1408.04	2758.21
	32.30	73.52	18993.50	81.35	1499.87
	40.37	192.99	19458.84	134.82	2901.02
	36.35	8.03	13156.51	143.06	2878.41
	46.01	14.28	364.65	512.47	1201.06
	39.93	278.69	719.82	329.64	1392.83
Average	41.22	154.00	10870.66	410.80	1794.80
SD	5.90	111.82	8304.29	432.97	948.95
CGI-200kDa/DNA	114.29	77.89	646.18	246.95	246.29
	75.91	45.94	223.41	1157.87	217.42
	294.41	327.88	469.42	176.12	340.54
	93.70	48.81	804.38	389.78	96.14
	51.17	95.11	3399.09	129.11	438.80
	69.60	96.71	5522.41	18.59	984.42
	315.82	619.95	126.17	110.87	38.97
	372.63	680.75	177.91	44.07	110.45
Average	173.44	249.13	1421.12	284.17	309.13
SD	130.76	263.95	1973.99	372.22	303.32
CGI-460kDa/DNA	383.76	94.40	30.07	131.15	220.61
	346.56	42.89	64.94	98.76	114.55
	279.07	64.89	168.20	81.67	647.61
	12.91	17.35	1221.74	62.89	72.20
	70.34	25.18	562.49	142.32	82.77
	58.80	86.96	581.86	165.96	174.44
	79.42	65.93	19.51	127.26	126.82
	148.11	89.77	85.50	13.87	60.21
Average	172.37	60.92	341.79	102.98	187.40
SD	143.61	29.70	423.28	49.16	193.63

## Appendix VII

### Cytotoxicity data of CS/DNA complexes in CHO-K1 cells

Table 20 Cytotoxicity data of CS-45kDa/DNA complexes with various chitosan salts.

Complex	N/P ratio				
	2	4	6	8	12
CAc-45kDa/DNA	88.24	112.01	106.44	102.93	95.15
	105.15	106.49	104.76	111.10	96.73
	98.16	109.37	92.41	106.30	94.23
	105.11	97.02	104.47	107.59	87.51
	100.31	99.95	105.43	107.59	96.11
	101.26	73.28	92.31	97.74	90.63
	Average	99.71	99.69	100.97	105.54
SD	6.25	14.12	6.70	4.64	3.59
CAs-45kDa/DNA	118.38	124.12	95.00	89.88	101.66
	117.87	98.73	121.34	106.08	114.06
	118.82	115.72	88.81	101.03	104.67
	113.45	126.84	90.27	93.17	93.36
	115.72	120.59	118.19	100.29	110.15
	117.49	115.72	122.61	93.52	101.07
	Average	116.95	116.95	106.04	97.33
SD	2.02	9.97	16.27	6.11	7.30
CHy-45kDa/DNA	109.90	112.69	90.77	106.73	90.34
	121.82	137.52	108.07	102.79	101.54
	111.73	124.69	114.70	109.56	119.51
	116.10	114.84	103.60	116.34	111.10
	106.49	117.74	107.74	107.45	116.82
	101.83	104.86	92.98	107.88	99.23
	Average	111.31	118.72	102.98	108.46
SD	7.05	11.26	9.33	4.47	11.27
CLa-45kDa/DNA	85.82	96.64	103.60	90.34	93.74
	99.86	110.43	109.95	106.87	86.98
	103.08	115.57	114.70	104.61	100.81
	105.05	109.75	103.22	109.75	105.99
	98.41	111.10	110.24	107.88	114.33
	96.59	116.48	104.23	105.57	115.15
	Average	98.13	110.00	107.66	104.17
SD	6.77	7.11	4.68	7.01	11.24

Table 21 Cytotoxicity data of CGI/DNA complexes with various chitosan MW.

Complex	N/P ratio				
	2	4	6	8	12
CGI-20kDa/DNA	106.82	108.33	100.37	101.33	106.10
	108.73	114.29	113.97	111.59	114.21
	85.82	97.11	100.53	95.52	141.65
	95.36	101.73	89.32	98.39	93.85
	104.43	98.39	116.36	115.41	103.40
	85.02	101.57	89.16	97.11	100.69
Average	97.70	103.57	101.62	103.22	109.98
SD	10.56	6.54	11.66	8.27	16.89
CGI-45kDa/DNA	97.90	94.34	106.79	87.89	95.75
	111.44	100.95	99.66	97.82	116.49
	102.17	99.98	98.02	98.72	94.30
	94.77	95.40	96.30	93.95	96.53
	97.08	94.77	93.36	92.74	94.07
	90.04	102.36	90.31	90.59	97.47
Average	98.90	97.97	97.41	93.62	99.10
SD	7.32	3.53	5.68	4.16	8.62
CGI-200kDa/DNA	100.83	91.53	93.09	104.93	91.65
	103.95	109.09	109.26	112.49	99.27
	103.14	90.72	103.08	117.92	102.44
	103.08	110.70	113.71	113.47	103.43
	106.60	105.56	106.78	116.19	105.74
	96.50	97.48	104.23	107.35	85.52
Average	102.35	100.85	105.02	112.06	98.01
SD	3.42	8.81	6.97	5.03	7.83
CGI-460kDa/DNA	98.75	95.39	113.16	105.24	104.33
	117.11	122.98	107.71	126.70	110.94
	116.36	114.49	115.22	95.15	100.41
	111.51	104.42	93.48	103.12	105.80
	116.94	103.30	98.91	102.62	85.46
	88.82	111.93	97.03	98.37	82.90
Average	108.25	108.75	104.25	105.20	98.31
SD	11.82	9.72	9.04	11.14	11.48

## BIOGRAPHY

**Date of birth** 13 March 1970

### Education

1993 B.Sc. Pharmacy, Faculty of Pharmacy, Mahidol University, Bangkok

1995 M.Sc. Industrial Pharmacy, Faculty of Pharmaceutical Sciences,  
Chulalongkorn University, Bangkok

### Employment

November 1995-

Department of Pharmaceutical Technology, Faculty of Pharmacy,  
Srinakharinwirot University

### Scholarship

July 2004 - March 2007

The Office of the Commission for Higher Education, Ministry of Education

### Publications

1. Weecharangsan W, Opanasopit P, Ngawhirunpat T, Apirakaramwong A, Rojanarata T, Ruktanonchai U, and Lee RJ, An investigation of chitosan salts as nonviral gene vectors in CHO-K1 cells. (submitted).
2. Weecharangsan W, Opanasopit P, Ngawhirunpat T, Rojanarata T, and Apirakaramwong A. Chitosan lactate as a nonviral gene delivery vector in COS-1 cells. *AAPS PharmSciTech*. 2006;7: E1-E6.

### Abstracts and Proceedings

1. Weecharangsan W, Opanasopit P, Ngawhirunpat T, Apirakaramwong A, Ruktanonchai U, and Lee RJ, An investigation of chitosan salts as nonviral gene vectors in CHO-K1 cells, The 2007 US-Thai Consortium Conference and Meeting 6-9 January 2007, Bangkok, Thailand, Podium presentation.
2. Weecharangsan W, Opanasopit P, Ngawhirunpat P, and Apirakaramwong A, Chitosan lactate as non-viral gene delivery vectors: cytotoxicity and transfection efficiency, The 2<sup>nd</sup> AASP Symposium & APEM Conference, 14-17 November 2005, Bangkok, Thailand, Poster Presentation.